2002-09-30

Roles of Lissencephaly Gene, LIS1, in Regulating Cytoplasmic Dynein Functions: a Dissertation

Chin-Yin Tai
University of Massachusetts Medical School

ROLES OF LISSENCEPHALY GENE, LIS1, IN REGULATING CYTOPLASMIC DYNEIN FUNCTIONS

A Dissertation Presented

By

Chin-Yin Tai

Submitted to the Faculty of the

University of Massachusetts Graduate School of Biomedical Sciences, Worcester

in partial fulfillment of the requirements for the degree of

DOCTOR OF PHILOSOPHY

CELL BIOLOGY

(September 30, 2002)

COPYRIGHTS

Tai, C.Y., Dujardin, D.L., Faulkner N.E., and Vallee, R.B. 2002. Role of dynein, dynactin, and CLIP-170 interactions in LIS1 kinetochore function. *J. Cell Biology* **156**:959-968.

ROLES OF LISSENCEPHALY GENE, LIS1, IN REGULATING CYTOPLASMIC DYNEIN FUNCTIONS

A Dissertation Presented
By
Chin-Yin Tai

Approved as to style and content by:

Dr. Stephen Lambert, Chair of Committee

Dr. Peter Pryciak, Member of Commttee

Dr. Dannel McCollum, Member of Committee

Dr. Tony Ip, Member of Committee

Dr. David Pellman, Member of Committee

Dr. Richard B. Vallee, Dissertation Mentor

Dr. John Sullivan, Dean of the
Graduate School of Biomedical Sciences

Department of Cell Biology
September, 20 2002

To my husband, Jen-Yeu

ACKOWLEDGEMENTS

I wish to express my gratitude to my thesis mentor, Dr. Richard Vallee, for giving me the opportunity to work in his laboratory, and for guiding and encouraging in my research. I would also like to thank all members of the Vallee lab who have helped and entertained me through out the years, especially Denis Dujardin and Patty Okamoto, both of whom passed on to me their expert knowledge in microscopy and molecular biology respectively. Atsushi Mikami helped me in protein purifications. Nicole Faulkner participated in numerous discussions in the LIS1 project to stimulate my scientific imaginations.

I also want to thank colleagues and friends on the third floor of Biotech IV, in particular Beth Luna and Joel Richter, for whom had provided me the access to use their equipments freely after the Vallee lab moved. Steve Lambert has provided friendly supervision of my work after Richard left. Yi-Shuian Huang has been my best friend and an aerobic exercise partner, who has endured my complaints.

ABSTRACT

Spontaneous mutations in the human LIS1 gene are responsible for Type I lissencephaly ("smooth brain"). The distribution of neurons within the cerebral cortex of lissencephalic children appears randomized, probably owing to a defect in neuronal migration during early development.

LIS1 has been implicated in the dynein pathway by genetic analyses in fungi. We previously reported that the vertebrate LIS1 co-localized with dynein at prometaphase kinetochores, and interference with LIS1 function at kinetochore caused misalignment of chromosomes onto the metaphase plate. This leads to a hypothesis that LIS1 might regulate kinetochore protein targeting. In order to test this hypothesis, I created dominant inhibitory constructs of LIS1. After removal of the endogenous LIS1 from the kinetochore by overexpression of the N-terminal self-association domain of LIS1, dynein and dynactin remained at the kinetochores. This result indicated that LIS1 is not required for dynein to localize at the kinetochore. Next, CLIP-170 was displaced from the kinetochores in the LIS1 full-length and the C-terminal WD-repeat overexpressers, suggesting a role for LIS1 in targeting CLIP-170 onto kinetochores.

LIS1 was co-immunoprecipitated with dynein and dynactin. Its association with kinetochores was mediated by dynein and dynactin, suggesting LIS1 might interact directly with subunits of dynein and/or dynactin complexes. I found that LIS1 interacted

with the heavy and intermediate chains (HC and IC) of dynein complex, and the dynamitin subunit of dynactin complex. In addition to kinetochore targeting, the LIS1 C-terminal WD-repeat domain was responsible for interactions with dynein and dynactin. Interestingly, LIS1 interacted with two distinct sites on HC: one in the stem region containing the subunit-binding domain, and the other in the first AAA motif of the motor domain, which is indispensable for the ATPase function of the motor protein. This LIS1-dynein motor domain interaction suggests a role for LIS1 in regulating dynein motor activity. To test this hypothesis, changes of dynein ATPase activity was measured in the presence of LIS1 protein. The ATPase activity of dynein was stimulated by the addition of a recombinant LIS1 protein.

Besides kinetochores, others and we have found LIS1 also localized at microtubule plus ends. LIS1 may mediate dynein and dynactin mitotic functions at these ends by interacting with astral microtubules at cortex, and associating with the spindle microtubules at kinetochores. Overexpression of LIS1 displaced dynein and dynactin from the microtubule plus ends, and mitotic progression was severely perturbed in LIS1 overexpressers. These results suggested that the role for LIS1 at microtubule plus ends is to regulate dynein and dynactin interactions with various subcellular structures.

Results from my thesis research clearly favored the conclusion that LIS1 activates dynein ATPase activity through its interaction with the motor domain, and this activation is important to establish an interaction between dynein and microtubule plus ends during

mitosis. I believe that my thesis work not only has provided ample implications regarding dynein dysfunction in disease formation, but also has laid a significant groundwork for more future studies in regulations of the increasing array of dynein functions.

TABLE OF CONTENTS

LIST OF TABLES

LIST OF FIGURES

CHAPTER I

CHAPTER II

CHAPTER III

INTRODUCTION

The microtubule network provides a framework for diverse activities such as cell division, cell motility, vesicular trafficking, organelle positioning, and the distribution of cell fate determinants. Microtubules are polymers consisting of heterodimers of α- and β-tubulins. The head-to-tail association of α/β tubulin heterodimer creates a polar microtubule filament, which provides the directionality for motor proteins, kinesins mostly moving towards the plus ends of microtubules, and cytoplasmic dyneins traveling towards the minus ends. All cytoskeleton-associated proteins convert chemical energy through the hydrolysis of ATP into mechanical forces.

Members in the dynein family are sub-divided into two categories: axonemal dyneins and cytoplasmic dyneins. Axonemal dyneins generate forces for ciliary and flagellar power strokes by sliding adjacent microtubules within the axoneme (Gibbons IR, 1965). Two different forms of cytoplasmic dyneins exist in higher eukaryotes, namely DHC1a/dynein 1 and DHC1b/dynein 2 (detailed in Chapter I) (Paschal et al., 1987; Tanaka et al., 1995; Vaisberg et al., 1996).

DHC1a/dynein 1, hereinafter refers to as cytoplasmic dynein, is the major form of cytoplasmic dynein. In addition, another multi-protein complex, dynactin, was identified through its ability to assist dynein in cargo-binding specificity and motor processivity (Gill et al., 1991; King and Schroer, 2000; Schroer and Sheetz, 1991). Studies of

cytoplasmic dynein and dynactin in the past decade largely focused on their regulation at the molecular level.

Studies of the disease-causing gene, LIS1, revealed a causal relation between LIS1 mutations and perturbation of cytoplasmic dynein functions. The disease, lissencephaly, is a childhood neurological disorder, which results in a disorganized cerebral cortex. It is hypothesized that defects in the cortical organization are the result of dysfunction in neuronal migration, possibly a dynein-mediated process. Earlier it was found that homologues of LIS1 participated in the cytoplasmic dynein functions in several genetically tractable systems (Geiser et al., 1997; Swan et al., 1999; Xiang et al., 1995). Loss-of-function mutations of LIS1 homologues in these organisms exhibited phenotypes identical to dynein mutants. In addition, a mutant allele of the *Aspergillus* LIS1 homologue, *nudF*, suppressed the phenotype of a particular allele of *nudA* mutant, which encodes the cytoplasmic dynein heavy chain (Willins et al., 1997). Although these results highlighted the indispensable role of LIS1 in dynein functions in lower eukaryotes, the role of LIS1 in mammalian dynein functions and the role of dynein in lissencephaly were less clear.

We started to investigate the functions of LIS1 in cytoplasmic dynein pathway in mammalian cells, and based on our results, we hypothesized that LIS1 participated in mitotic dynein functions (Faulkner et al., 2000). We found that LIS1 colocalized with dynein and dynactin at numerous subcellular structures including kinetochores, cell

cortex, spindle, and spindle poles. We examined the functions of LIS1 at some of these sites. First, injection of an anti-LIS1 antibody interfered with chromosome alignment during metaphase. Injection of an anti-dynein antibody produced a similar phenotype. These results suggested that both LIS1 and dynein affected mitotic chromosome alignment, possibly through their interactions at kinetochores. Second, overexpression of LIS1 in polarized epithelial cells caused mis-orientation of mitotic spindles as well as displacement of dynein and dynactin from cell cortex (Faulkner et al., 2000). This suggested that LIS1 participated in the regulation of cortical dynein/dynactin targeting and hence mediating spindle orientation. Together, these results pointed to roles for LIS1 in mitotic dynein function, especially spindle orientation and chromosome alignment at the metaphase plate. Specific mechanisms of how LIS1 regulates these activities were mostly unknown.

The goal of my thesis work was to understand how LIS1 functioned with cytoplasmic dynein to regulate mitotic progression. First, I wanted to examine the functional characteristics of the two structural domains of LIS1 protein. The sequence analysis of LIS1 protein showed two distinct domains: a N-terminal domain containing a 28 a.a. coiled-coil structure (a.a. 51-78), and a C-terminal domain containing seven WD repeats. I created two LIS1 fragments, LIS1 N (a.a. 1-87) and LIS1 WD (a.a. 88-414), and studied their subcellular localization and the mitotic phenotypes associated with their overexpression. The N-terminal domain functioned as the dimerization domain for self-association, and the C-terminal WD-repeat domain was identified as the kinetochore-

targeting domain. Overexpression of either the LIS1 N or the LIS1 WD fragments resulted in severe perturbation of mitotic progression.

Second, I investigated LIS1's function at the mitotic kinetochores. This question was approached by identifying the hierarchical relationship among dynein, dynactin and LIS1. Others have shown that dynactin linked dynein to the kinetochores (Starr et al., 1998). It was unclear whether dynactin was also involved in the kinetochore targeting of LIS1, or vice versa. We found that dynactin mediated the kinetochore localization of LIS1, and LIS1 was not required for the kinetochore targeting of dynein and dynactin (detailed in Chapter II). In addition, I asked whether overexpression of LIS1 disrupted the kinetochore localization of several other kinetochore proteins. Among them, CLIP-170 has been shown to localize at the kinetochore through dynein and dynactin (Dujardin et al., 1998). I found that CLIP-170 was displaced from the kinetochore in LIS1 overexpressers. Together, my work suggested that the kinetochore localized LIS1 acted as a linker between dynein/dynactin and CLIP-170.

Third, I asked whether there was a specific protein-protein interaction between LIS1 and dynein/dynactin. I found that LIS1 was co-immunoprecipitated by a panel of antibodies made against subunits of dynein and dynactin (Faulkner et al., 2000). I then asked which subunit in the dynein and dynactin protein complexes specifically contributes to this interaction. Heavy and intermediate chains of the dynein complex, and the dynamitin subunit of the dynactin complex were found to interact with LIS1 directly

(detailed in Chapter II). Next, domain analyses were carried out to further dissect the regions in LIS1 protein required for these interactions. The WD-repeat domain was found to mediate all these interactions with dynein and dynactin, whereas the N-terminal domain was involved in self-association.

Fourth, I found that two distinct sites within the dynein HC interacted with LIS1, one in the subunit-binding domain, and the other in the ATPase domain (detailed in Chapter II). These interactions suggested a mechanistic role for LIS1 in regulating motor activity. Recombinant LIS1 was found to activate the ATPase activity of the purified dynein complex by 1.6 fold (detailed in Chapter III). In addition, the majority of LIS1 protein did not co-sediment with dynein, suggesting the interaction between LIS1 and dynein was transient.

Lastly, others and we have found that LIS1, dynein and dynactin localized at the microtubule plus ends (Coquelle et al., 2002; Faulkner et al., 2000), and that the p150^{Glued} subunit of dynactin mediated the microtubule plus end localization of dynactin (Vaughan et al., 1999). Overexpression of LIS1 displaced the p150^{Glued} from the microtubule plus ends (Faulkner et al., 2000). I then asked whether dynein could associate with the microtubule plus ends also through p150^{Glued} subunit, and whether LIS1 overexpression could displace dynein from the microtubule plus ends as well. I found that dynein depended on the p150^{Glued} to localize at microtubule plus ends. In addition, overexpression of LIS1 displaced dynein and dynactin from the plus ends.

CHAPTER I

REVIEW OF LIS1 IN DISEASE AND IN THE CYTOPLASMIC DYNEIN PATHWAY

Lissencephaly

Pathology

Lissencephaly ("smooth brain" in Greek) represents a severe developmental brain disorder. The hallmark of the disease is exemplified by a clear decrease in convolutions of cerebral cortex (pachygyria) or the complete lack of it (agyria).

Infant patients often suffer from poor feeding and impaired development of the visual system, and they often die from severe seizures before their second birthday. Children who survive often have mental retardation and impaired physical development. One in 40,000 infants is born with this disease in the United States each year (Leventer et al., 2001b; Walsh, 1999).

Clinically, lissencephaly is divided into two subtypes based on morphological defects. Type I lissencephaly includes Miller-Dieker syndrome (MDS) and isolated

lissencephaly sequence (ILS). MDS children exhibit distinct facial abnormalities, such as broad forehead, slight indentation of the temple, upturned tip of the nose, thin upper lip and small jaw, whereas ILS children do not have obvious facial defects. Type II lissencephalic patients have other birth defects, for example hydrocephalus, cloudy cornea, muscular dystrophy, etc.

Proposed mechanism and genetics of the disease

Failure of neuronal migration is thought to be the cause of cortical disorganizations found in lissencephalic brains (Rakic, 1988). The process of neuronal migration is regulated in both temporal and spatial manners. After the completion of the last round of cell division at the ventricular zone, neurons migrate along the radial glials to the cerebral cortex (Rakic, 1988; Rakic, 1990). Human cerebral cortex consists of six distinct layers, and the ordered waves of neuronal migrations create an inside-out arrangement of these layers (Gupta et al., 2002; Lambert de Rouvroit and Goffinet, 2001; McConnell, 1988; Rakic, 1978). Disruptions of the formation of cortical layers observed in lissencephalic patients suggested that factors affecting the process of neuronal migration were defective. These factors could be involved in either the temporal or the spatial controls of neuronal migration.

Risk factors contributing to the formation of lissencephaly could be either non-genetic or genetic. The non-genetic risk factors include viral infections and shortage of blood supply in early pregnancy. Genetic elements associated with the disease have been

identified and cloned including *LIS1* and others (see Table 1 for complete list) (des Portes et al., 1998; Gleeson et al., 1998; Reiner et al., 1993). Mutations in *LIS1* result in Type I lissencephaly. A large deletion of *LIS1* locus and its neighboring gene, *HIC1*, result in MDS with distinct facial defects. *HIC1* encodes an unknown Zinc finger protein and expresses specifically in mesenchymes (Grimm et al., 1999). This suggests that the facial defects of MDS patients may be a result of deletions into the *HIC1* gene. Only one gene was identified to be involved in Type II lissencephaly. *FCMD*, encodes a putative extracellular matrix (ECM)-associating protein (Kobayashi et al., 1998). Together, mutations in several different genes have been implicated in the formation of lissencephaly, suggesting a complex network of multi-protein regulated processes underlies the formation of the disease.

Table 1: Genetics of human neocortex organization disorders[1,2]

Gene mutated	Disease	Mode of inheritance	Protein function	First identified by
LIS1	MDS and ILS	Sporadic	involves in dynein/dynactin and PAFAH pathways	(Reiner et al., 1993)
DCX	ILS and SBH	X-linked	regulates microtubule dynamics	(Gleeson et al., 1998)
RELN	LCH	Recessive	a large extracellular matrix (ECM)-associating protein; involves in signaling transduction	(Hong et al., 2000)
FLNA	PH	Dominant	actin-binding protein; involves in regulating actin cytoskeleton	(Fox et al., 1998)
PEX2, PXR1	Zellweger syndrome	Recessive	peroxisome biogenesis; abnormal lipid metabolism	(Baes et al., 1997; Faust and Hatten, 1997)
FCMD	Fykuyama congenital muscular dystrophy (FCMD)-cobblestone complex type II LIS & myopathy		putative ECM protein	(Kobayashi et al., 1998)

[1] Abbreviations used in the table: DCX, doublecortin; RELN, reelin; FLNA, filamin A, α; MDS, Miller-Dieker syndrome; ILS, isolated lissencephaly sequence; SBH, subcortical band heterotopia; LCH, lissencephaly with cerebellar hypoplasia; PH, periventricular heterotopia; LIS, lissencephaly.

[2] Modified from (Gupta et al., 2002; Ross and Walsh, 2001)

LIS1 mutations in patients: from severity of clinical defects to structure of protein

Reduced amount of LIS1 protein is found in lissencephalic patients with missense mutations in LIS1 locus, and truncated LIS1 proteins were undetectable in patients carrying nonsense mutations, frameshift mutations or small deletions of the LIS1 gene (Cardoso et al., 2000; Sapir et al., 1999). This suggests that a decrease in the amount of LIS1 proteins in brain causes lissencephaly. Different types of LIS1 mutations were compared with the severity of brain disorganizations. Patients carrying LIS1 missense mutations have milder cortical malformations than patients with other types of mutations, implying that the mutated LIS1 proteins are partially functioning (Leventer et al., 2001a).

LIS1 encodes a 45 kDa polypeptide containing a coiled-coil domain at the N-terminus and seven WD repeats at its C-terminus. At least four alternatively spliced LIS1 transcripts were identified, and only one size of LIS1 protein was detected (Reiner et al., 1993). The sites of mutations in LIS1 proteins characterized in lissencephalic patients are scattered through out the entire protein, and similarities in the severity of diseased phenotypes were found while comparing mutations in the two structural domains of LIS1 (Leventer et al., 2001a). This indicates the two domains of LIS1 protein are equally important for its function.

Mouse model of lissencephaly

Three reduced dosage of LIS1 mutant mice were designed to test whether the decrease of LIS1 expression affects the severity of phenotypes (Hirotsune et al., 1998).

The homozygous *LIS1* null mutation resulted in early post-implantation embryonic lethality, suggesting that proper LIS1 function is important for early embryonic development. Heterozygous *LIS1* mice exhibited the phenotype of cortical disorganization, which is reminiscent of human lissencephaly. When examining brains from the mutant mice carrying two hypomorphic alleles of *LIS1* mutations was found that the organizational disruptions were more prominent in the compound heterozygote than those in either one of the single heterozygotes. This result demonstrated that further reduction of LIS1 level enhances the severity of abnormalities.

Despite the fact that histological analyses from the cerebella of these *LIS1* heterozygous mice showed no obvious disorganizations, the authors chose to use cerebellar neurons from these mice to measure neuronal migration. *LIS1* +/- neurons moved at a much slower speed when compared with wildtype neurons. Although cerebellar neurons derived from the *LIS1* heterozygous mice exhibited defects in neuronal migration even with the lack of disruptions in the cerebella, this result did not directly address the question why there are abnormalities found in the cerebral cortex in *LIS1* mutant mice, and lissencephalic patients.

Knowing that cortical organization in LIS1 mutant mice was disrupted, it was important to examine whether other functions of these neurons were also defective. Electrophysiological tests of the *LIS1* mutant mice identified abnormal neuronal activities in the cerebral cortex (Fleck et al., 2000). The abnormal patterns of the

electrophysiological readouts suggested that the disruption of cortical organization resulted in misconnections of neurons. Frequent severe seizures in lissencephalic patients could be the direct result of the misfiring from these disorganized neurons.

Cytoplasmic dynein and dynactin: structure and functions

Cytoplasmic dyneins convert the chemical energy from ATP hydrolysis into mechanical force to travel toward the minus end along microtubules at 1μm/sec (Paschal et al., 1987).

Two forms of cytoplasmic dyneins

DHC1a or dynein 1, the major form found in all eukaryotes, is a large protein complex with a molecular weight of 1.2 mDa (Vallee et al., 1988). Its constituent subunits were named according to their respective sizes: two 530 kDa heavy chains (HC), two 74 kDa intermediate chains (IC), four 53-59 kDa light-intermediate chains (LIC) and a number of 10-13 kDa light chains (LC) (King et al., 2002; Vallee et al., 1988). Except for the LIC subunits found exclusively in higher eukaryotes, homologues of the rest of the subunits were isolated and identified from fungi to human. In mammalian cells, this major form of cytoplasmic dynein participates in a wide range of functions inside the cell, including: retrograde transport of vesicles, Golgi positioning, RNA transport, chromosome capture and alignment, spindle orientation, spindle pole focusing, centrosome reorientation, nuclear migration, viral particle transport, melanosome movements, nuclear envelope breakdown, and the list of functions is still growing (Banks and Heald, 2001; Dujardin and Vallee, 2002; Goldstein and Yang, 2000; Kamal and Goldstein, 2000; Karcher et al., 2002; Stebbings, 2001).

DHC1b or dynein 2, the minor form of cytoplasmic dynein found in most of the ciliated eukaryotic cells and, has functions restricted to intraflagellar transport (IFT) (Mikami et al., 2002; Pazour et al., 1999; Signor et al., 1999) and Golgi organization(Grissom et al., 2002; Vaisberg et al., 1996). It contains a monomeric HC and a monomeric LIC, and unlike DHC1a/dynein1, it lacks any of the ICs and the LCs (Grissom et al., 2002; Mikami et al., 2002). Hereafter, cytoplasmic dynein refers to the DHC1a/dynein 1.

The heavy chains (HCs)

The motor and microtubule-binding activities of cytoplasmic dynein reside in the two identical HC subunits (Gee et al., 1997; Mazumdar et al., 1996). The N-terminal 150 kDa half contains the binding sites for LIC and IC (Tynan et al., 2000a), whereas the C-terminal 380 kDa forms a hollow centered globular head with a stalk structure (for microtubule-binding) protruding from a ring of six AAA (ATPase associated with cellular activities) subdomains (Gee et al., 1997; Mocz and Gibbons, 2001; Neuwald et al., 1999).

The AAA domain is an evolutionarily conserved module found in proteins involved in DNA replication, membrane fusion, proteolysis, cytoskleleton reorganization, protein chaperoning and motility (Ogura and Wilkinson, 2001). Most AAA domains are about 35-40 kDa. Each AAA domain contains two sub-domains: an N-terminal domain

containing a nucleotide binding pocket (P-loop), and a C-terminal α-helical domain involved in substrate recognition (Ogura and Wilkinson, 2001). In axonemal dynein, vanadate-mediated photocleavage severed the ATP hydrolytic core (P-loop) of the first AAA domain, and destroyed most of the motor activities (Gibbons and Gibbons, 1987). Later, we found that mutation in the P-loop motif of the first AAA domain of cytoplasmic dynein HC abolished the photocleavage property and promoted a rigor-like state (Gee et al., 1997), indicating that the first AAA domain of the HC is responsible for the ATPase activity of the motor domain.

The intermediate chains (ICs)

ICs interact with HCs, LCs, and the p150^{Glued} subunit of dynactin (Karki and Holzbaur, 1995; Lo et al., 2001; Ma et al., 1999; Mok et al., 2001; Susalka et al., 2002; Vaughan and Vallee, 1995). ICs regulate not only dynein ATPase activity, but also serve as a bridge between dynein complex and herpes simplex virus (Kini and Collins, 2001; Ye et al., 2000). ICs' phosphorylation states determine their affinity towards dynactin (Lane et al., 2001; Vaughan et al., 2001).

Two genes (IC1 and IC2) transcribing five alternatively spliced variants (IC1A, IC1B, IC2A, IC2B and IC2C) have been identified and characterized for ICs (Paschal et al., 1992; Vaughan and Vallee, 1995). The two isoforms encoded by IC1 are brain specific, and their functions remain to be determined (Pfister et al., 1996a; Pfister et al., 1996b). IC2C is the most ubiquitously expressed isoform in all tissues tested (Vaughan

and Vallee, 1995). The structure of IC proteins contains several distinct domains: a N-terminal coiled-coil domain binds dynactin (Vaughan and Vallee, 1995), followed by a region of variable sequence due to alternative splicing, followed by the LCs (Tctex-1 and LC8) binding sites (Lo et al., 2001; Mok et al., 2001), and the C-terminal four WD-like repeats possibly involving in binding to the HC (Ma et al., 1999).

The light intermediate chains (LICs)

Two isoforms of LICs (LIC1 and LIC2) were found in all tissues (Hughes et al., 1995). Homo-oligomers of each isoform interacted separately with the dimeric HC subunits of cytoplasmic dynein (Tynan et al., 2000b). LIC1 is involved in association with pericentrin, a pericentriolar matrix associated protein, which represents a cargo of dynein complex to be delivered to the centrosomes (Purohit et al., 1999). LIC2 was not involved in transporting pericentrin and it did not co-exist with LIC1 in the same dynein complex, suggesting that LICs played a role in defining cargo specificity of dynein complex (Tynan et al., 2000b). LICs were phosphorylated by cdc2/cyclin B protein kinase, resulting in separation of dynein from the vesicles during mitosis (Addinall et al., 2001; Niclas et al., 1996). These results clearly demonstrated that the significance of LIC subunits is to diversify motor functions and to couple with cell cycle progression.

The light chains (LCs)

Cytoplasmic dynein contains several light chains, which were also found in the axonemal dyneins (Bowman et al., 1999; King et al., 1996; Tai et al., 1999). Each LC

interacts with several different kinds of cargos, suggesting a role for these LCs in cargo-binding specificity. For example, the 14 kDa LC, Tctex-1 interacted directly with rhodospin to translocate rhodospin-bearing vesicles across the connecting cilium, whereas RP3, sharing 75% homology with the Tctex-1, did not interact with rhodopsin (Tai et al., 1999). Interestingly, the 8 kDa LC (LC8) was found to co-precipitate with myosin V (Benashski et al., 1997; Espindola et al., 2000). The exact function of LC8 in the myosin V pathway is unclear, however, it may represent a link between a microtubule motor, dynein, and an actin motor, myosin V.

The dynactin complex

Dynactin complex was initially characterized as a high molecular weight dynein activator in chicks (Gill et al., 1991; Schroer and Sheetz, 1991), and was subsequently found to participate in mediating motor processivity along the microtubule and in cargo-binding (Burkhardt et al., 1997; Holleran et al., 1998; King and Schroer, 2000). Transmission electron microscopy of the dynactin complex revealed two sub-domains: a short actin-like filament connecting to a shoulder-sidearm projection structure (Eckley et al., 1999). Further biochemical analyses identified components in these two sub-domains: Arp1, CapZ, p62, Arp11, p27 and p25 were in the actin-like short filament, whereas p150^{Glued}, dynamitin and p24 resided in the shoulder-sidearm projection (Eckley et al., 1999; Garces et al., 1999). Overexpression of the dynamitin subunit resulted in splitting the dynactin complex into smaller protein complexes (Echeverri et al., 1996), and the location of the dynamitin subunit was identified at the junction between the two

sub-domains by immuno-EM (Eckley et al., 1999). Thus, dynamitin is thought to serve as a hinge between the two sub-domains of dynactin. Overexpression of dynamitin has been widely applied to study different aspects of dynein and dynactin.

Dynactin also has its own microtubule-binding ability conferred by the N-terminus of the p150^{Glued} subunit (Waterman-Storer et al., 1995). The microtubule-binding domain of p150^{Glued} has been shown to localize preferentially to the plus ends of microtubules (Vaughan et al., 1999), and phosphorylation of this domain negatively regulated its binding activity, leading to the dissociation of dynactin complex from microtubules (Vaughan et al., 2002). The p150^{Glued} subunit interacted to IC and Arp1 simultaneously through its central coiled-coil region (Karki and Holzbaur, 1995; Vaughan and Vallee, 1995; Waterman-Storer et al., 1995). The Arp1 subunit interacted with spectrin, suggesting Arp1 links dynactin complex to the spectrin-containing vesicles (Holleran et al., 1996).

Co-purifications of dynein and dynactin

To purify a single complex containing both dynein and dynactin proved to be extremely difficult. Dynein and dynactin were separated as two protein complexes in most of the purification methods. They exhibited the same sedimentation profiles by either sucrose gradient centrifugation or gel filtration chromatography (Paschal et al., 1993). Recently, a supercomplex containing both dynein and dynactin was observed when the rat brain extracts were fractionated in a low-salt (20 mM Tris HCl pH7.6)

sucrose gradient (Kini and Collins, 2001), suggesting a weak interaction between dynein and dynactin. Phosphorylation of IC has also been shown to inhibit the binding of p150^{Glued} (Vaughan et al., 2001), suggesting a regulated interaction between dynein and dynactin.

LIS1 functions

Although extensive studies on the mutation spectrums of *LIS1* gene in humans and mice demonstrated clear correlations between disease severities and the *LIS1* mutant loci, the exact function of this gene product is still elusive. This section is focused on recent studies of LIS1 protein functions, and is categorized according to the individual function.

LIS1 in cytoplasmic dynein pathway

In *A. nidulans*, cells with mutations in the subunits of dynein/dynactin and the LIS1 homologue, *nudF,* showed defects in post-mitotic nuclear migration along the hyphae (Xiang et al., 1994). In *S. cerevisiae,* mutants of dynein, dynactin and the LIS1 homologue, *pac1*, showed defects in nuclear positioning during mitosis (Geiser et al., 1997; Xiang et al., 1995) (see Table 2 for summary of dynein/dynactin homologues in various organisms). In *A. nidulans*, allele-specific suppression was observed between LIS1 homologue, *nudF*, and dynein heavy chain (DHC), *nudA*, implying that LIS1 might interact with DHC directly (Willins et al., 1995). Over the years, this interaction was demonstrated in several eukaryotic model systems, and was detailed in Chapter II (Hoffmann et al., 2001; Sasaki et al., 2000; Tai et al., 2002).

Table 2: Homologues of dynein and dynactin-related genes in fungi and fly[1]

Higher eukaryotes	***S. cerevisiae***	***A. nidulans***	***N. crassa***	***D. melanogaster***
Cytoplasmic dynein				
Heavy chain	*DYN1/DHC1*	*NUDA*	*RO-1*	*Dhc*
Intermediate chain	*PAC11*	*NUDI*		*Cdic*
Light intermediate chain				
Light chain				
LC8	*DYN2*	*NUDK*		*ddlc1*
Tctex-1				*dtctex-1*
RP3				
LC7				*roadblock*
Dynactin				
Shoulder-sidearm subcomplex				
p150^{Glued}	*NIP100*	*NUDM*	*RO-3*	*glued*
dynamitin	*JNM1*			
p24				
Actin-like filament				
Arp1	*ARP1/ACT5*		*RO-4*	*gridlock*
CapZ				
p62			*RO-2*	
p25			*RO-12*	
p27				
Arp11			*RO-7*	
Other components				
LIS1/PAFAH1b β	*PAC1*	*NUDF*		*DLIS1*
NUDC		*NUDC*		
NudE/NudEL		*NUDE*	*RO-11*	

[1] Modified from (Lambert de Rouvroit and Goffinet, 2001) with additional information from (Bruno et al., 1996; Caggese et al., 2001; Dick et al., 1996; Holzbaur et al., 1991; Lee et al., 2001; Minke et al., 1999; Nurminsky et al., 1998; Rasmusson et al., 1994; Swan et al., 1999).

Others and we made several observations suggesting LIS1 functions in the dynein pathway of mammalian cells. First, LIS1 colocalized with dynein and dynactin at the kinetochore, cell cortex, spindle, spindle poles, microtubule plus ends, nuclear envelope (Coquelle et al., 2002; Faulkner et al., 2000). Second, LIS1 co-immunoprecipitated with dynein and dynactin from bovine brain cytosolic extract (Faulkner et al., 2000; Smith et al., 2000). To demonstrate LIS1 functions in the dynein pathway, we altered the amounts of LIS1 protein expressed in cell lines, and asked whether these changes interfered with normal dynein functions. Overexpression of LIS1 in cultured mammalian cells disrupted cortical dynein localization and the majority of transfected cells contained misoriented spindles, suggesting the involvement of LIS1 in spindle orientation during mitosis (Faulkner et al., 2000). In fly, LIS1 and dynein HC homologues colocalized at the cell cortex in oocytes, and dynein HC was missing from the cortical site in the fly *LIS1* mutant (Swan et al., 1999). This was consistent with the suggestion that LIS1 functions in cortical dynein localization, which in turns regulated microtubule-cortex interactions. Furthermore, anti-LIS1 antibody injected cells exhibited failures in chromosome alignment at the metaphase plate (Faulkner et al., 2000). This phenotype was also observed in the anti-dynein antibody injected cells (Faulkner et al., 2000). In *D. melanogaster*, decrease of neuroblast proliferations was observed in both *Dlis1* and *Dhc* mutants (Liu et al., 2000). These results strengthened the notion that LIS1 was involved in mitotic dynein function. In addition, dynactin was displaced from the microtubule plus ends in LIS1-overexpressing cells, whereas other plus-end binding proteins, EB1 and CLIP-170, remained bound (Faulkner et al., 2000), indicating that the disruption of

dynactin at plus ends was not an indirect effect of altering microtubule dynamics at these ends (Faulkner et al., 2000). Together, mammalian LIS1 was found to participate in mitotic dynein functions, such as spindle orientation and metaphase chromosome capturing. These mitotic effects of LIS1 could be summarized with a role for LIS1 in dynein pathway at microtubule plus ends (Figure 1; Vallee et al., 2001).

Figure 1. Three-way interactions among LIS1, dynein/dynactin and microtubule plus end in mammalian cells. The radial array of microtubule network emanated from the centrosomes utilizes plus ends to probe the periphery of the cell in all cell cycle phases. In interphase (A), LIS1 colocalizes with dynein and dynactin at growing microtubule plus ends (C). Mitotic microtubules are divided into two sets: the mitotic spindle captures chromosomes at kinetochores, a proteineous structure located at centromeres, and the astral microtubules interact with the cell cortex underlying the plasma membrane (B). During mitosis, one set of LIS1, dynein and dynactin localizes at cell cortex to mediate interactions with astral microtubule plus ends (C), and, another set of these proteins resides at the kinetochores to capture the plus ends of the incoming spindle microtubules (D). This figure is modified from the Figure 3 of Vallee et al., 2001.

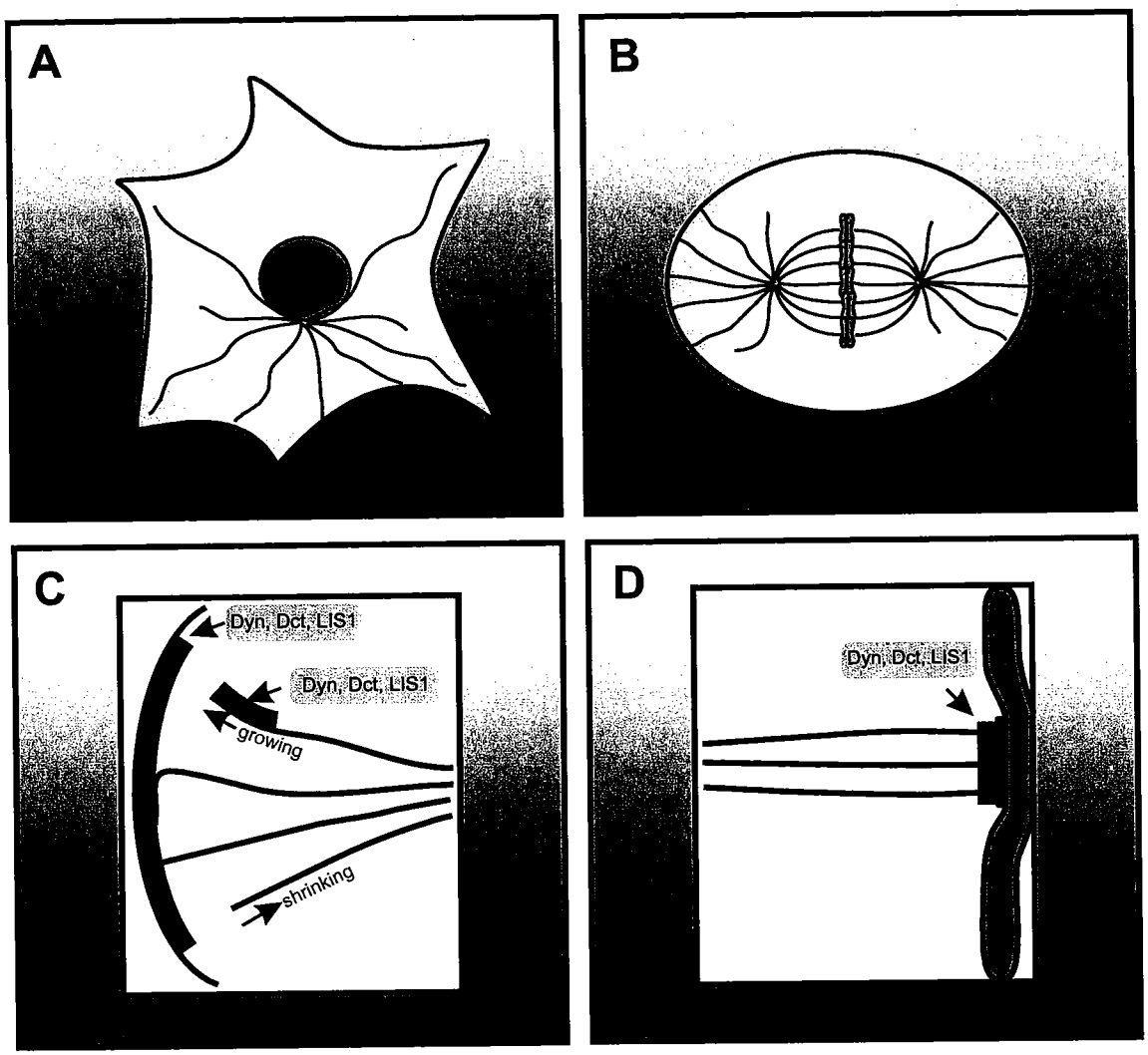
A
B
C
Dyn, Dct, LIS1
Dyn, Dct, LIS1
growing
shrinking
D
Dyn, Dct, LIS1

LIS1 in the regulation of microtubule dynamics

Whether or not LIS1 is a microtubule-associated protein (MAP), and if it directly regulates microtubule dynamics are two outstanding questions. Members in the MAP family interact with microtubules directly. LIS1 colocalized with microtubules in various mammalian cell lines was observed by one group of researchers, suggesting LIS1 might serve as a MAP (Coquelle et al., 2002; Sapir et al., 1997). This was supported by genetic and biochemical analyses in *A. nidulans*. First, genetic data showed allele-specific suppression between the α-tubulin and LIS1 homologue, *nudF,* mutants (Willins et al., 1995). Recently, a tagged NudF protein purified from fungal cell extracts has shown to interact with purified α-tubulin (Hoffmann et al., 2001). However, we and another group of researchers failed to localize mammalian LIS1 at microtubules (Faulkner et al., 2000; Smith et al., 2000). These results indicate that LIS1 in *A. nidulans* acts like a MAP. However, it remains to be clarified whether the mammalian LIS1 belongs to the MAP family.

The reductions of both catastrophe and rescue frequencies of microtubule dynamics were observed in the *nudF* mutant, suggesting that LIS1 is involved in regulating microtubule dynamics (Han et al., 2001). *In vitro* translated mammalian LIS1 was co-pelleted with microtubules, possibly through unidentified MAPs in the lysates used for the *in vitro* translation (Sapir et al., 1997). This LIS1 protein reduced catastrophe frequency of microtubules.

The possible site for LIS1 to modulate microtubule dynamics is at the microtubule plus ends. A family of proteins, named microtubule-plus-end tracking proteins (+TIPs), has been identified in recent years, including dynactin, CLIP-170, EB1, APC, CLIP115, CLASPs, and LIS1 (reviewed in McNally, 2001; Schuyler and Pellman, 2001). Members in the +TIPs family have been observed to localize specifically at the plus ends of microtubules regardless whether the interactions are direct or indirect. GFP-tagged LIS1 has been observed to localize at microtubule plus ends (Faulkner Ph.D. thesis), possibly through the interaction with another +TIP, CLIP-170 (Coquelle et al., 2002). In *A. nidulans*, GFP-tagged NudF protein also localized at the microtubule plus ends (Han et al., 2001). However, the homologue of CLIP-170 has yet to be identified in this organism. Overexpression of either LIS1 or the C-terminal Zinc finger of CLIP-170 displaced dynactin from the microtubule plus ends, suggesting these two proteins work in concert to regulate dynactin targeting at the plus ends (Faulkner et al., 2000; Valetti et al., 1999). It is very likely that LIS1 regulates microtubule dynamics through multiple interactions with dynactin and CLIP-170.

LIS1 in the organization of microtubule network

The vertebrate LIS1 localized at interphase centrosomes (Smith et al., 2000), and we found it localized at mitotic spindle poles (Faulkner et al., 2000; Tai et al., 2002). The interphase microtubule network became unfocused in LIS1 overexpressing cells (Smith et al., 2000), but we did not observe this phenotype when we performed similar overexpression experiments (Faulkner et al., 2000; Tai et al., 2002). We found a

significant increase of multiple spindle poles in LIS1 overexpressing cells (Faulkner et al., 2000; Tai et al., 2002). LIS1 homologue, NudF, has been demonstrated to interact directly with γ-tubulin in *A. nidulans* (Hoffmann et al., 2001). The exact function of NudF in γ-tubulin pathway remains to be examined.

LIS1 in axonal transport

The mushroom body is a specialized region in the central nervous system of fruit fly, which controls the learning and memory abilities. It contains ~200 neurons, and the development of individual neuron is well studied. A mushroom body-specific null allele of *DLIS1* exhibited defects in axonal transport with obvious swelling along the axons (Liu et al., 2000). A *Dhc* hypomorphic allele mutant showed that the swelling only occurred at the axonal termini with occasional swellings along the axons, different from the swelling patterns seen in *DLIS1* mutant (Liu et al., 2000). In a mouse sciatic nerve ligation experiment, LIS1 and dynein were found to accumulate at both proximal and distal ends of the ligation site, whereas a representative kinesin isoform, KIF5C, accumulated only at the proximal end, suggesting LIS1 colocalizes with dynein during axonal transport (Sasaki et al., 2000). From the fly genetic and the mouse localization data, it is tempting to postulate that LIS1 is involved in dynein-mediated axonal transport.

LIS1 in Golgi positioning

LIS1 may play a role in organizing Golgi apparatus around the nucleus (Smith et al., 2000). A more spread out pattern of Golgi staining was observed in the mouse

embryonic fibroblasts (MEFs) from *LIS1* +/- mice when compared with wildtype MEFs. Transfection of a LIS1-GFP construct into the *LIS1* +/- MEFs restored the tightness of Golgi stacks to the wildtype level. Since the microtubule network in these *LIS1*+/- MEFs became more bundled and less focused around the nuclei, it is possible that the reduced compactness may be an indirect effect of microtubule network disruption caused by the dysfunction of LIS1.

LIS1 in PAFAH pathway

LIS1 protein was co-purified with platelet-activating factor acetylhydrolase Ib (PAFAH Ib), and was considered to be the non-catalytic subunit of this heterotrimeric enzyme complex (Hattori et al., 1994; Hattori et al., 1993). PAFAH represents a group of enzymes that removes an acetate group from the sn-2 position of platelet-activating factor (PAF) and results in the inactivation of PAF (Arai et al., 2002). PAF is a lipid mediator, which evokes potent pro-inflammatory responses in various tissues (reviewed in McManus and Pinckard, 2000). The role of PAF in neuronal migration was also tested by performing a cerebellar granule cell migration assay in the presence or absence of the constitutive active derivative of PAF (Bix and Clark, 1998). PAF was found to be a negative regulator of neuronal migration. Excess amount of PAF inside the cell had negative effect on neuronal migration similar to the reduced dosage phenotypes of LIS1 mutant mice. This suggests the role of LIS1 in neuronal migration might be regulated through the PAFAH complex.

In summary, LIS1 involves in a wide range of cellular activities, including: nuclear migration, chromosome alignment onto the metaphase plate, spindle orientation, microtubule dynamics, Golgi positioning, centrosome functions, and PAF metabolism. All these events could be independent or interdependent of each other, and they could be either dependent or independent of dynein.

From LIS1 cellular functions to the mechanisms of lissencephaly formation

Models for lissencephaly formation emerged as the cellular functions of LIS1 became clear. There have been two models proposed, and both agree that a nuclear migration defect results in lissencephaly (Rakic, 1988; Rakic, 1990).

It has been suggested that a disruption of communications between the centrosomes and the leading edge of the migrating neurons resulted in reduced efficiency of cell motility (Feng and Walsh, 2001; Gupta et al., 2002; Lambert de Rouvroit and Goffinet, 2001). As I discussed earlier, LIS1 localized at centrosomes, and fibroblasts isolated from *LIS1* mutant mice showed disorganization of microtubule network around the centrosome, suggesting a role for LIS1 in regulating microtubule focusing at centrosomes (Smith et al., 2000). LIS1-interacting proteins, NudE/NudEL and NudC are also localized at centrosomes (Aumais et al., 2001; Feng et al., 2000; Niethammer et al., 2000; Sasaki et al., 2000). Overexpression of LIS1-interacting fragment of NudE caused brain disorganization in *Xenopus* (Feng et al., 2000). LIS1, NudE/EL and NudC also colocalized at axonal growth cones, suggesting potential roles for these proteins at leading edge as well as at centrosomes (Aumais et al., 2001; Niethammer et al., 2000). In addition, LIS1 was indicated in regulating microtubule dynamics directly, further strengthened a role for LIS1 in modulating microtubule dynamics at centrosomes and at the leading edge during neuronal migration.

A cell division-coupled neuronal migration model was proposed when LIS1 was found to function in mitosis (Vallee et al., 2000). This model suggested that the final destination of neurons in the cortical layers is determined during the last round of the cell cycle. LIS1 was found to be involved in mitotic dynein activities including chromosome alignment and spindle orientation (Faulkner et al., 2000). Delays in mitosis of cultured mammalian cells were observed when LIS1 functions were perturbed by anti-LIS1 antibody injection or overexpression. This delay in mitosis could result in delay in the timing of neuronal differentiation, and further disrupts the orders of successive waves of neuronal migration.

An interesting observation made by F.C. Sauer in 1935 was that during cell division of neuronal progenitors, a series of oscillatory movements of the nucleus couple with the progression of cell cycle (Sauer, 1935). A series of transplantation experiments was performed to determine whether a particular cell cycle stage of an individual neuron dictated it's final destination in the neocortex (McConnell and Kaznowski, 1991). When the progenitor cells were injected with [^{3}H]thymidine during S phase and implanted into the host ventricular zone either during S or during G2/M phases, these progenitors had different fates. The S-phase implanted neurons migrated according to the fate of the host neurons, whereas the G2/M implanted neurons still migrated according to their own fate before transplantation. This suggested there was certainly a commitment step between late S and G2/M phases and this further strengthened the argument that cell cycle did play a role in neuronal migration. In addition, asymmetric cell division was found in

these cortical progenitors (Chenn and McConnell, 1995). LIS1 overexpression disrupted spindle orientation in polarized epithelial cells (Faulkner et al., 2000), this could contribute to the mitotic delay of neuronal progenitor cells (Figure 2). The *DLIS1* mutation in *Drosophila* showed a decrease in neuroblast proliferations (Liu et al., 2000), consistent with a role of LIS1 in cell division. It is unclear whether there are defects in mitoses of these mice, but the correlations between cell cycle and nuclear migration are indisputable.

Figure 2. Potential roles for LIS1 in lissencephaly formation. Diagram shows neuronal progenitor cells in the ventricular zone of the vertebrate central nervous system. Defects in neuronal distribution observed in lissencephalic brains could arise directly from changes in A, interkinetic nuclear oscillatory movement at G1/S transition; B, mitosis of neuronal progenitors, that delays due to chromosome misalignment or spindle mis-orientation caused by dosage changes of LIS1 (Faulkner et al., 2000) could result in delays in neuronal migration; C, postmitotic neuronal migration (orange) along the radial glia (blue), a potential role for LIS1 in regulating microtubule dynamics of the migrating neurons could result in mispositioning of these neurons at the wrong cortical layers. Modified after Vallee et al., 2000.

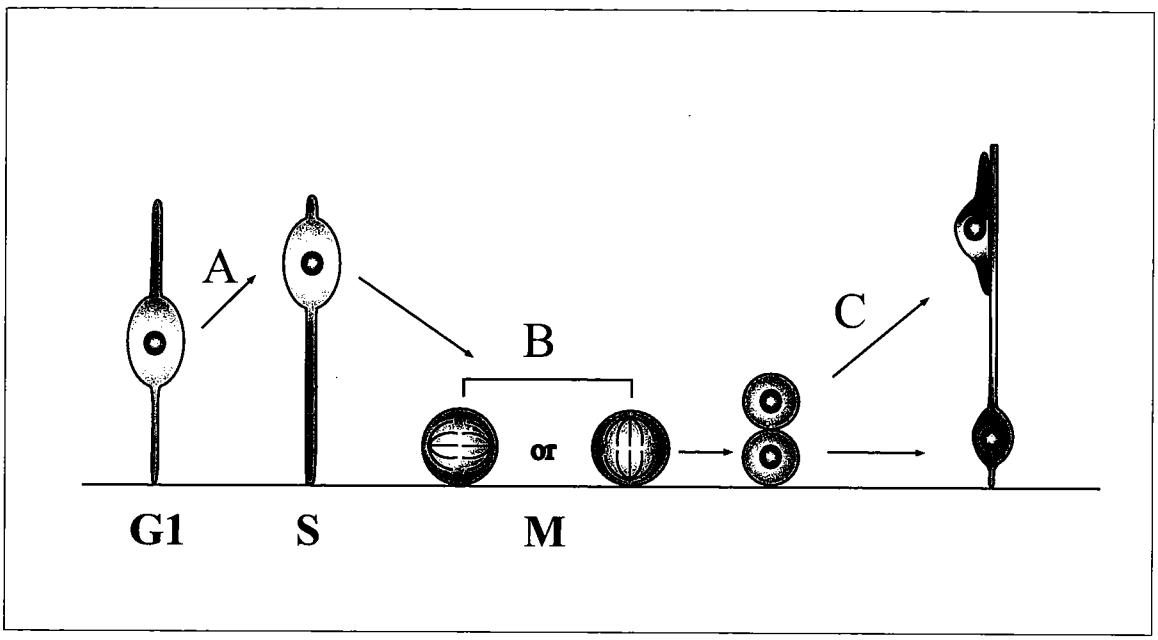
A
B
or
C
G1
S
M

CHAPTER II

ROLE OF DYNEIN, DYNACTIN, AND CLIP-170 INTERACTIONS IN LIS1 KINETOCHORE FUNCTION

Introduction

Mutations in the human LIS1 gene are responsible for the autosomal dominant brain developmental disease type I lissencephaly (Reiner et al., 1993). This condition involves gross disorganization of neurons within the cerebral cortex, and is thought to reflect a failure in normal neuronal migration during early development.

Genetic studies in lower eukaryotes have indicated that LIS1 homologues participate in dynein-mediated nuclear migration (Geiser et al., 1997; Xiang et al., 1994). In vertebrates LIS1 was initially identified as a noncatalytic subunit of brain platelet-activating factor acetylhydrolase (PAFAH) (Hattori et al., 1993). We, and others, have more recently found LIS1 to interact biochemically with cytoplasmic dynein and dynactin (Faulkner et al., 2000; Sasaki et al., 2000; Smith et al., 2000). We also obtained evidence for a role for LIS1 in vertebrate cell division, raising the possibility that the errors in neuronal distribution characteristic of lissencephaly arise from defects in the

genesis of neuronal progenitors. Overexpression of LIS1, application of LIS1 antisense oligonucleotides, and microinjection of anti-LIS1 antibody all produced potent mitotic defects, including spindle misorientation and chromosome misalignment at the metaphase plate (Faulkner et al., 2000). Consistent with a mitotic function, LIS1 localized prominently to prometaphase kinetochores and to the cell cortex of dividing vertebrate cultured cells, known binding sites for cytoplasmic dynein and its accessory complex dynactin.

The molecular relationship between dynein, dynactin and LIS1 is poorly understood. Dynein and dynactin are each large, multisubunit complexes. Dynein consists of a heavy chain (HC), responsible for ATPase activity and force production, plus a variety of accessory subunits (intermediate, light intermediate, and light chains: ICs, LICs, and LCs) implicated in binding to diverse forms of subcellular cargo (Tai et al., 2001; Tynan et al., 2000b; Vaughan and Vallee, 1995; Ye et al., 2000). Dynactin consists of a short filament of the actin-related protein Arp1 and a variety of associated polypeptides. Dynactin has been found to link dynein to the prometaphase kinetochore (Echeverri et al., 1996) and the surface of Golgi membranes (Burkhardt et al., 1997; Roghi and Allan, 1999), suggesting that it participates in dynein cargo binding. Dynactin has also been reported to stimulate dynein processivity (King and Schroer, 2000). The ICs of cytoplasmic dynein interact directly with the p150^{Glued} subunit of dynactin in *in vitro* assays (Karki and Holzbaur, 1995; Vaughan and Vallee, 1995). However, the interaction

between the two intact complexes has been observed only at very limited levels (Kini and Collins, 2001), suggesting that it is weak or regulated (Vaughan et al., 2001). LIS1 has been reported to interact with a portion of the cytoplasmic dynein heavy chain in yeast two-hybrid and coexpression/coimmunoprecipitation assays (Sasaki et al., 2000). Whether it interacts with other subunits of dynein, whether it interacts with dynactin independently, and how these interactions relate to dynein function and subcellular organization is poorly understood.

How the structural organization of LIS1 relates to its function is also poorly understood. LIS1 is predicted to consist of two distinct domains. The N-terminal 97 a.a. contains a short region of predicted coiled-coil, which has been implicated in self-association (Ahn and Morris, 2001). The C-terminal 317 a.a. contains a series of seven WD-repeats, which in the β subunit of the heterotrimeric G proteins and other polypeptides constitute a β-propeller fold (Wall et al., 1995). C-terminal deletions of LIS1 are sufficient to cause lissencephaly (Cardoso et al., 2000), indicating that the WD-repeat domain is important functionally. This region has been implicated in binding to the catalytic subunit of PAFAH
(Kitagawa et al., 2000; Niethammer et al., 2000; Sweeney et al., 2000). Whether this is its sole function, or whether it also functions in the dynein pathway is unknown. LIS1 has been reported to interact with two additional classes of protein in the dynein pathway, NudC and NudE/NudEL

(Efimov and Morris, 2000; Feng et al., 2000; Morris et al., 1998; Niethammer et al., 2000) , but their role in LIS1 function and their binding sites within LIS1 are uncertain.

We report here that LIS1 associates with kinetochores through its WD-repeat domain. Using dominant inhibitory dynactin and LIS1 constructs, we find LIS1 to be linked to the kinetochore through the motor protein complexes, rather than the reverse. We find the WD-repeat domain of LIS1 interacts with three distinct subunits of the dynein and dynactin complexes, representing both motor and cargo binding regions. Overexpression of full-length LIS1 and its WD-repeat fragment specifically displaced CLIP-170 from mitotic kinetochores. Together, these results suggest a direct role for LIS1 in novel forms of dynein/dynactin regulation.

Materials and Methods

Mammalian expression constructs

Most of the heavy chain tagged constructs are described elsewhere (Gee et al., 1997; Mazumdar et al., 1996), except N907C1138myc, N1141C1405flag, N1406C1669flag, N1670C1873flag, N1874C2124flag and N1874C2124^{K1910E}flag constructs, which were made by adding a NotI site, a Kozak consensus sequence, myc tag or flag tag at the appropriate location by polymerase chain reaction (PCR) using VENT DNA polymerase (New England Biolabs, Beverly, MA), then cloned into the NotI site of pCMVβ (Clontech, Palo Alto, CA). LIS1 fragments were created by applying the similar strategy with a HA tag added at the N-terminus of each fragment. The N-terminal 87 amino acids of LIS1 was used as the N-terminal construct, 88 to 414 amino acids was used as the WD-repeat domain construct, and an internal deletion of 51 to 78 amino acids of LIS1 was used as the Coiled-coil deletion construct. Dynein intermediate chain, light intermediate chain constructs are described previously (Tynan et al., 2000b; Vaughan and Vallee, 1995), and light chain constructs were obtained from Dr. Stephen King at the University of Connecticut Health Center, Farmington, CT. Non-tagged p150^{Glued} (Vaughan and Vallee, 1995), dynamitin (Echeverri et al., 1996), Arp1 (Clark and Meyer, 1999) and p62-myc (Garces et al., 1999) are described elsewhere. *myc* tagged dynamitin fragment constructs are described previously (Echeverri, Ph. D. thesis). All PCR-amplified constructs were sequenced

confirmed by the Nucleic Acid Facility located at the University of Massachusetts Medical School.

Antibodies

Anti-myc polyclonal antibody has been described elsewhere (Gee et al., 1997); anti-HA polyclonal and monoclonal and anti-myc monoclonal antibodies were purchased from Covance (Richmond, VA). Anti-LIS1 monoclonal antibody was provided by Dr. Orly Reiner (Weizmann Institute, Rohovot, Isreal) and has been characterized previously (Faulkner et al., 2000); anti-CLIP-170 monoclonal antibody was provided by Dr. Holly Goodson (University of Norte Dame, IN); anti-tubulin monoclonal antibody was from Amersham Pharmacia Biotech (clone DM1A, Piscataway, NJ). Antibodies against Bub1, BubR1 and CENP-E were provided by Dr. Tim Yen (Fox Chase Cancer Center, PA), anti-Mad2 antibody was provided by Drs. Bonnie Howell and Edward Salmon (University of North Carolina, NC). Anti-dynein IC antibody was purchased from Chemicon (Temecula, CA). Secondary horseradish peroxidase-conjugated donkey anti-mouse and anti-rabbit antibodies were purchased from Jackson Immunoresearch Laboratories, Inc. (West Grove, PA). For immunofluorescence, Cy3-conjugated donkey anti-mouse and anti-rabbit antibodies were purchased from Jackson Immunoresearch Laboratories and Alexa 488 anti-mouse and anti-rabbit antibodies were purchased from Molecular Probe (Eugene, OR).

Cell culture and transfection

COS-7, HeLa cells were grown in Dulbecco's modified Eagle's medium with 10% fetal bovine serum and penicillin/streptomycin (GIBCO Invitrogen Corp., Carlsbad, CA). For transient transfection, cells were plated either in a 10-cm petridish or onto 18mm coverslips, grown to 70 to 80% confluencies, then transfected with the appropriate amount of DNA mixed with lipofectAMINE (for 10-cm dish) and lipofectAMINE PLUS (for coverslips) (GIBCO Invitrogen Corp.). Transient expression was allowed for 40 to 48 hours.

Immunoprecipitation

Co-immunocprecipitation procedure is described previously (Tynan et al., 2000b). COS-7 cells were transfected with plasmid DNA purified from either Qiagen Maxiprep or QIAprep Spin miniprep kits (Qiagen, Valencia, CA) with LipofectAMINE reagents for overnight at 37^0C. Forty-eight hours after the addition of DNA/liposome mixture, cells were washed twice with PBS and lysed with modified RIPA buffer (100mM NaCl, 1mM EGTA, 50mM Tris, pH8.0, 1% IGEPAL CA-630) with freshly added protease inhibitor mixture: 2ug/ml of aprotinin, leupeptin (Sigma, St. Louis, MO) and 1mM of AEBSF (Roche Molecular Biochemicals, Indianapolis, IN). Cells then were incubated on ice for 20 min and spun at 13,000rpm for 10 min in a microfuge. Protein G beads (Amersham Biosciences) or flag M2 affinity resin (Sigma) were used for all immunoprecipitations. Extracts were mixed with RIPA-washed beads and incubated at 4^0C overnight with gentle rotation. Beads then were washed three time with RIPA at room temperature 10 min each and boiled in 5x SDS-PAGE sample buffer for 5 min. The entire eluate with 4% of

supernatant were loaded into 5-15% SDS-polyacrylamide gel and transferred onto Immobilon-P membrane (Millipore Corp., Bedford, MA). Immunoblotting was performed with various antibodies against tags or specific proteins.

Yeast two-hybrid assay

The LexA-based two-hybrid assay (Gyuris et al., 1993) was used to assess interactions between LIS1 fragments and various dynein/dynactin subunits including: IC2C, dynamitin, HC N547C649, HC N748C907 and HC N1874C2124. All LIS1 fragments were cloned into the pEG202 bait vector by PCR and tested for auto-activation of the reporter. LIS1 N bait construct activated reporter in the absence of prey and was omitted in the two-hybrid assay. IC2C, dynamitin and HC fragments were cloned into pJG4-5 prey vector by PCR. Interactions were scored by using the β-gal filter assay.

Immunofluorescence Microscopy

For kinetochore staining, cells were either extracted with 0.5% (Fig. 2 and 3) or 0.01% Triton X-100 (Fig. 5B)(Sigma) for 1 min or without the extraction (Fig. 4A) and fixed in 3% paraformaldehyde (EMS, Ft. Washington, PA) in PHEM buffer (120mM PIPES, 50mM HEPES, 20mM EGTA and 4mM Magnesium acetate, pH6.9) for 20 min at room temperature. Cells then were permeabilized with -20^{0}C methanol for 4 min. All primary and secondary antibodies incubation were performed at 37^{0}C for one hour. After all antibody incubations, cells were incubated with 0.1ug/ml of DAPI (Sigma) for 10 min before mounting with Prolong Antifade solution (Molecular Probe).

Immunofluorescence images were obtained by using Leica DM IRBE microscope equipped with Hamamatsu ORCA 100 CCD camera and processed by MetaMorph software (Universal Imaging Group). Confocal microscopy was carried out with a Nikon Diaphot 200 microscope using BioRad MRC1000 system with a Kr/Ar laser. Each image was obtained from the total projection (20-24 stacks, 0.3μm per step), and background subtraction was processed by the MetaMorph, pseudocolored and cropped by Adobe Photoshop 5.5 and Corel DRAW 9.0.

Results

Phenotypic Effects of LIS1 Fragments

Previous work from this lab implicated LIS1 in mitotic chromosome alignment and spindle orientation (Faulkner et al., 2000). In order to determine which portion of the LIS1 molecule is involved in these activities, we constructed two cDNAs encoding HA-tagged fragments of LIS1 corresponding to the N-terminal 87 a. a. comparable to the 89 a. a. product resulting from a known disease-causing deletion (Cardoso et al., 2000), and the C-terminal 327 a.a. respectively (Fig. 1A). The N-terminal fragment contains a 28 a.a. predicted coiled-coil domain, whereas the C-terminal fragment contains seven WD-repeat motifs. To our surprise, overexpression of each fragment produced a dramatic increase in mitotic index comparable to that observed with full-length LIS1 (Fig. 1B and C), with a greater number of multipolar spindles and more dramatic disruption of spindle organization (Fig. 1B). The more severe phenotype is reminiscent of that produced by overexpression of the dynamitin subunit of dynactin (Echeverri et al., 1996). However, as reported previously for full-length LIS1 (Faulkner et al., 2000), and unlike dynamitin, no effect on Golgi morphology was detectable with the LIS1 fragments (data not shown).

Figure 1. Phenotypic analysis of LIS1 fragments. (A) Schematic diagram of LIS1 domains, showing a predicted coiled-coil region (filled box) from a. a. 51 to 78 and a series of seven WD repeats (shaded boxes) between a. a. 97 and 408. (B) Effects of overexpression of LIS1 fragments on mitotic spindle morphology. Spindle defects (untransfected, 4%; LIS1 FL, 36%; LIS1 WD, 65.4%; LIS1 N, 61.2%) including multiple spindle poles, detached pole and unfocused poles. (C) Perturbation of mitosis by LIS1 fragment overexpression. Cell cycle stage was scored for nontransfected control cells (control), and cells overexpressing full-length LIS1 (Ox LIS1 FL), and the N– and C-terminal fragments (Ox LIS1 N, Ox LIS1 WD). I, interphase; PM, prometaphase, M, metaphase, A, anaphase, T, telophase. Full-length, – and C-terminal fragments all produced similar pronounced increases dramatic increases in mitosis. Values are means ± standard deviation from four independent experiments with ~ 2000 total cells counted in each case.

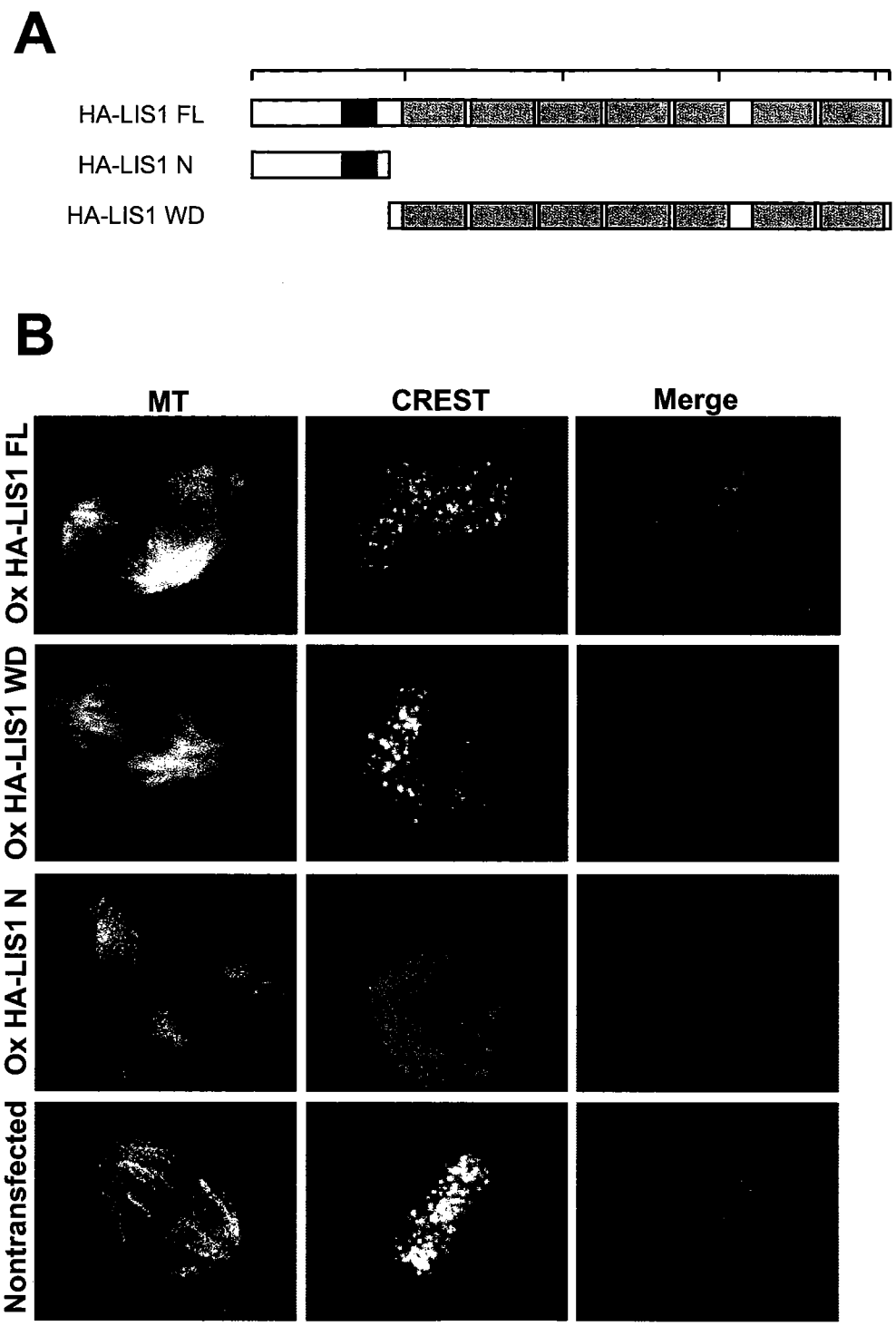
A
HA-LIS1 FL
HA-LIS1 N
HA-LIS1 WD
B
MT
CREST
Merge
Ox HA-LIS1 FL
Ox HA-LIS1 WD
Ox HA-LIS1 N
Nontransfected

C

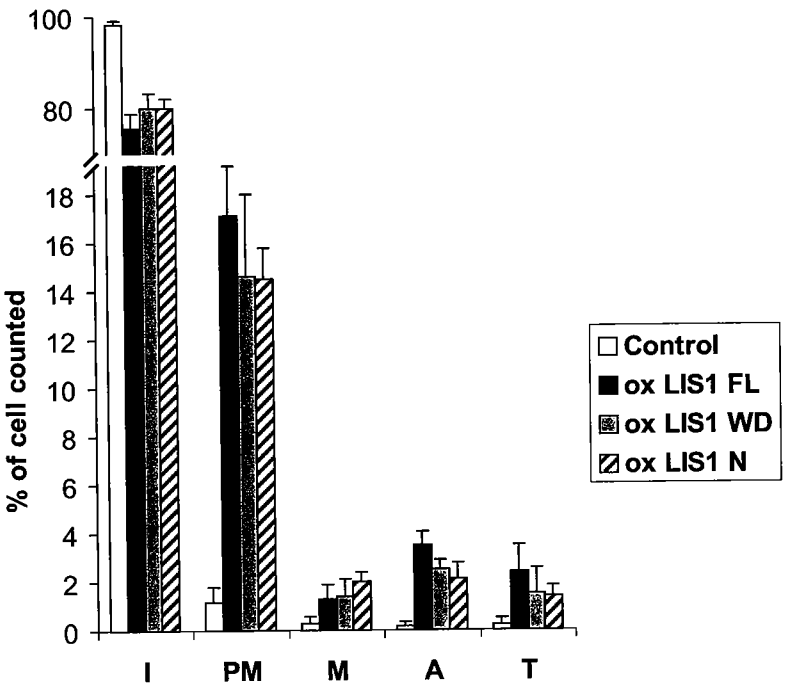
100
80
18
16
14
12
10
8
6
4
2
0
% of cell counted
I
PM
M
A
T
Control
ox LIS1 FL
ox LIS1 WD
ox LIS1 N

To gain insight into the manner in which the individual fragments produced these effects, we examined their ability to associate with prometaphase kinetochores, a site at which we had previously observed endogenous LIS1 using immunofluorescence microscopy (Faulkner et al., 2000). We also treated cells with nocodazole, which allows outer kinetochore components to accumulate above their normal levels (Echeverri et al., 1996; Hoffman et al., 2001; King et al., 2000). Full-length HA-tagged LIS1 exhibited dramatic localization to prometaphase kinetochores identified by co-staining with CREST antiserum in both COS-7 (Fig. 2A upper row) and HeLa cells (data not shown), adding strong support to the identification of LIS1 as a kinetochore component. Within the kinetochore LIS1 staining was slightly peripheral to the CREST signal, consistent with outer kinetochore localization. In cells exposed to nocodazole for prolonged periods, (see below) LIS1 exhibited an elongated crescent shape as observed for dynein and other outer kinetochore components (Echeverri et al., 1996; Hoffman et al., 2001; King et al., 2000). Clear kinetochore localization was also observed with the WD-repeat fragment of LIS1 alone. This effect was more pronounced in nocodazole-treated cells (Fig. 2A middle row), but was also readily observed in untreated cells (Fig. 2B). In contrast, specific localization of the N-terminal LIS1 fragment was not generally observed (Fig. 2A lower row), though very weak kinetochore staining could be detected in occasional cells (data not shown). Together, these results indicate that the WD-repeat domain of LIS1 is sufficient for kinetochore targeting.

Figure 2. Kinetochore localization of LIS1 fragments. (A) Transfected COS-7 cells were treated with nocodazole before fixation for immunofluorescence. Cells were triple labeled for LIS1 and its fragments using anti-HA monoclonal antibody (green); inner kinetochore antigens using CREST human autoimmune antiserum (red); and DNA using DAPI (blue). (B) Kinetochore localization in non-nocodazole treated cell. Merged images of DNA (blue) and anti-HA antibody labeled LIS1 signals (green) in COS-7 cells transfected with either HA-LIS1 FL or HA-LIS1 WD constructs. Bars: 5μm.

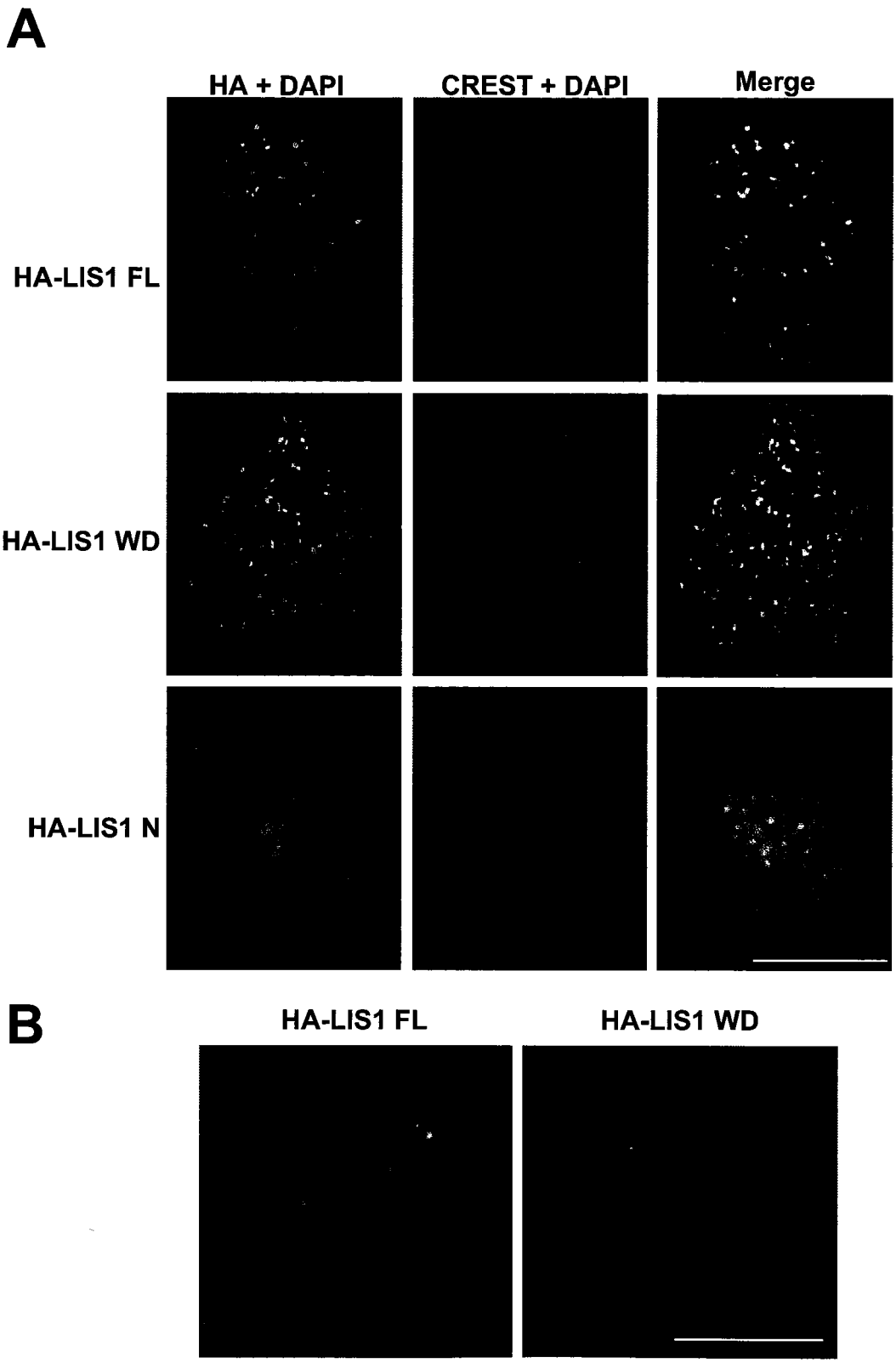
A
HA + DAPI
CREST + DAPI
Merge
HA-LIS1 FL
HA-LIS1 WD
HA-LIS1 N
B
HA-LIS1 FL
HA-LIS1 WD

Hierarchy of LIS1 interactions at the kinetochore

Despite this difference in behavior, the two fragments produce phenotypes of comparable severity (see above). The N-terminus of the LIS1-related *Aspergillus* protein NudF has been implicated in self-association (Ahn and Morris, 2001), raising the possibility that the corresponding portion of LIS1 might interact with the endogenous full-length protein and interfere with its behavior. In coexpression experiments, we observed the N-terminal fragment to coimmunoprecipitate with itself and full-length LIS1, but not with the WD region (Fig. 3A). In contrast to previous results with *NudF*, removal of the predicted coiled-coil had no effect on self-association, suggesting that the entire N-terminal domain participates in this activity. To determine whether the N-terminal domain can displace the endogenous wild-type protein from kinetochores we examined cells overexpressing the N-terminal construct for endogenous LIS1 staining. For this purpose we used a monoclonal antibody (Sapir et al., 1997), which we determined to react with the WD-repeat region of LIS1 (Fig. 3B). In high expressers, the endogenous LIS1 kinetochore staining was, indeed, dramatically reduced (Fig. 3C, right column).

Figure 3. Effects of LIS1 fragments on kinetochore composition. (A) Self-association of LIS1 N-terminal fragment. myc-tagged LIS1 full-length cDNA was co-expressed with different HA-tagged LIS1 fragments (Fig. 1) and HA-tagged LIS1 coiled-coil deletion construct (HA-LIS1 ΔC-C), and anti-HA immunoprecipitates were immunoblotted with anti-myc antibody. Clear co-immunoprecipitation was observed only between constructs including the N-terminal region of LIS1. (B) Specificity of LIS1 monoclonal antibody for WD-repeat region. COS-7 cells were transfected with HA-tagged LIS1 constructs. Cell lysates were loaded into 5-15% gradient gel and analyzed by immunoblotting with anti-HA monoclonal antibody, which recognized all LIS1 constructs and monoclonal anti-LIS1 (Faulkner et al., 2000; Sapir et al., 1997). The latter recognized endogenous and full-length HA-LIS1 (arrow), as well as the slightly smaller WD-repeat fragment, but not the 10kD LIS1 N-terminal fragment (open arrow head). (C) Effect of LIS1 N on endogenous LIS1 localization. In contrast to nontransfected cells, endogenous LIS1 protein detected with the LIS1 monoclonal antibody was displaced from kinetochores by LIS1 N overexpression. (D) Effect of LIS1 N and LIS1 WD on endogenous dynein IC localization. Dynein staining at the kinetochore persisted in cells overexpressing either fragment. Bars: 5μm.

A

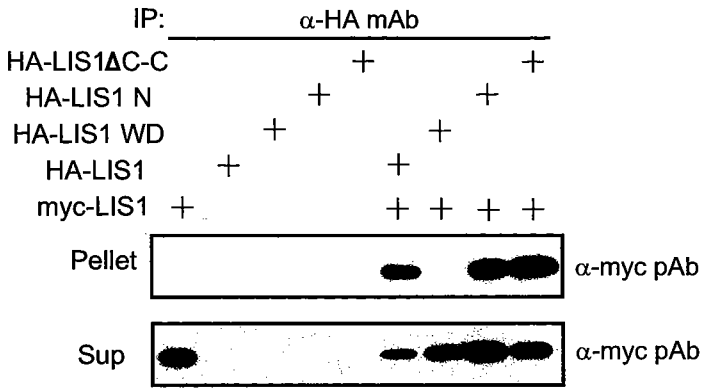
IP:
α-HA mAb
HA-LIS1ΔC-C
HA-LIS1 N
HA-LIS1 WD
HA-LIS1
myc-LIS1
Pellet
α-myc pAb
Sup
α-myc pAb

B

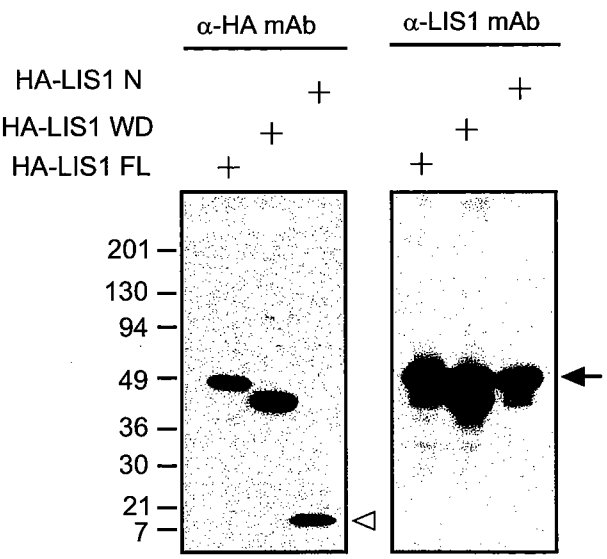
α-HA mAb
α-LIS1 mAb
HA-LIS1 N
HA-LIS1 WD
HA-LIS1 FL
201
130
94
49
36
30
21
7

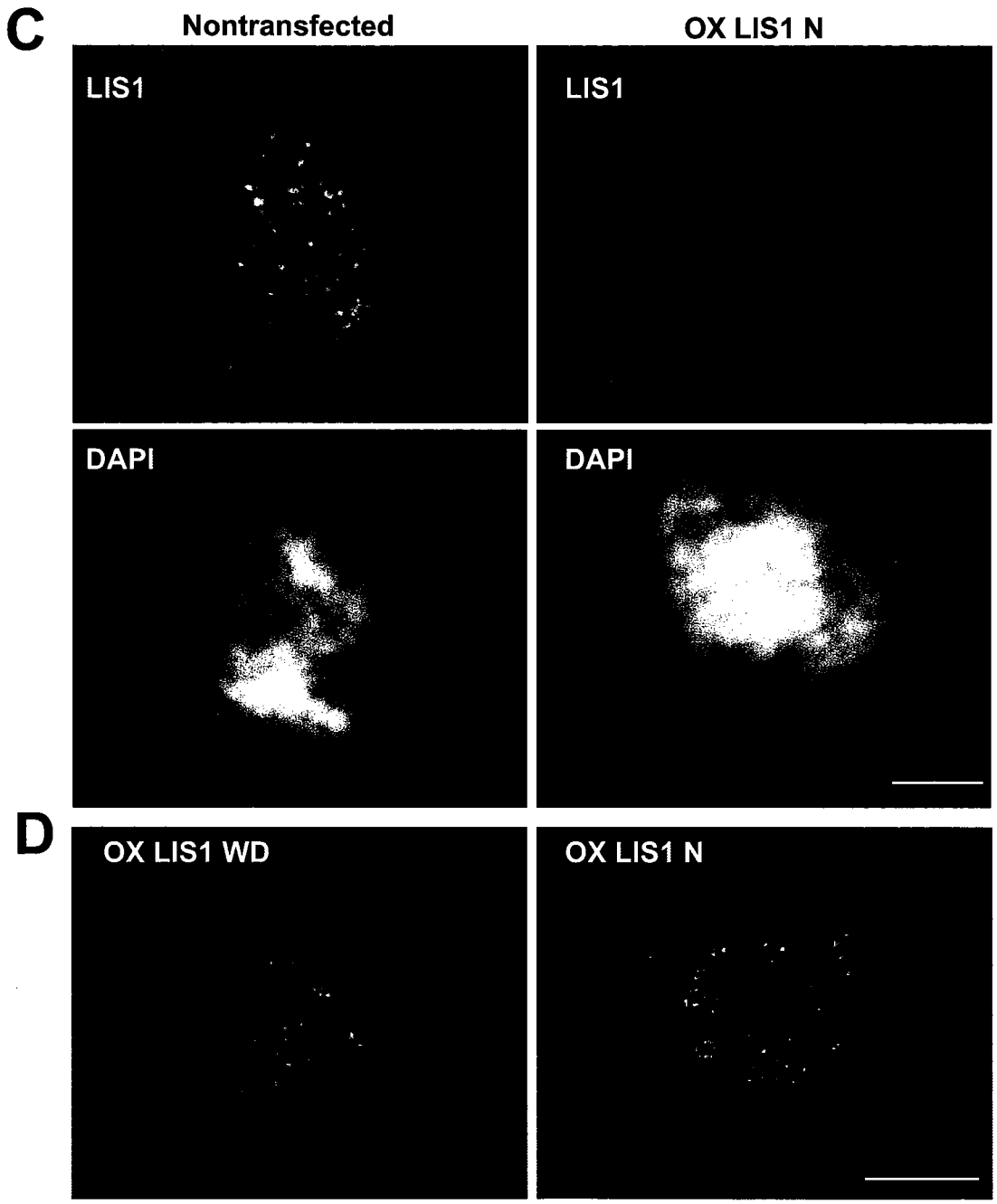
C
Nontransfected
OX LIS1 N
LIS1
LIS1
DAPI
DAPI
D
OX LIS1 WD
OX LIS1 N

We previously reported that dynein and dynactin remain at the prometaphase kinetochore in LIS1 overexpressing cells (Faulkner et al., 2000), though our current data (Fig. 2) indicate that the full-length epitope-tagged LIS1 protein occupies the kinetochore under these conditions. To test the effects of removing endogenous LIS1 from this site, we overexpressed the N-terminal LIS1 fragment. Again, no effect on the dynein (Fig. 3D) and dynactin (data not shown) signals was observed in cells overexpressing LIS1 fragment *vs.* untransfected cells (data not shown).

To test whether LIS1 displaced other kinetochore proteins, we stained cells overexpressing full-length LIS1, and the N– and WD-repeat fragments with antibodies against CENP-E, CENP-F, Bub1, BubR1, Mad2, and CLIP-170. No effect was observed except in the case of CLIP-170, which was completely displaced by the full-length and WD-repeat LIS1 constructs (Fig. 4 and data not shown).

Figure 4. Displacement of CLIP-170 by overexpression of LIS1 fragments. HeLa cells were transfected with LIS1 constructs and treated with 10μM nocodazole for 1 hr prior to fixation for immunofluorescence. (A) CLIP-170 staining in LIS1 overexpressers. Both LIS1 FL and WD constructs clearly displaced CLIP-170 from kinetochores, whereas the LIS1 N-terminal fragment had no effect. (B) CENP-E staining in LIS1 overexpressers. CENP-E kinetochore signals were not unaffected by the overexpression of any of the LIS1 constructs. Bars: 10μm.

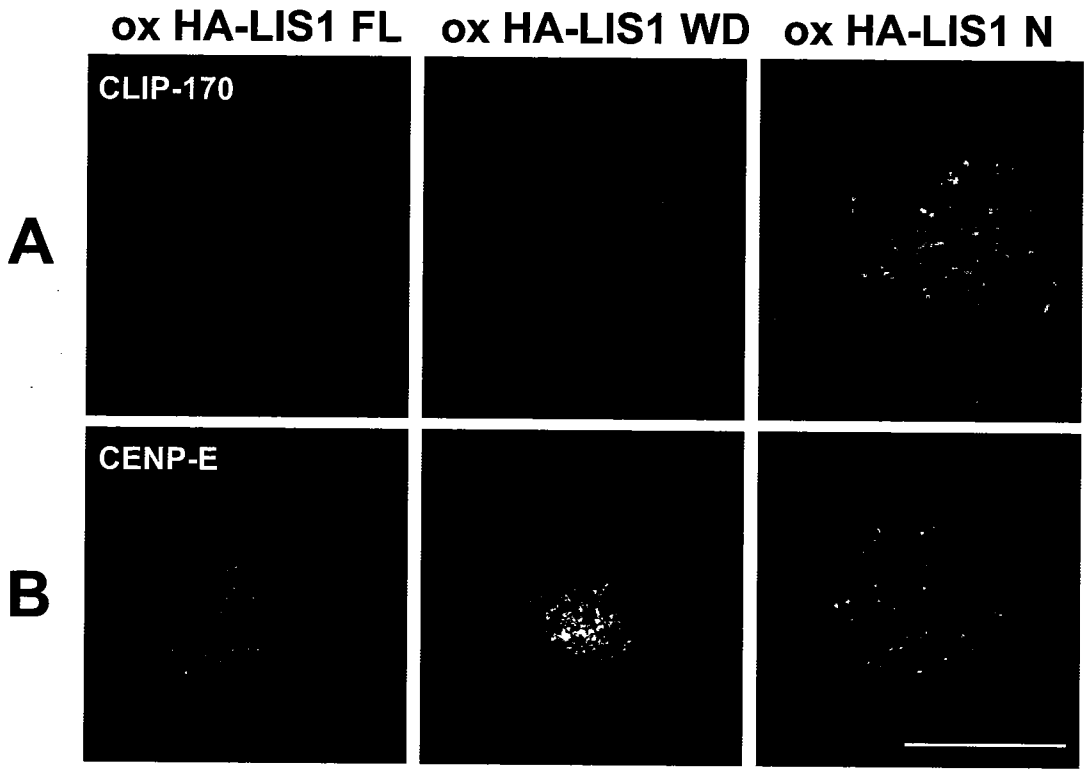
ox HA-LIS1 FL
ox HA-LIS1 WD
ox HA-LIS1 N
CLIP-170
A
CENP-E
B

To test whether LIS1 requires dynein/dynactin for kinetochore binding, we overexpressed the dynamitin subunit of dynactin, which dissociates dynactin into smaller subcomplexes and releases dynein from the kinetochore (Echeverri et al., 1996). We now find that epitope-tagged dynamitin persists at the kinetochore under these conditions (Fig. 5A). This behavior suggests an additional effect of dynamitin overexpression, competition for binding to the dynein/dynactin anchoring protein ZW10 (Starr et al., 1998). As expected, Arp1, a dynactin subunit, was displaced from the kinetochore (Fig. 5B upper-left panel). The LIS1 signal was also greatly diminished (Fig. 5B upper-right panel). Together, our data indicate that the localization of LIS1 to the kinetochore requires dynein and dynactin rather than the reverse.

Figure 5. Displacement of LIS1 by dynamitin overexpression. (A) Confocal images of COS-7 cells transfected with dynamitin-myc stained with polyclonal anti-myc antibody (green) and CREST human autoantiserum. In addition to its disruptive effect on the dynactin complex, overexpressed dynamitin associates with kinetochores. (B) Nocodazole-treated COS-7 cells transfected with dynamitin-GFP and stained with anti-Arp1, anti-LIS1, and DAPI. Arp1 and LIS1 were clearly reduced. Bars: 10μm.

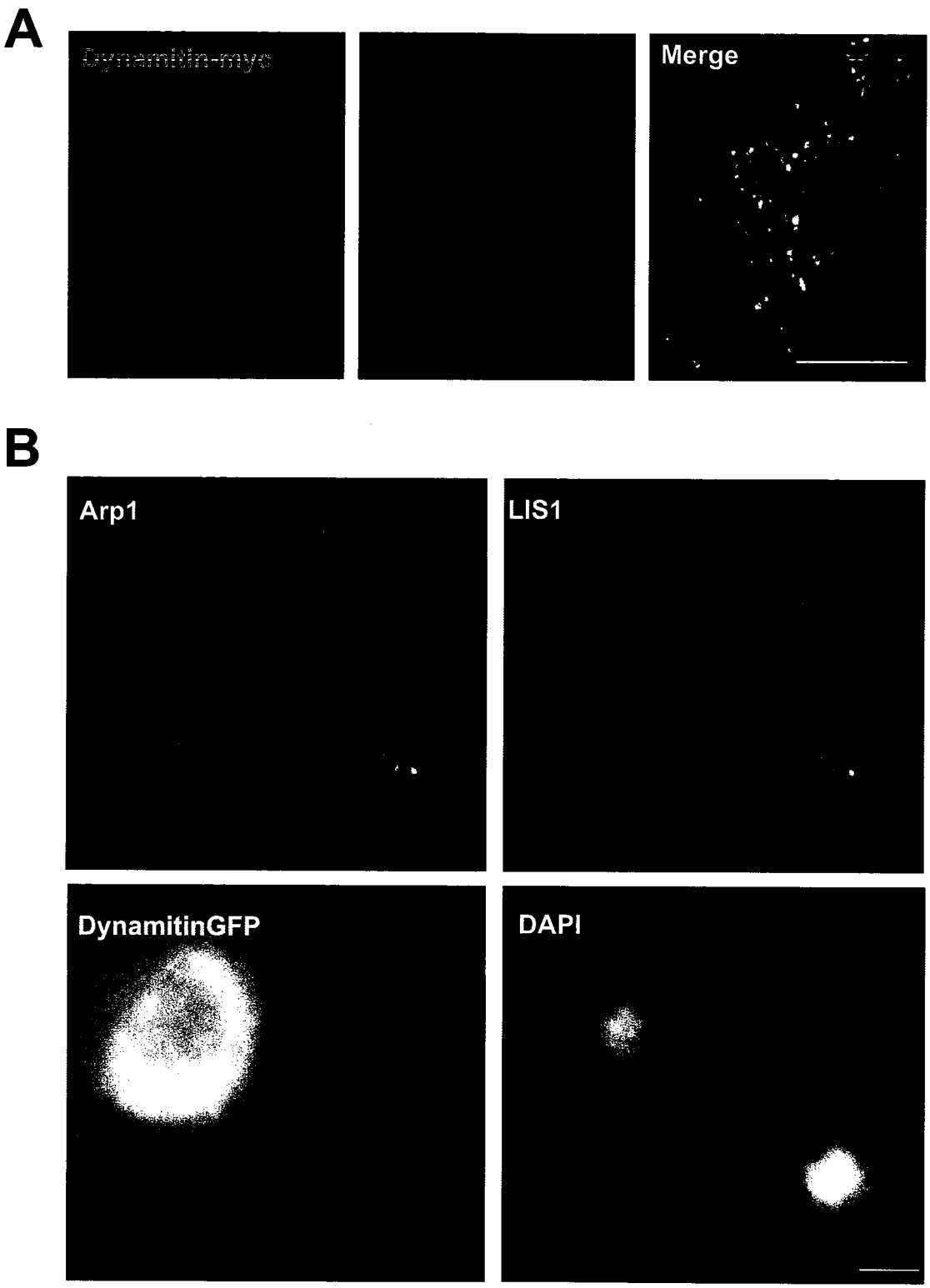
A
Dynamitin-myc
Merge
B
Arp1
LIS1
DynamitinGFP
DAPI

LIS1 interacts through its WD-repeat domain with multiple sites in dynein and dynactin

The dependence of LIS1 kinetochore targeting on dynein and dynactin supports a physiological interaction with the two complexes. To define the molecular basis for these interactions further, we explored whether LIS1 can interact with subunits in each complex. LIS1 was coexpressed with cytoplasmic dynein and dynactin subunits, and interactions were assessed by coimmunoprecipitation.

Both the heavy and intermediate chains of cytoplasmic dynein coimmunoprecipitated with LIS1, as did the dynamitin subunit of dynactin (Fig. 6A). Light intermediate chains (LIC1 and LIC2) and light chains (Tctex-1, RP3 and LC8) of the dynein complex, and the p150^{Glued}, Arp1 and p62 subunits of the dynactin complex were all negative in this assay. These results indicate that LIS1 interacts with each complex independently and, in the case of cytoplasmic dynein, through multiple subunit interactions. We also examined these interactions by immunoprecipitation from the [^{35}S] methionine labeled total cell extract. In each case (HC, IC2C, dynamitin), LIS1 was the major non-dynein/dynactin polypeptide pulled down, with minor background bands also visible (data not shown).

Figure 6. Interaction of LIS1 with multiple dynein and dynactin subunits. (A) Coimmunoprecipitation of LIS1 with dynein and dynactin subunits. Full-length HA- or myc-LIS1 was co-transfected with HC-FLAG, IC2C-myc, LIC2-FLAG, LC8-VSVG, Tctex-1-HA, RP3-HA,p150^{Glued}, dynamitin, Arp1 and p62-myc. Immunoprecipitation was performed with anti-HA or anti-myc antibody and blotted with antibodies against the epitope tag of individual dynein subunit, or anti-p150^{Glued}, anti-dynamitin, anti-Arp1. Interactions were observed with the dynein HC and IC, and dynamitin. IC1A was also positive in this assay (not shown). (B) Two-hybrid assay of LIS1 with dynamitin, HC and IC. LIS1 fragments were cloned into the LexA-based bait vector and full-length dynamitin, IC2C, HC N547C649, HC N748C907 and HC N1874C2124 fragments (Fig. 8) were cloned into the prey vector. Dynamitin, IC, HC N748C907 and HC N1874C2124 were all positive in this assay. The negative HC fragment (HC N547C649) was also negative in the coimmunoprecipitation assay (Fig. 9).

A

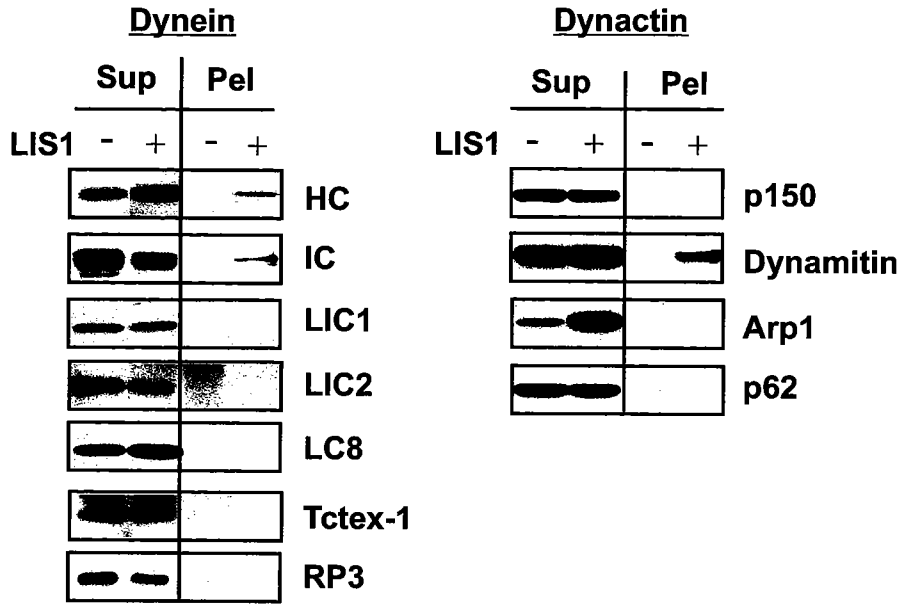

B

Two-hybrid prey clones	Two-hybrid bait clones	
	LIS1 FL	LIS1 WD
Dynamitin	++	++
IC	+	+
HC N547C649	–	–
HC N748C907	+	+
HC N1874C2124	+	+

We also used the yeast two-hybrid assay as a further test for interaction specificity. A positive reaction was observed between LIS1 and the cytoplasmic dynein heavy and intermediate chains, and dynamitin (Fig. 6B). In the case of the heavy chain, three fragments were analyzed for interactions. Only HC N649C907 and HC N1874C2124 showed positive reactions, whereas HC N547C649 did not (see next section for further detail). Thus, together our data support a direct interaction between LIS1 and each of three distinct dynein and dynactin subunits.

To gain further insight into the molecular basis for the observed interactions, we tested which region of LIS1 is involved. No interaction was detected using the N-terminal region of LIS1. Instead, each of the LIS1 interacting subunits coimmunoprecipitated with the WD-repeat domain of LIS1 alone (Fig. 7). These results are consistent with a role for the WD-repeat domain in linking LIS1 to the kinetochore through dynein and dynactin (see above).

Figure 7. WD-repeat domain of LIS1 mediates dynein and dynactin subunit interactions. COS-7 cells were singly- or doubly-transfected with HA-LIS1 FL, HA-LIS1 WD, HA-LIS1 N, *vs.* (A) IC2C-myc; (B) dynamitin-myc; and (C) HC-C1140-myc (D) HC-N1874C2124-FLAG constructs. Immunoprecipitations were performed by using (A and B) anti-*myc* antibody or (C) anti-HA antibody or (D) FLAG M2 beads. The immunoprecipitates (right panels) were immunoblotted with either anti-myc antibody (A) or (B and C) anti-HA antibody. Supernatants (left panels) were used to monitor protein expression. Each dynein and dynactin subunit immunoprecipitated with HA-LIS1 FL and HA-LIS1 WD, but not with HA-LIS1 N.

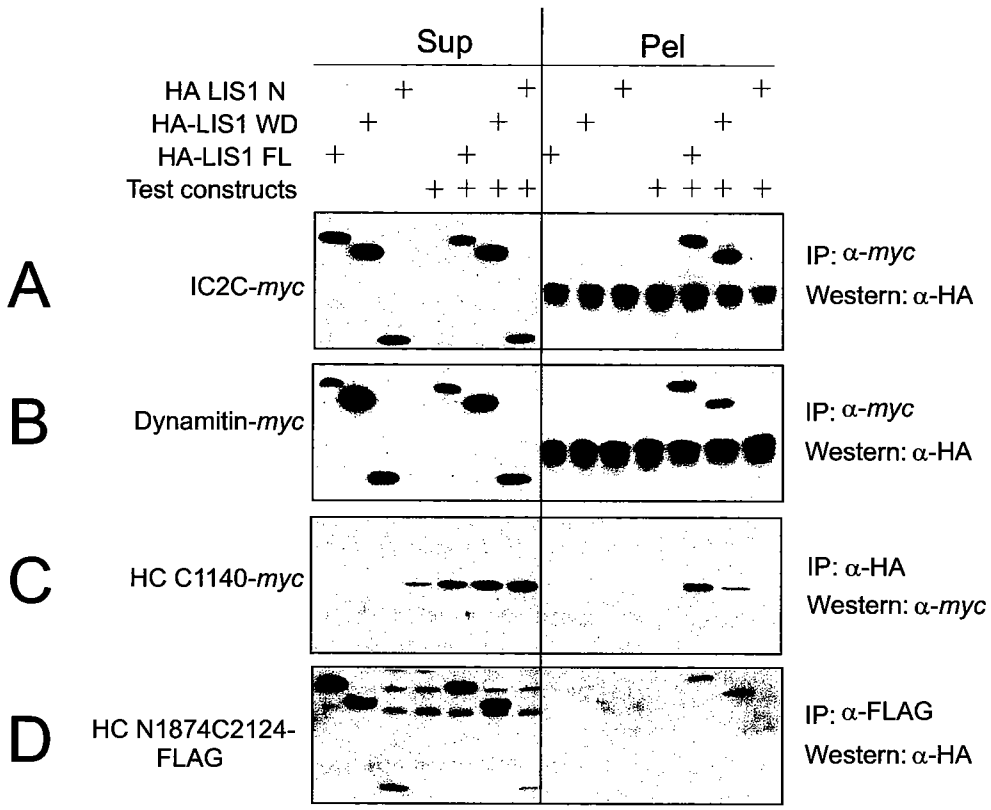
Sup
Pel
HA LIS1 N
HA-LIS1 WD
HA-LIS1 FL
Test constructs
A
IC2C-myc
IP: α-myc
Western: α-HA
B
Dynamitin-myc
IP: α-myc
Western: α-HA
C
HC C1140-myc
IP: α-HA
Western: α-myc
D
HC N1874C2124-FLAG
IP: α-FLAG
Western: α-HA

LIS1-binding domain of dynamitin differs from the ZW-10 interacting domain

The 121-143 a.a. of dynamitin has been demonstrated by a yeast two-hybrid assay to interact with ZW10, and this interaction was essential for dynactin kinetochore targeting (Starr et al., 1998). Overexpression of dynamitin displaced LIS1 from the kinetochore (Fig. 5). LIS1 was found to interact with dynamitin via its WD-repeat domain (Fig. 7). The mapping of LIS1-interacting domain of dynamitin should provide new insight into the detailed protein-protein interactions at the kinetochore.

Dynamitin consists of several domains: a helix-turn-helix (HTH) domain overlapped with a coiled-coil domain, two other coiled-coil domains located at the downstream of the HTH domain (Fig. 8A; Echeverri et al., 1996). A series of *myc*-tagged dynamitin fragment constructs cooverexpressed and coimmunoprecipitated with HA tagged LIS1 full-length construct in COS-7 cells (Fig. 8B). The 218-311 a.a. region of dynamitin (p50N218C311myc) provided the optimal binding for LIS1. Reduced interaction was observed when LIS1 immunoprecipitated with the dynamitin fragment lacking the 251-311 a.a. (p50C251myc). Two proline residues were inserted separately to disrupt each of the two coiled-coil domains of dynamitin (p50L236Pmyc and p50V295Pmyc), and they did not affect the interactions. These results indicated that the two coiled-coil domains at the C-terminus of dynamitin were responsible for the interaction of LIS1.

Figure 8. LIS1 binds to the C-terminal region of dynamitin. The HA-LIS1 FL construct was cotransfected with myc-tagged dynamitin (p50) constructs in COS-7 cells. Immunoprecipitates of myc-tagged dynamitin fragments were blotted for HA-LIS1. (A) Schematic representation of dynamitin at top with three predicted coiled-coil domains (gray), and a helix-turn-helix motif (transparent blue) overlapped with the first coiled-coil domain (Echeverri et al, 1996). Filled bars represent positive interactions with LIS1, and open bars represent negative interactions. (B) Anti-HA immunoblots of dynamitin fragment immunoprecipitates showing LIS1.

A

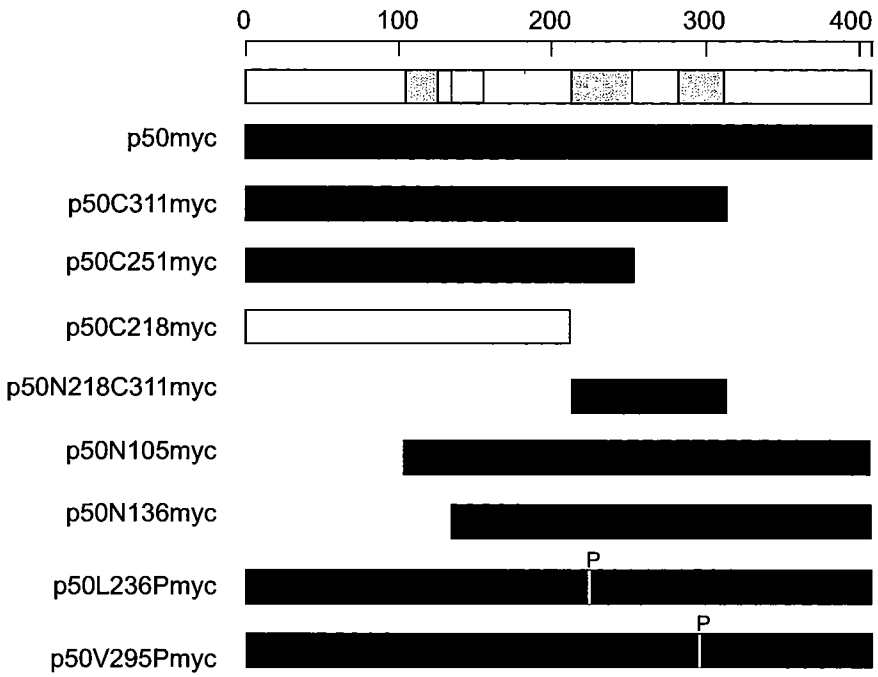
0
100
200
300
400
p50myc
p50C311myc
p50C251myc
p50C218myc
p50N218C311myc
p50N105myc
p50N136myc
P
p50L236Pmyc
P
p50V295Pmyc

B

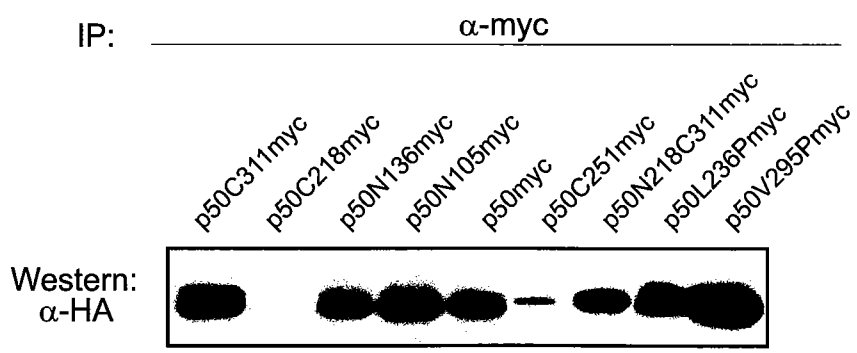
IP:
α-myc
p50C311myc
p50C218myc
p50N136myc
p50N105myc
p50myc
p50C251myc
p50N218C311myc
p50L236Pmyc
p50V295Pmyc
Western:
α-HA

Two distinct sites of heavy chain interact with LIS1

The dynein heavy chain consists of two major functional regions. The N-terminal 1100-1300 a.a. are thought to constitute the "stem" of the molecule, and contain the known sites for interaction with the cargo-binding ICs, LICs, and LCs (Habura et al., 1999; Mok et al., 2001; Tynan et al., 2000a). The remainder of the molecule represents the motor domain. The site for microtubule binding is located at the tip of a projecting stalk (a.a. 3160-3506)(Gee et al., 1997), which resides within a series of recently predicted AAA ATPase domains (Neuwald et al., 1999). Photocleavage (Gibbons and Gibbons, 1987) or mutation (Gee et al., 1997) of the P-loop of the first AAA domain abolishes ATPase activity, implicating this site most clearly in ATP hydrolysis and force production.

The identity of the site within the HC with which LIS1 interacts should provide important insight into LIS1 function. To investigate this issue systematically we coexpressed LIS1 with a series of motor domain and stem fragments and subfragments (Fig. 9). Surprisingly, clear binding was observed with HC fragments corresponding to each major domain (e. g., N1137flag corresponding to the entire motor domain; C1140myc corresponding to the stem domain). Analysis of subfragments of the motor domain indicated that one LIS1 binding site is located toward the N-terminus of this region. During the course of this study a LIS1-binding fragment from the same region encompassing part, but not all, of the first two AAA domains was also identified in a

yeast two-hybrid screen (Sasaki et al., 2000). Recently, the same fragment was also found to interact with the *Aspergillus* LIS1 homologue, NUDF (Hoffmann et al., 2001). To determine whether the LIS1 binding site corresponded to a predicted HC functional domain we designed a fragment (N1874C2124flag) corresponding to the boundaries of the first AAA repeat (Neuwald et al., 1999). Clear binding with LIS1 was observed. To determine whether LIS1 binding is affected by ATP binding state, full-length HC and AAA domain constructs containing K to E mutations in the first P-loop element were tested (Fig. 9A, B: K1910Eflag; N1874C2124^{K1910E}flag). No effect on LIS1 binding was detected, indicating that the LIS1-heavy chain interaction does not require a functional ATPase site.

LIS1 also bound to a single discrete site within the stem region close to the binding sites for the other dynein accessory subunits (Fig. 9A, C; and *cf.* Fig. 6B). This site was independent of that for IC binding, and overlapped with that for LIC binding. To test whether LIS1 competes with the LICs for HC binding, we immunoprecipitated the LICs. LIS1 was present in the precipitates (data not shown), indicating that LIS1 and the LICs can coexist within the same dynein complex.

Figure 9. Two distinct sites of HC interact with LIS1. The HA-LIS1 FL construct was cotransfected with myc-tagged dynein stem-region and FLAG tagged motor-domain constructs. HC fragment immunoprecipitates were immunoblotted for HA-LIS1. (A) Diagrammatic representation of dynein heavy chain at top, showing IC- (orange) LIC- (yellow) and HC-HC (green) interaction sites (Tynan et al., 2000a), as well as microtubule-binding stalk (gray: coiled-coil; red: microtubule-binding site) (Gee et al., 1997) and AAA domains (blue; Neuwald et al., 1999). Filled bars represent positive interactions with LIS1, and empty bars represent negative interactions. White line in constructs represents K to E mutation at a.a. 1910. Deduced interaction regions are marked by dotted lines and correspond to amino acids 649-907 and 1874-2124. (B, C) Anti-HA immunoblots of HC fragment immunoprecipitates showing LIS1.

A

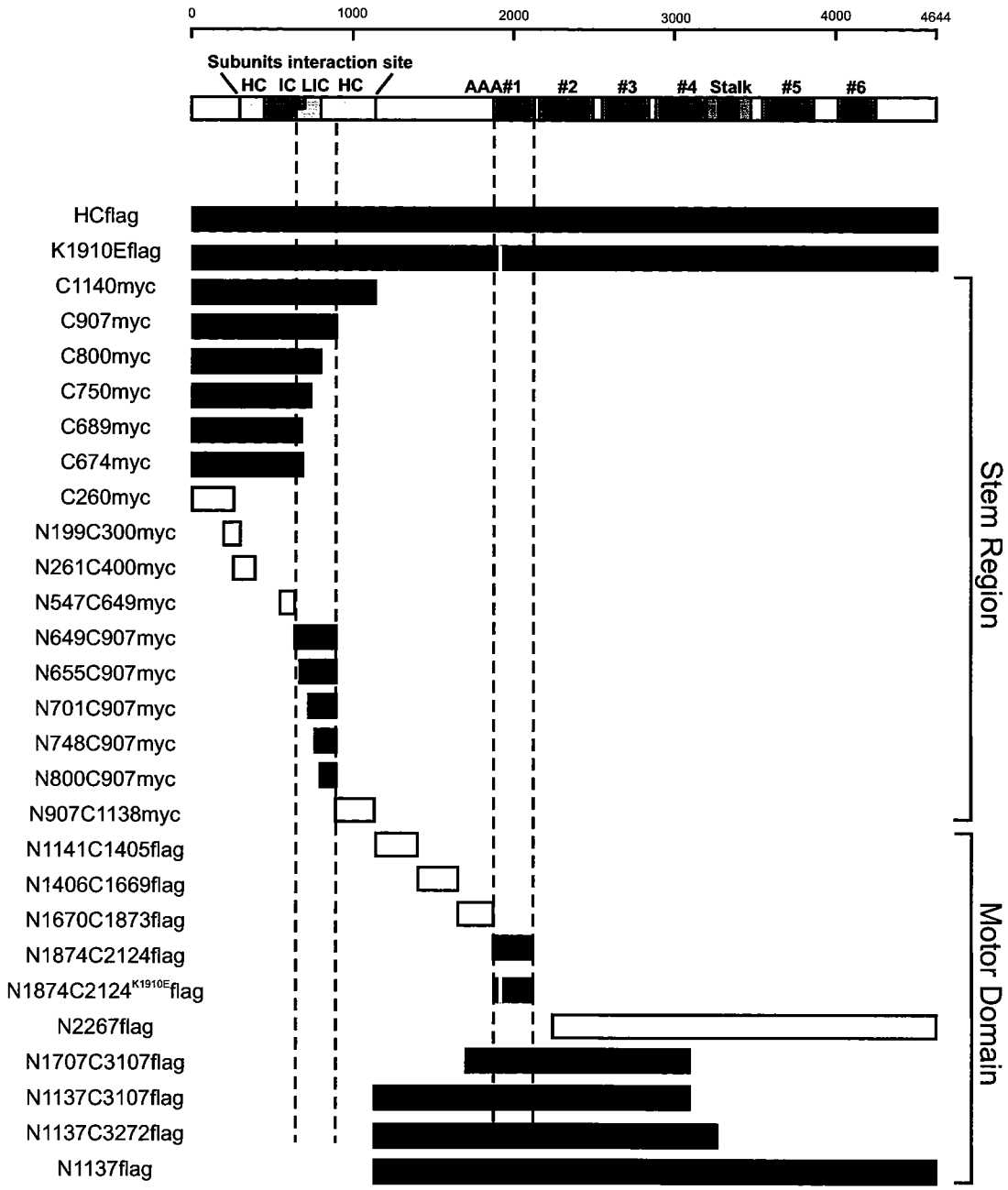
0
1000
2000
3000
4000
4644
Subunits interaction site
HC IC LIC HC
AAA#1
#2
#3
#4
Stalk
#5
#6
HCflag
K1910Eflag
C1140myc
C907myc
C800myc
C750myc
C689myc
C674myc
C260myc
N199C300myc
N261C400myc
N547C649myc
N649C907myc
N655C907myc
N701C907myc
N748C907myc
N800C907myc
N907C1138myc
N1141C1405flag
N1406C1669flag
N1670C1873flag
N1874C2124flag
N1874C2124K1910Eflag
N2267flag
N1707C3107flag
N1137C3107flag
N1137C3272flag
N1137flag
Stem Region
Motor Domain

B

HC flag-tagged Fragments

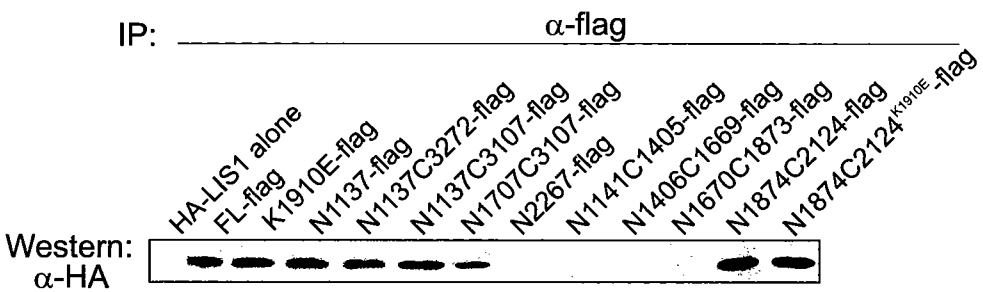

C

HC *myc*-tagged Fragments

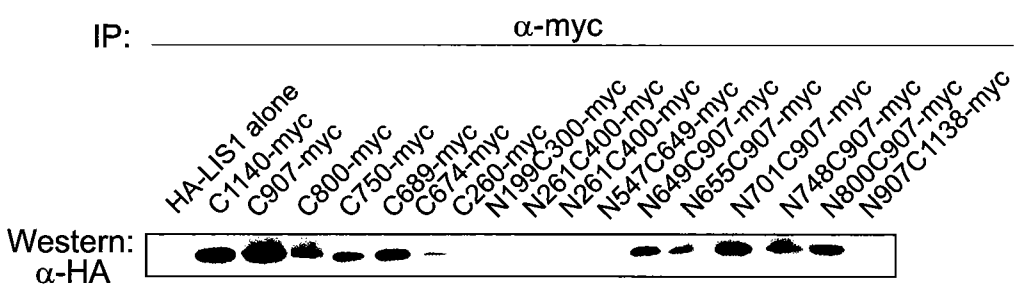

Discussion

Distinct Roles for LIS1 Domains

As for full-length LIS1, overexpression of the LIS1 N-terminal and WD-repeat domains produced pronounced increases in mitotic index. Neither fragment affected Golgi organization (*cf.* Smith et al., 2000), again indicating a role in a restricted range of dynein functions (Faulkner et al., 2000). The N-terminal region is involved in self-association (Fig. 3A; Ahn and Morris, 2001), but, so far, not in interactions with dynein, dynactin (Fig. 7), α-PAFAH or NudEL
(Kitagawa et al., 2000; Niethammer et al., 2000; Sweeney et al., 2000). The N-terminal domain failed to bind to kinetochores, but displaced endogenous full-length LIS1 (Fig. 3). We suggest that this behavior is likely to reflect a weakened affinity of the of LIS1-N/full-length LIS1 heterodimer for kinetochores. The resulting loss of endogenous LIS1 from this and, potentially, other sites seems likely to contribute to the mitotic phenotype.

In contrast, the WD-repeat fragment showed no evidence of self-association, mediated all of the heterologous LIS1 interactions identified in this study, and targeted to kinetochores very efficiently (Fig. 2A). The mechanism by which this region affects mitosis may involve competition with full-length LIS1 for dynein and dynactin binding, and displacement of CLIP-170 from the kinetochore (see below). Although α-PAFAH interacts with the WD-repeat region of LIS1

(Kitagawa et al., 2000; Niethammer et al., 2000; Sweeney et al., 2000), it was undetectable in our cell lysates (data not shown) and fails to associate with dynein (Niethammer et al., 2000; Tai et al., unpublished observations). It cannot, therefore, account for the mitotic effects we observed. The precise sites of LIS1 interaction with NudE, NudEL, and NudC are not known, nor has their fate been determined in LIS1 overexpressing cells.

Role of LIS1 in Kinetochore Organization and Function

As in the case of full-length LIS1 (Faulkner et al., 2000), the fragments failed to displace dynein and dynactin from the kinetochore despite the efficient displacement of endogenous LIS1 by the N-terminal fragment. The latter result argues strongly against a role for LIS1 in anchoring dynein and dynactin at the kinetochore. Conversely, LIS1 was displaced by dynamitin overexpression, which removes dynein and dynactin from the kinetochore. Together, our results are most clearly consistent with a model in which LIS1 is linked to the kinetochore through either dynein or dynactin or both (Fig. 10A).

Figure 10. Schematic representations of LIS1 interactions. (A) Effect of LIS1 overexpression at kinetochores and microtubule plus ends. (See text for detailed discussion and references.) For clarity dynactin is represented only by its dynamitin (p50) and p150^{Glued} subunits, and dynein only by its heavy (HC) and intermediate (IC) chains, and the interaction of the HC with microtubules is omitted. CLIP-170 associates with the kinetochore through dynein and dynactin, but the specific link is unknown. LIS1 is found in the current study to interact with p50, HC, and IC. Overexpression of dynamitin (dotted orange line) removes all polypeptides depicted. Overexpression of either full-length LIS1 and LIS1 WD (dotted green line) has no effect on the association of dynein and dynactin with the kinetochore, but dissociates CLIP-170 from this site and interferes with the interaction of p150^{Glued} with microtubules (see Faulkner et al., 2000). Further potential direct effects of overexpressed LIS1 or LIS1 fragments on dynein and dynactin subunits are discussed in the text. (B) Interaction of LIS1 with two dynein HC sites. (I) LIS1 is shown interacting independently with the cargo binding dynein stem domain or the first AAA unit within motor domain. (II) The proximity of these two sites within the folded dynein molecule may allow LIS1 to interact with both simultaneously.

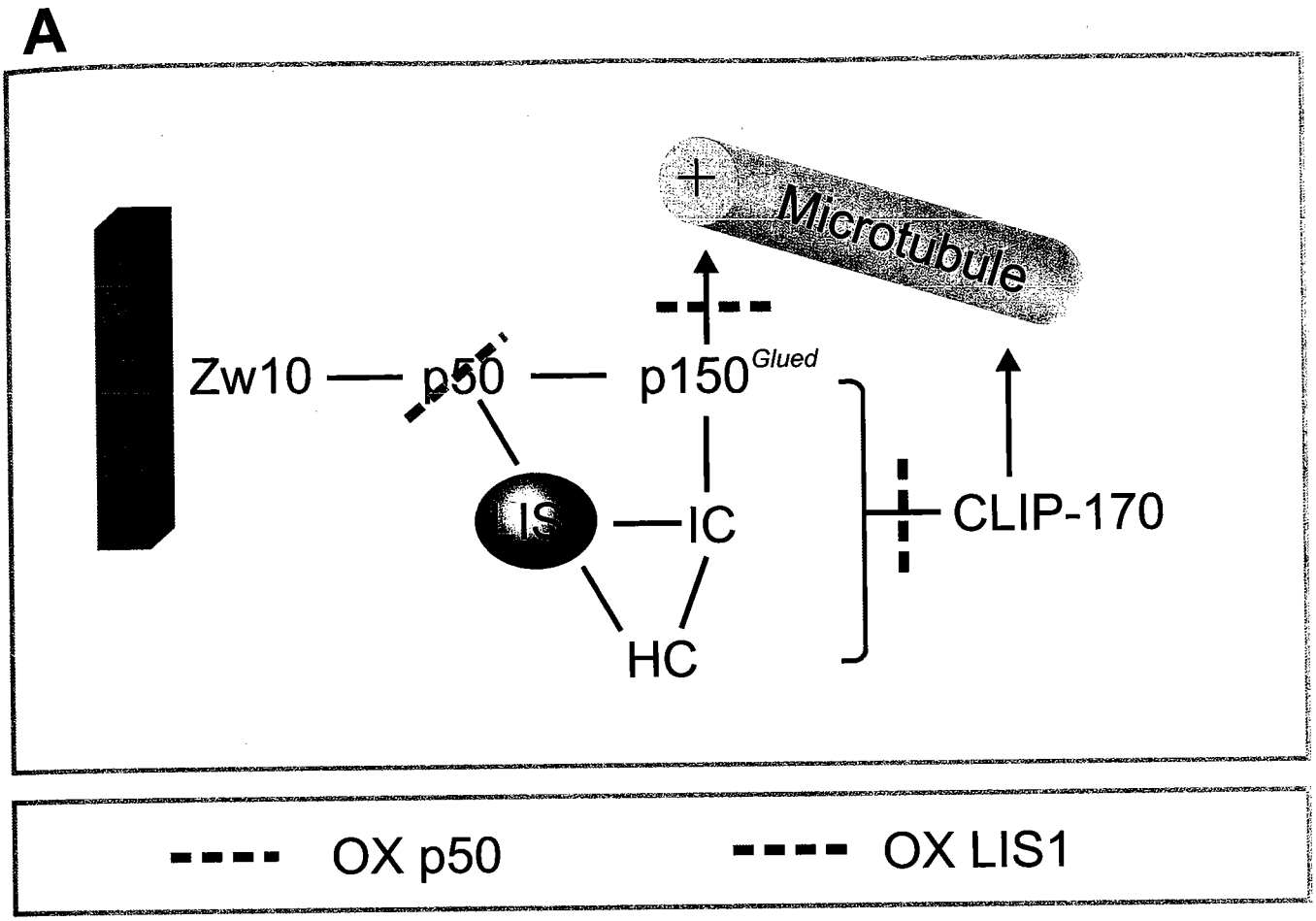
A
+
Microtubule
Zw10
p50
p150Glued
LIS1
IC
HC
CLIP-170
OX p50
OX LIS1
B
I
or
II

CLIP-170 was displaced from kinetochores by overexpression of LIS1 or its WD domain (Fig. 4). Because CLIP-170 can also be displaced by dynamitin overexpression, it is likely to associate with the kinetochore indirectly through dynein or dynactin (Dujardin et al., 1998). LIS1 overexpression appears to interfere with the latter link (Fig. 4), suggesting that LIS1 may mediate the interaction between CLIP-170 and the motor protein complexes. Although this is an appealing model, it is disputed by the effects of LIS1-N overexpression, which displaces endogenous LIS1 from the kinetochore (Fig. 3C) without affecting CLIP-170 (Fig. 4).

All three LIS1 constructs produce more severe accumulation of cells in mitosis and more dramatic alterations in spindle morphology than are generated by a dominant negative CLIP-170 fragment (Dujardin et al., 1998), suggesting a greater overlap in LIS1 and dynein functions. Loss of CLIP-170 almost certainly contributes to the LIS1 or LIS1-WD overexpression phenotypes, but is unlikely to explain fully the greater range of LIS1 phenotypic defects. It is uncertain whether this difference reflects a role for LIS1 in a wider range of mitotic dynein functions than CLIP170. Our evidence for an interaction between LIS1 and subunits of dynein and dynactin suggests a direct form of regulation in which CLIP170 is unlikely to participate. In this regard we have already found that LIS1 displaces the p150^{Glued} subunit of dynactin from growing microtubule ends (Faulkner et al., 2000; Chapter III), an effect which may well weaken the interaction between kinetochores and microtubules during mitosis.

LIS1 Interactions with Dynein and Dynactin

We have found LIS1 to interact with three different polypeptides, two in the dynein complex and a third in the dynactin complex. The ability of LIS1 to interact with subunits of both cytoplasmic dynein and dynactin suggests an important new role in linking the two complexes together. Despite extensive genetic and biochemical evidence for an interaction between the dynein IC and p150^{Glued} subunits (Karki and Holzbaur, 1995; McGrail et al., 1995; Vaughan and Vallee, 1995), only limited evidence for the copurification of the complexes has been obtained (Kini and Collins, 2001; Paschal et al., 1993). Phosphorylation of the ICs has recently been reported to regulate this interaction (Vaughan et al., 2001), and the current study suggests that LIS1 acts as a protein cofactor, which also contributes to the stability of the cocomplex.

The LIS1-binding domain of dynamitin resided in the C-terminal two coiled-coil domains, which was separated from the ZW10 binding domain, suggesting LIS1 did not compete with ZW10 for the binding of dynamitin. In addition, another effort was made to identify the LIS1-binding site within IC. IC can be divided into two structural domains: a coiled-coil domain located at the extremity of the N-terminus, which interacts with p150^{Glued} (Vaughan and Vallee, 1995); four WD-repeat like structure at the C-terminus, which is implicated in HC binding (Ma et al., 1999). Binding sites for Tctex-1 (Mok et al., 2001) and LC8 (Lo et al., 2001) are located between the two structural

domains. The fragments of the ubiquitous expressed isoform, IC2C, was cloned into the pCMV expression vector (pCDNA3.1, Invitrogen) with the myc tag inserted at the 3'-ends of each fragment. Four IC constructs were made in: the N-terminal 1-260 a.a. (IC2C C260myc); C-terminal 261-613 a.a. (IC2C N261myc); N-terminal 1-123 a.a. (IC2C C123myc); N-terminal 123-280 a.a. (IC2C N123C280myc). Preliminary result showed LIS1-binding site was located around the N-terminal 1-260 a.a. (data not shown). Unfortunately, the two smaller N-terminal fragments did not express well to identify a site in them.

The association of LIS1 with the first AAA domain of the dynein heavy chain strongly predicts an additional role in regulating motor activity. Although the mechanism by which the multiple dynein AAA domains coordinate their behavior to produce force and transmit it through the stalk is not understood, the importance of the first AAA domain has been clearly demonstrated (Gee et al., 1997; Gibbons and Gibbons, 1987).

Thus, LIS1 interacts with both cargo-binding and force producing regions of dynein itself, as well as with dynactin, suggesting a role for LIS1 in a complex and novel forms of regulation (Fig. 10B). Conceivably, LIS1 might serve to signal whether the dynein complex is associated with cargo (such as the mitotic kinetochore) and regulate motor activity accordingly. Alternatively, it could serve to stiffen the linkage between the stem and motor domains of dynein *via* a mechanism reminiscent of the role of light chains in stabilizing the myosin neck region (Lowey et al., 1993). Further study of the

functional properties of LIS1 is likely to provide important new insight not only into mechanisms of brain development, but into dynein regulation and function as well.

CHAPTER III

FURTHER ANALYSES OF LIS1 IN DYNEIN/DYNACTIN MICROTUBULE PLUS-END BINDING AND MOTOR ACTIVITIES

Introduction

A group of specialized proteins called plus ends tracking proteins (+TIPs) have been identified since 1999 (reviewed in Schuyler and Pellman, 2001). These proteins showed dynamic movements like comets streaking towards the plus ends of microtubules.

The functions of these +TIPs at the microtubule plus ends are mostly unclear. CLIP-170 was the only +TIPs whose function has been directly linked to the regulation of microtubule dynamics (Diamantopoulos et al., 1999). The function of dynactin at microtubule plus ends was suggested to recruit cytoplasmic dynein (Palazzo et al., 2001; Vaughan et al., 1999; Vaughan et al., 2002), based on the observation that dynactin appeared at the microtubule plus ends prior to the arrival of cytoplasmic dynein (Vaughan et al., 1999). It was unclear in addition to dynactin whether other factors were also required for dynein to be localized at microtubule plus ends.

Previously, we found that LIS1 localized at microtubule plus ends (Coquelle et al., 2002; Faulkner, Ph.D. thesis), and overexpression of LIS1 displaced dynactin from the microtubule plus ends (Faulkner et al., 2000). Lately, I demonstrated that LIS1 interacted with dynein independent of dynactin (Tai et al., 2002), suggesting that LIS1 served as an alternative recruiting factor for dynein when dynactin was displaced from the microtubule plus ends.

In the first part of this Chapter, I determined the protein factors required for dynein to be localized at the microtubule plus ends. First, I wanted to find a cell line suitable for detecting dynein plus end signals, instead of using the COS-7 cells, which requires a step of room-temperature incubation in order to detect the weak dynein plus end staining (Vaughan et al., 1999). I found that in HeLa cells, clear dynein microtubule plus end signals were detected consistently without the need of shifting temperature. Next, I tested whether the intact complex of dynactin was required for dynein plus end targeting. It has been shown that dynein interacted with dynactin through the direct binding between ICs and p150^{Glued} (Karki and Holzbaur, 1995; Vaughan and Vallee, 1995). Overexpression of dynamitin splits dynactin into smaller sub-complexes, and the p150^{Glued} subunit remained bound to the plus ends (Vaughan et al., 1999). With just the p150^{Glued} at microtubule plus ends, it was thought that dynein should remain at microtubule plus ends in the dynamitin overexpressing cells, and my results proved this idea. This finding further indicated that dynein microtubule plus end targeting does not

require an intact dynactin complex. Finally, I examined whether LIS1 could replace dynactin as the plus-end targeting factor for dynein in the absence of dynactin. Overexpression of LIS1 removed dynactin from the microtubule plus ends, which resulted in the displacement of dynein as well, indicating that the p150^{Glued}-containing dynactin sub-complex was absolutely required for dynein plus end targeting and LIS1 could not replace dynactin for this role.

The second part of this chapter further characterized the protein-protein interactions between LIS1 and the dynein complex. The work in Chapter II demonstrated LIS1-dynein interactions through the co-overexpression and co-immunoprecipitation assay, which did not reflect the actual affinity between these proteins at the endogenous level. Here, I found the majority of LIS1 did not co-sediment with dynein and dynactin in a sucrose density gradient centrifugation, suggesting their interactions were weak, transient or regulated. Second, LIS1 was co-immunoprecipitated with the intact complexes of dynein and dynactin, indicating that LIS1 was interacting with the whole complexes rather than the individual subunits.

In Chapter II, LIS1 was found to interact with the ATPase domain of dynein HC, suggesting a role for LIS1 in regulating the ATPase activity of dynein HC (Tai et al., 2002). In an *in vitro* assay, I found that LIS1 stimulated dynein ATPase activity in a dose-dependent manner. This result highlighted the functional significance of LIS1 interacting with the motor domain of dynein HC.

Materials and Methods

Expression constructs and recombinant protein purification

HA tagged LIS1 fragment constructs were described in Chapter II. 6His tagged LIS1 baculoviral expression construct was generated by PCR amplification with Bgl II and EcoR I restriction sites at 5' and 3' ends, and then cloned into pBlueBacHis2B vector (Invitrogen). PCR amplified region was confirmed by DNA sequencing performed by UMass Nucleic Acid Facility.

Isolation and purification of β-gal$^+$(blue) plaques containing the recombinant virus were obtained according to the manufacture's recommendations (Clontech). The purity of the viruses was determined by PCR of purified viral DNAs. Maximal protein expression in Sf9 cells was observed after 72 hours of infection. Every $2x10^7$ infected cells was lysed with 4 ml of insect lysis buffer (100 mM Tris pH 7.5, 130 mM NaCl, 1% Triton X-100) with protease inhibitor cocktail (1mM AEBSF, 2 μg/ml of aprotinin, leupeptin and pepstatin A) on ice for 40 minutes and then briefly sonicated to shear chromosomal DNA for 3x30 seconds. Lysate was then spun in a tabletop centrifuge at full speed at 4^0C for 10 minutes. During the 10-min spin, the Ni-NTA beads (Qiagen) were washed three times with the lysis buffer and added the precleared lysate upon the completion of the spin. Binding was performed at 4^0C for 1 hour with gentle head-to-tail rotation. Beads were then washed three times with washing buffer (50 mM Sodium Phosphate buffer pH 8.0, 300 mM NaCl, 10% glycerol, 20 mM imidazole) at 4^0C for 10

minutes each. Protein was eluted with 3x beads vol. of elution buffer (50 mM Sodium Phosphate buffer pH 8.0, 300 mM NaCl, 10% glycerol, 250 mM imidazole) at 4^0C for 1hour. Purified protein was then dialyzed in Tris/KCl buffer (20 mM Tris HCl pH7.6, 50 mM KCl, 5 mM $MgCl_2$, and 0.5 mM EDTA) overnight at 4^0C with one change after six hours.

Antibodies

Anti-myc polyclonal antibody has been described elsewhere (Gee et al., 1997); anti-HA polyclonal and monoclonal and anti-myc monoclonal antibodies were purchased from Covance (Richmond, VA). Anti-LIS1 monoclonal antibody was provided by Dr. Orly Reiner (Weizmann Institute, Rohovot, Isreal) and has been characterized previously (Faulkner et al., 2000); anti-CLIP-170 monoclonal antibody was provided by Dr. Holly Goodson (University of Norte Dame, IN). Anti-dynein IC monoclonal antibody was purchased from Chemicon (Temecula, CA). Anti-EB1 and anti-p150^{Glued} monoclonal antibodies were purchased from Transduction Laboratories. Anti-p150^{Glued} polyclonal antibody (DART) was described elsewhere (Vaughan and Vallee, 1995; Vaughan et al., 2002). Anti-His monoclonal antibody was purchase from Clontech. Secondary horseradish peroxidase-conjugated donkey anti-mouse and anti-rabbit antibodies were purchased from Jackson Immunoresearch Laboratories, Inc. (West Grove, PA). For immunofluorescence, Cy3-conjugated donkey anti-mouse and anti-rabbit antibodies were purchased from Jackson Immunoresearch Laboratories and Alexa 488 anti-mouse and anti-rabbit antibodies were purchased from Molecular Probe (Eugene, OR).

Cell culture and transfection

HeLa cells were grown in Dulbecco's modified Eagle's medium with 10% fetal bovine serum and penicillin/streptomycin (GIBCO Invitrogen Corp., Carlsbad, CA). For transient transfection, cells were plated either in 10-cm petridishes or onto 18mm coverslips grown to 70 to 80% confluencies, then transfected with the appropriate amount of DNA mixed with lipofectAMINE (for 10-cm dish) and lipofectAMINE PLUS (for coverslips) (GIBCO Invitrogen Corp.). Transient expression was allowed for 40 to 48 hours.

Sf9 cells were maintained in the TNM-FH medium (Pharmingen) at 27^0C. For protein production, cells were plated at 70% confluency in 15-cm petridishes and appropriate amount of viral stock was then added. For viral stock production, cells were plated to 50% confluency and half strength of viral stock was added. Between 7 to 10 days, the cells were completely lysed and the debris was separated by centrifugating at 1000 rpm for 10 minutes. The supernatant was then stored in the dark at 4^0C.

Sucrose gradients and immunoprecipitations

Four confluent 10-cm petridishes of COS-7 cells were washed twice with PBS and lysed with Tris/KCl buffer (20 mM Tris HCl pH7.6, 50 mM KCl, 5 mM $MgCl_2$, and 0.5 mM EDTA) +1% Triton X-100 with freshly added protease inhibitor mixture: 2ug/ml of aprotinin, leupeptin (Sigma, St. Louis, MO) and 1mM of AEBSF (Roche Molecular

Biochemicals, Indianapolis, IN). Cells then were incubated on ice for 20 min and spun at 13,000rpm for 10 min in a microfuge. 1ml of the lysate was loaded onto a 10-ml 10-40% sucrose gradient in Tris/KCl buffer. Centrifugation was for 30,000 rpm at 4^0C for 20 hours in an SW41Ti rotor (Beckman Coulter). 500 μL of fractions were collected from the bottom for further analyses. 100 μL of selected fractions incubated with or without antibodies and buffer-washed Protein G beads (Amersham Biosciences) at 4^0C overnight with gentle rotation. Beads then were washed five times with Tris/KCl + 1% Triton X-100 buffer at room temperature 10 min each and boiled in 5x SDS-PAGE sample buffer for 5 min. The entire eluate and 4% of supernatant were loaded into 5-15% SDS-polyacrylamide gel and transferred onto Immobilon-P membrane (Millipore Corp., Bedford, MA). Immunoblotting was performed with various antibodies against specific proteins.

Cytoplasmic dynein purifications and biochemical assays

Calf brain white matter (40-50 gm) was dissected and from two fresh calf brains and processed as described previously (Paschal et al., 1987; Paschal et al., 1991). The tissue was transferred into a 100-mL capacity Teflon pestle homogenizer in 1.0 vol of extraction buffer (EB; 50 mM Pipes pH7.0, 50 mM Hepes pH7.0, 2 mM $MgCl_2$, 1 mM EDTA) with freshly added 1mM DTT and protease inhibitor mixture (1mM AEBSF, 10 mg/ml of aprotinin, leupeptin, pepstatin A). Homogenization was performed with 6 to 10 passes at 2000rpm on ice. The homogenate was centrifuged in a 45Ti rotor (Beckman Coulter) at 18,000 rpm for 30 minutes at 4^0C. The supernatant was further centrifuged in

a 60Ti rotor (Beckman Coulter) at 45,000 rpm for 1 hour at 4^0C to obtain the high-speed cytosolic extract (CE). The CE was immediately transferred into a 50-mL Falcon tube and then taxol (Sigma) was added to 30 μM, and incubated at 37^0C for 30 minutes. Sample was loaded onto four 10-mL of 10% sucrose cushion in EB + DTT + 5 μL of taxol in 60Ti tubes. Taxol-stabilized microtubules were centrifuged in a prewarmed 60Ti rotor at 30,000 rpm at RT for 30 minutes. Microtubule pellets were resuspended with 0.2 vol of EB + DTT + 10 μL of taxol and centrifuged again. This buffer-wash step was repeated again and the final microtubule pellet was resuspended with 0.1 vol of EB + 3 mM MgGTP + 10 μL of taxol. The sample was incubated at 37^0C for 15 minutes, and centrifuged again in a Ti60 rotor at 30,000 rpm at RT for 30 minutes. The pellet was resuspended gently with 0.1 vol of EB + 10 mM MgATP + 10 μL of taxol, and incubated at 37^0C for 15 minutes. Again, centrifugation was performed in a Ti60 rotor at 35,000 rpm at RT for 30 minutes. The final eluate was loaded onto 2 10-mL 5-20% sucrose gradient in Tris/KCl + 1 mM DTT. Centrifugation was performed in an SW41Ti rotor at 32,000 rpm for 16 hours at 4^0C. 500-μL fractions were collected from the top and the same fraction from the two gradients was pooled together. Fractions containing dynein were identified by coomassie-stained SDS-polyacrylamide gel and quantified by Bradford method (Bio-Rad).

Radioactive ATPase assay was performed immediately after obtaining dynein (Paschal et al., 1991). The reactions were assembled on ice in a 40-μL vol, with dynein, LIS1 protein and Tris/KCl buffer, and then the 10 μL of 5 mM [γ-^{32}P] MgATP (1 μL of

10 μCi/μL [γ-^{32}P] ATP in 400 μL of 5 mM MgATP stock) was added at RT. Samples were then incubated at 37^{0}C for 30 minutes. 100 μL of silicotungstic acid solution (20 mM in 10 mM H_2SO_4) was added to stop the reaction, followed by the addition of 300 μL of charcoal suspension (Sigma; acid-washed, stirred in 3 vol of deionized water) and 600 μL of 5 mg/ml BSA (Sigma). After vortexing, the mixture was centrifuged in a tabletop microfuge at 12,000 rpm for 2 minutes. 500 μL of supernatant from each tube was added into a 3.5-mL of scintillation cocktail and then fed into a scintillation counter (Beckman) to quantify the Pi release.

Immunofluorescence Microscopy

For microtubule plus ends staining, cells were rinsed briefly with -20^{0}C 100% methanol and then fixed in -20^{0}C 100% methanol for 10 min. All primary and secondary antibody incubations were performed at 37^{0}C for one hour. After all antibody incubations, cells were incubated with 0.1ug/ml of DAPI (Sigma) for 10 min before mounting with Prolong Antifade solution (Molecular Probe). Immunofluorescence images were obtained by using Leica DM IRBE microscope equipped with Hamamatsu ORCA 100 CCD camera and processed by MetaMorph software (Universal Imagining Group). Each image was then cropped and/or pseudocolored by Adobe Photoshop 5.5 and Corel DRAW 9.0.

Results

Dynein localization at the microtubule plus ends in HeLa cells

In COS-7 cells, the staining of microtubule plus end-associated dynein was weak and could only be observed after cells being pre-incubated at room temperature for 1 minute prior to fixation (Vaughan et al., 1999). It became difficult to judge the alteration in the localization of dynein at the microtubule plus ends when additional experimental manipulations were required.

I found dynein plus end signals are very prominent without the temperature shift in HeLa cells (Fig. 1A upper left panel). In general, the staining pattern of dynein at the plus ends overlapped with that of p150^{Glued} (length of IC signals: 0.48 μm ± 0.13; length of p150^{Glued} signals: 0.54 μm ± 0.13) (Fig. 1A). However, IC and p150^{Glued} were not always colocalized (Fig. 1A, open arrow heads). The punctate staining patterns of IC and p150^{Glued} were distinct from the uniformed and longer staining of EB1 (0.75 μm ± 0.2). Relatively, it seemed that p150^{Glued} co-localized more often with ICs than with EB1 at the plus ends.

Figure 1. Colocalization of dynein, dynactin and EB1 at microtubule plus ends in HeLa cells. (A) Double labeling of p150^{Glued} (dynactin) and IC (dynein). The microtubule plus end localizations of p150^{Glued} and IC were detected by a polyclonal anti-p150^{Glued} antibody and a monoclonal anti-IC antibody, respectively. The merged image (red, IC; green, p150^{Glued}) shows overlapped microtubule plus end labeling pattern for these two proteins (yellow arrows). Non-colocalization is indicated with open arrow heads (green, positive for p150^{Glued} but negative for IC; red, positive for IC but negative for p150^{Glued}). (B) Double labeling of p150^{Glued} and EB1. The microtubule plus end localizations of p150^{Glued} and EB1 were detected by a polyclonal anti-p150^{Glued} antibody and a monoclonal anti-EB1 antibody. The merged image (red, p150^{Glued}; green, EB1) shows that the plus-end staining of p150^{Glued} is much shorter compared with that of EB1. The green open arrow heads indicate positive staining for EB1 but negative staining for p150^{Glued}. Yellow arrows in both (A) and (B) indicate the co-localization of the two proteins detected in each experiments. Bar, 5μm.

A

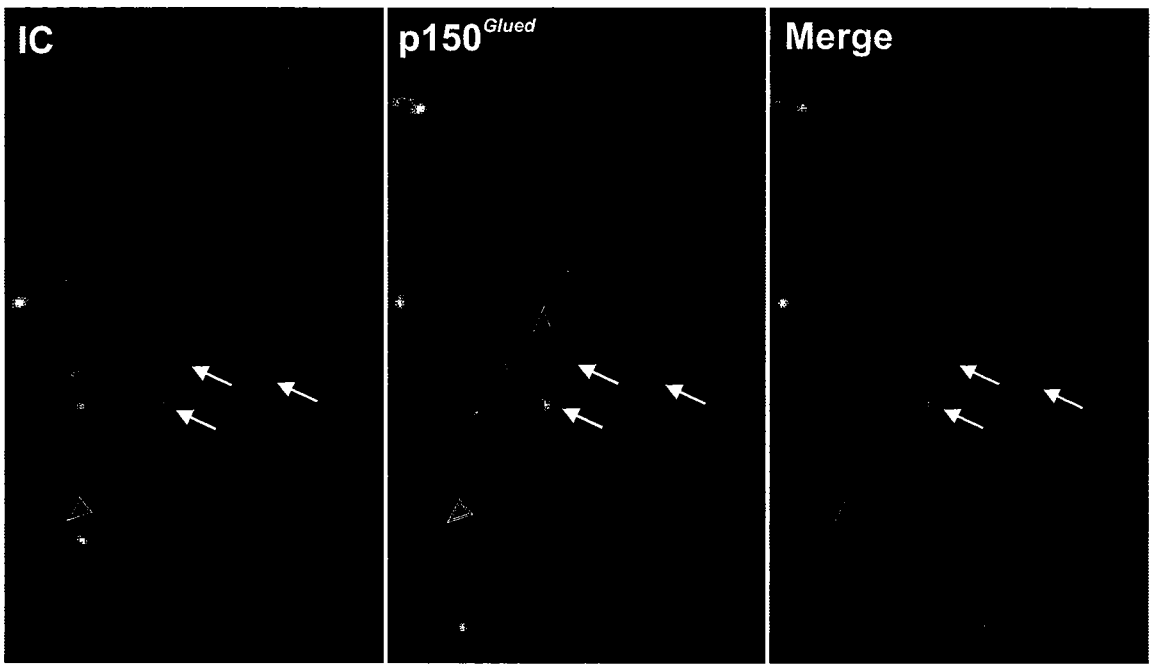

B

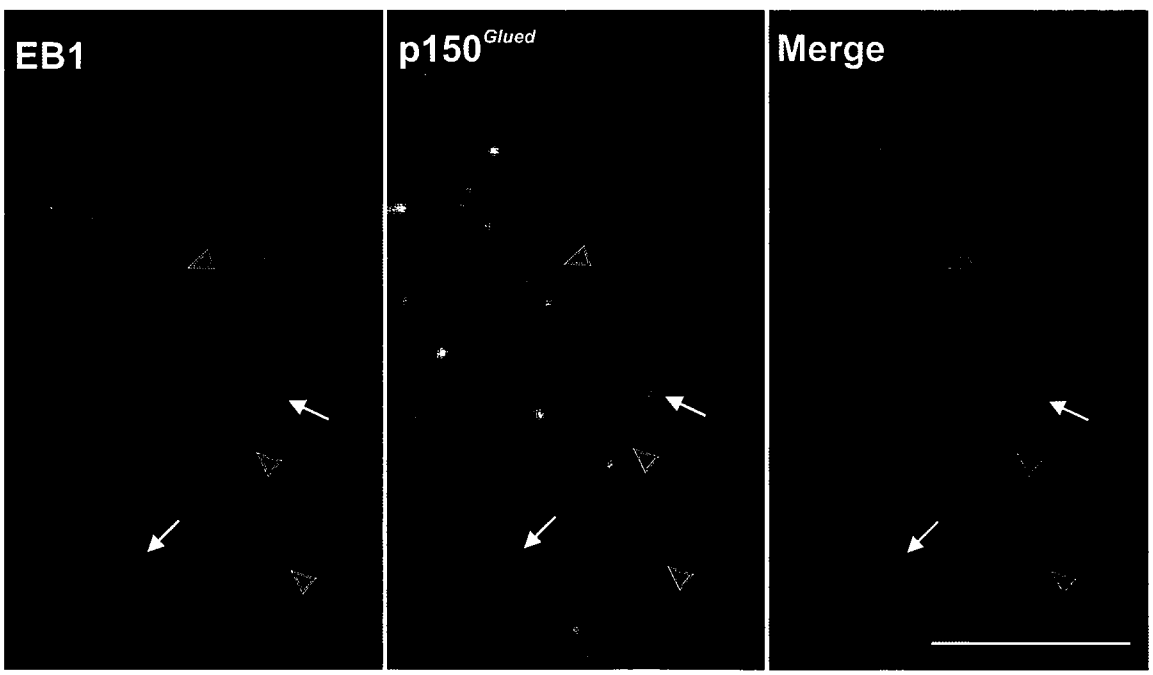

Dynactin and LIS1 in dynein targeting to the microtubule plus ends

Dynein binds to dynactin via the interaction of IC and p150^{Glued} (Karki and Holzbaur, 1995; Vaughan and Vallee, 1995). Overexpression of dynamitin splits the dynactin into sub-complexes (Echeverri et al., 1996). Arp1 was displaced from the microtubule plus ends, and p150^{Glued} remained bound (Fig. 2 upper two rows) (Vaughan et al., 1999). It was interesting to ask whether dynein could still localize at the microtubule plus ends in the absence of an intact dynactin by the overexpression of dynamitin. I found that dynein remained bound to the microtubule plus ends in dynamitin-overexpressing cells (Fig. 2 bottom row).

Figure 2. Effects of overexpressing myc-tagged dynamitin on the microtubule plus end localization of dynein and dynactin. HeLa cells were transfected with a myc-tagged dynamitin construct for 48 hours, then were double-labeled with the following pairs of antibodies: upper row, a polyclonal affinity purified Arp1 antibody plus a monoclonal anti-myc antibody; middle row, a polyclonal anti-p150^{Glued} antibody plus a monoclonal anti-myc antibody; bottom row, a monoclonal anti-IC antibody plus a polyclonal anti-myc antibody. Clearly, the Arp1 subunit of dynactin was displaced from the microtubule plus ends, whereas both p150^{Glued} and IC remained at the microtubule plus ends. Bar, 10μm. Insets, 2x enlarged.

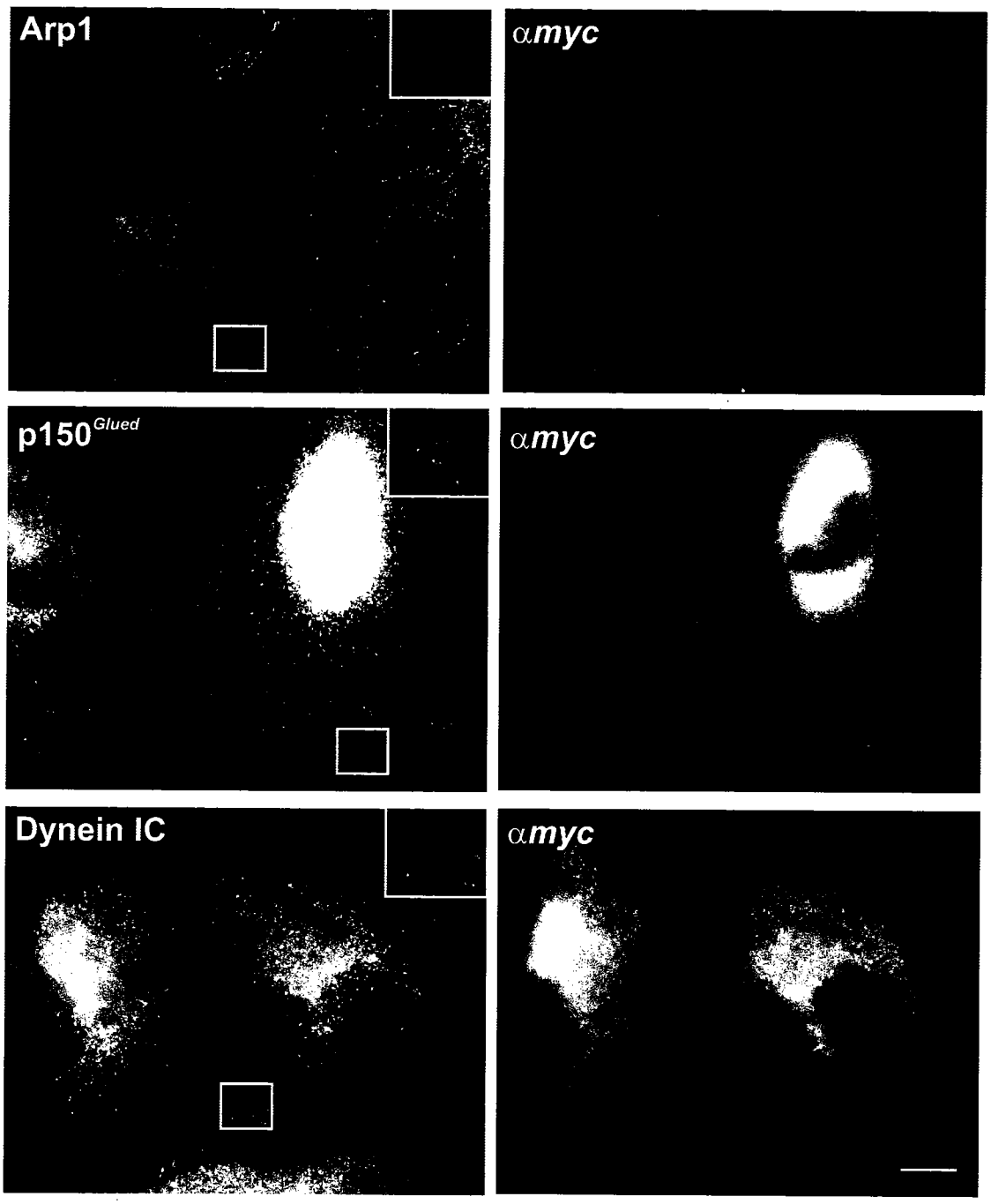
Arp1
αmyc
p150Glued
αmyc
Dynein IC
αmyc

Since the p150^{Glued}-containing sub-complex of dynactin was still able to bind microtubule plus ends, it was worthwhile to ask if dynein binding to the plus ends is p150^{Glued}-dependent. HeLa cells were transfected with LIS1 constructs to displace p150^{Glued} from the microtubule tips (Faulkner et al., 2000). It was found that both p150^{Glued} and dynein were displaced from the microtubule ends (Fig. 3A & B). Furthermore, all three LIS1 fragments (FL, WD, and N) were capable of removing dynein and dynactin from the microtubule plus ends. The displacement of dynein by overexpression of all three LIS1 polypeptide is specific, because CLIP-170 remained bound at the plus ends in all LIS1 overexpressers (Fig. 3C).

Figure 3. Overexpression of LIS1 fragments displaces p150^{Glued} and dynein from microtubule plus ends. HeLa cells were transfected with HA-tagged LIS1 fragment constructs (FL, WD and N), and were doubly labeled for LIS1 along with either p150^{Glued} (A), dynein IC (B) or CLIP-170 (C). Dynein IC and p150^{Glued} were displaced from the microtubule plus ends in all three LIS1 fragment-overexpressing cells (A, B), whereas CLIP-170 remained (C). Bar, 10μm. Insets, 2x enlarged.

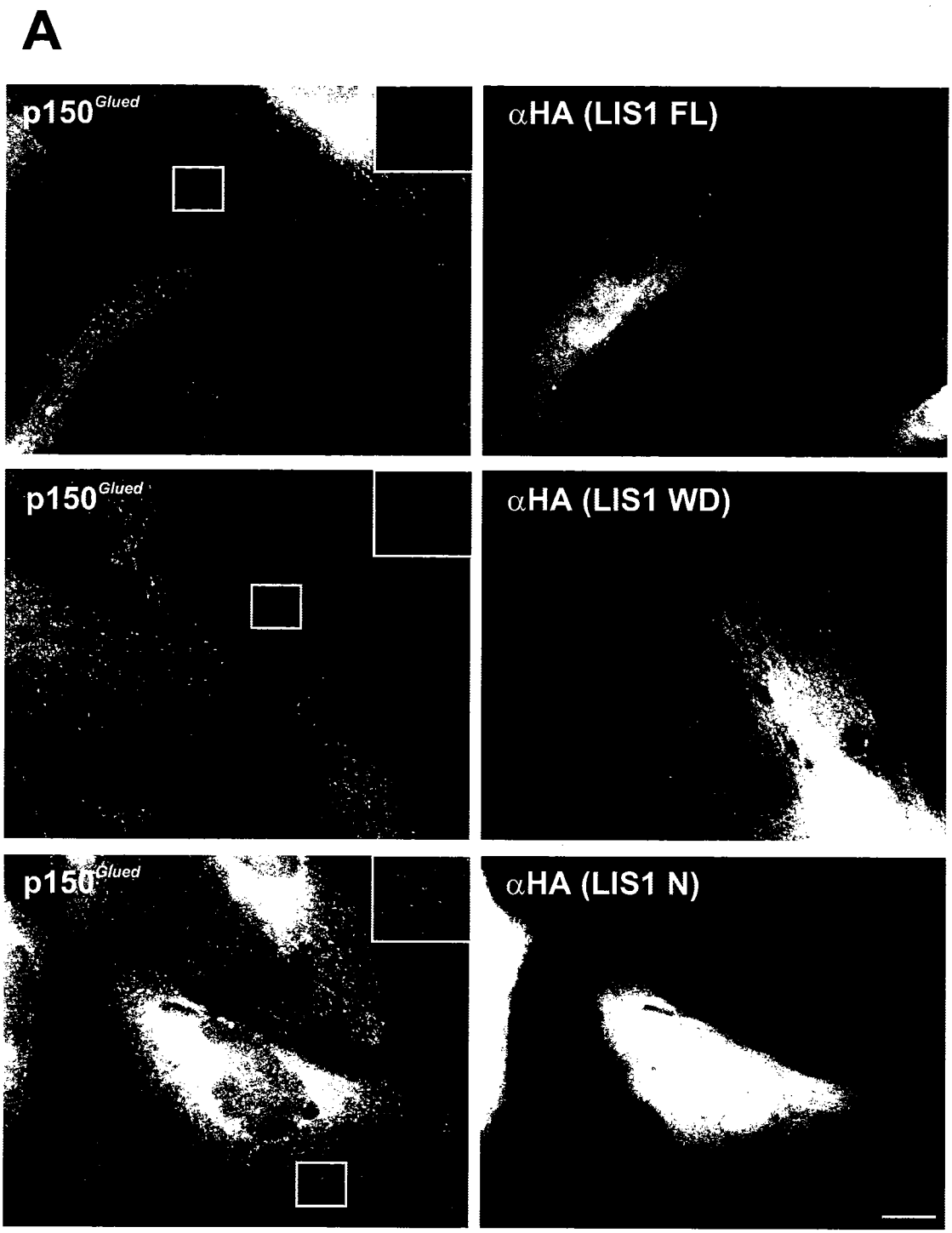
A
p150Glued
αHA (LIS1 FL)
p150Glued
αHA (LIS1 WD)
p150Glued
αHA (LIS1 N)

B

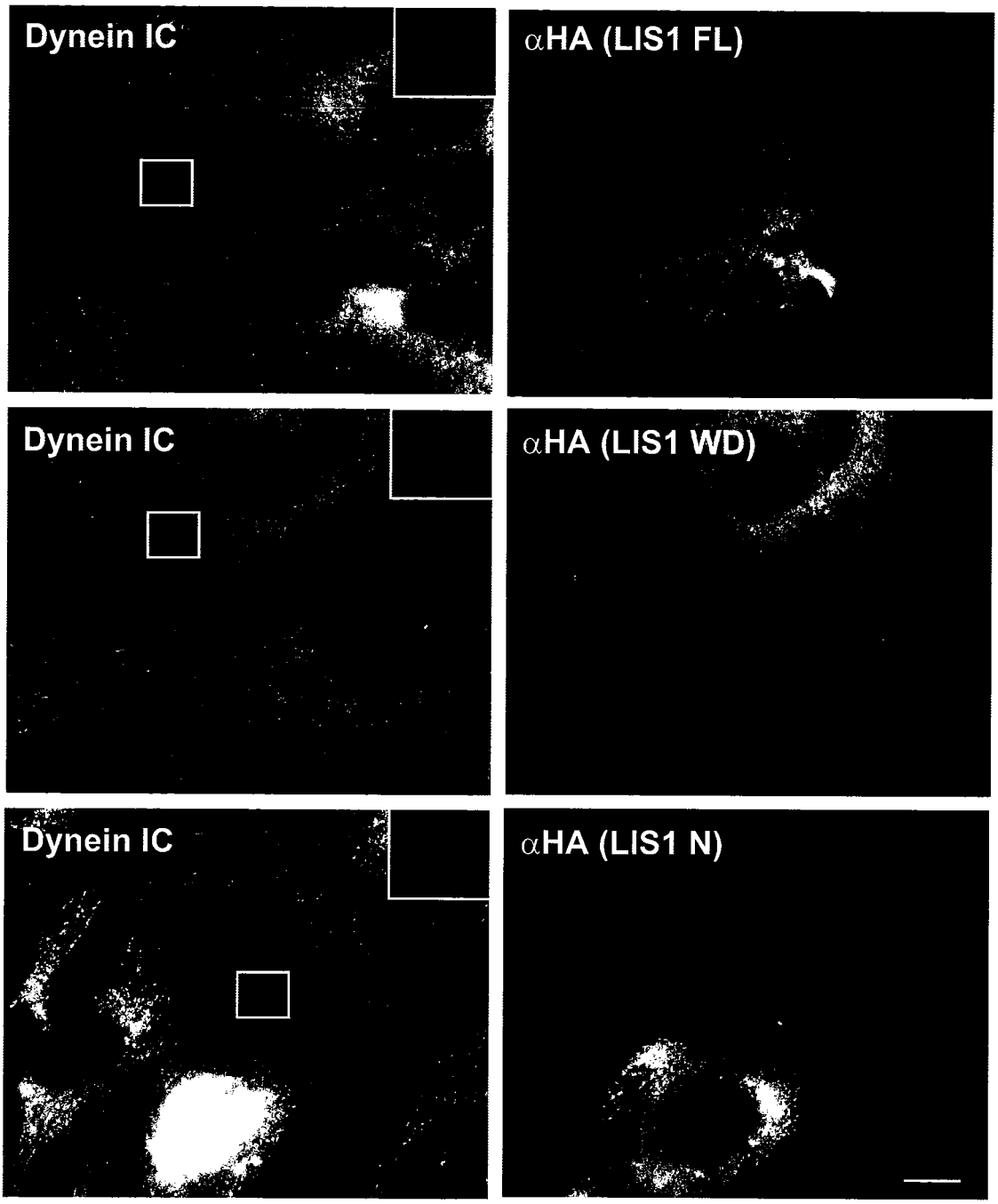
Dynein IC
αHA (LIS1 FL)
Dynein IC
αHA (LIS1 WD)
Dynein IC
αHA (LIS1 N)

C

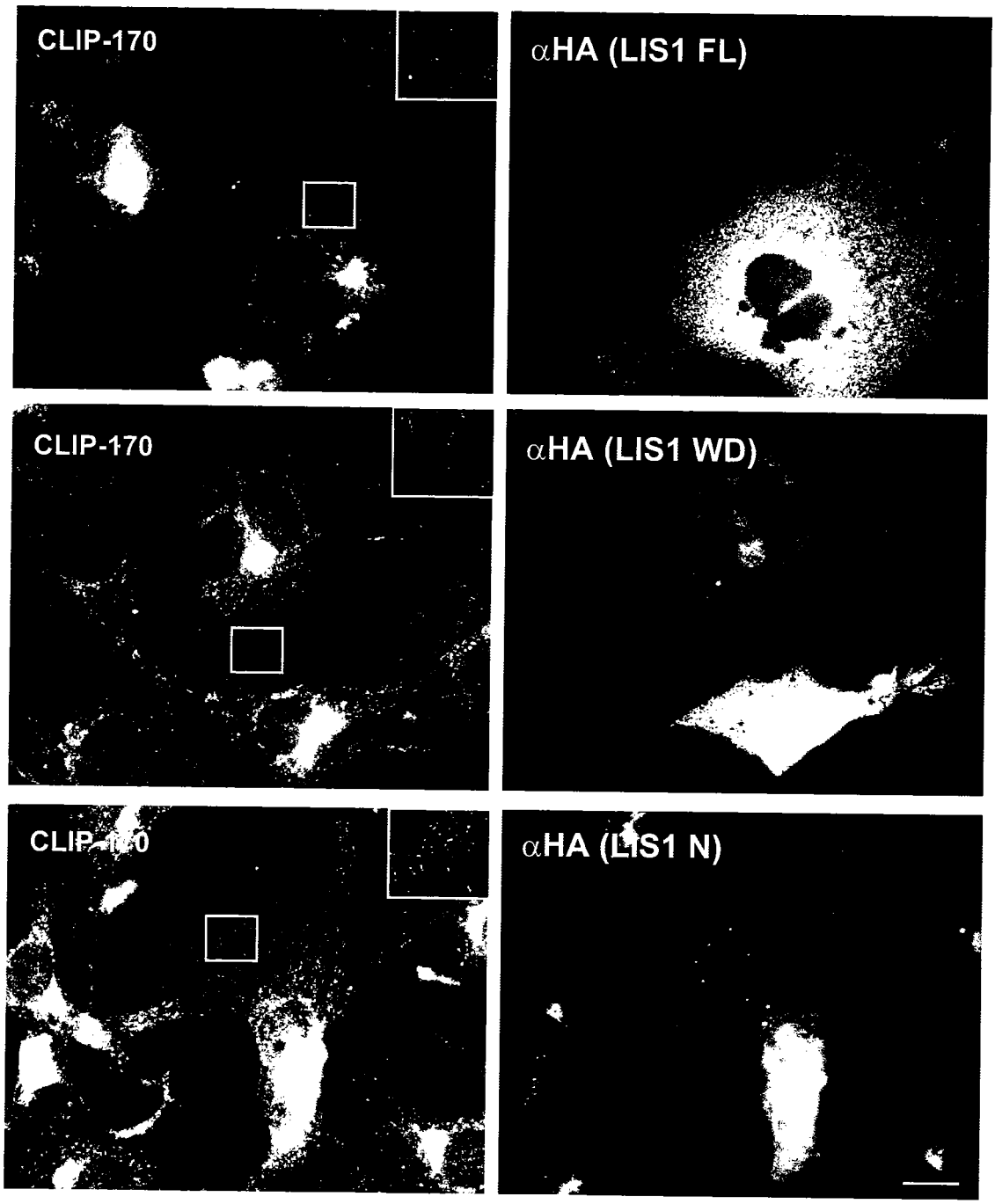

Detailed analyses of LIS1, dynein and dynactin interactions

Previously, I found that the majority of LIS1 protein remained in the supernatant when either dynein or dynactin was immunoprecipitated from the COS-7 cell lysates, suggesting that only a small portion of the entire LIS1 protein pool interacted with dynein and dynactin. In addition, it was unclear whether the LIS1 protein found in the dynein and dynactin co-precipitates was interacting with intact dynein and dynactin complexes.

I performed sucrose density gradient centrifugation to demonstrate that LIS1 could interact with both intact complexes of dynein and dynactin. The S values of a dynein-dynactin supercomplex should be at 30S (Kini and Collins, 2001), and the 20S peak of dynein and dynactin represented two separate complexes. LIS1 sedimented at the low-S fractions, and was clearly separated from the 20S dynein and dynactin fractions (Fig. 4A). Furthermore, a small amount of LIS1 was present in the 20S fractions (Fig. 4A), and was associated with dynein and dynactin (Fig. 4B). The same result was obtained when calf brain extract was used (data not shown).

Figure 4. Sedimentation profile and immunoprecipitation of dynein, dynactin and LIS1. (A) COS-7 cell extract was subjected to sucrose gradient centrifugation and blotted for dynein (IC), dynactin ($p150^{Glued}$) and LIS1. (B) Immunoprecipitation of LIS1 from selected fractions and blotted for dynein (IC) and dynactin ($p150^{Glued}$).

A

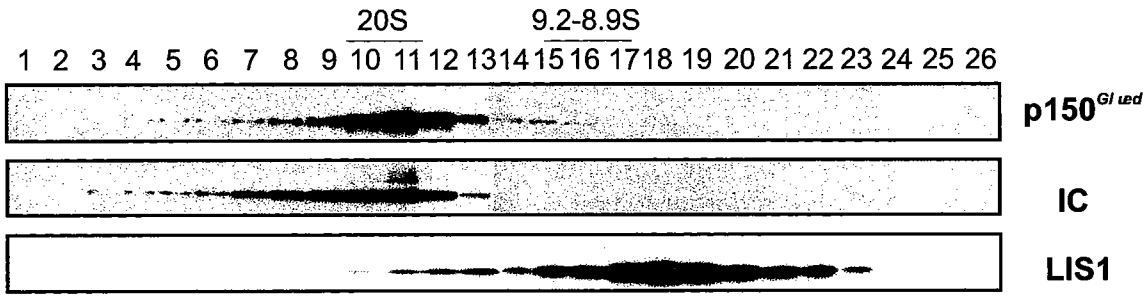
20S
9.2-8.9S
1 2 3 4 5 6 7 8 9 10 11 12 13 14 15 16 17 18 19 20 21 22 23 24 25 26
p150Glued
IC
LIS1

B

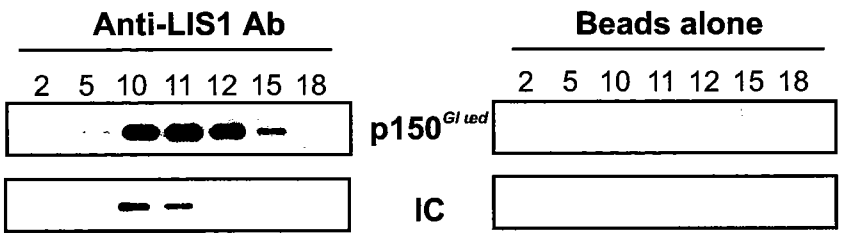
Anti-LIS1 Ab
Beads alone
2 5 10 11 12 15 18
2 5 10 11 12 15 18
p150Glued
IC

The effect of LIS1 in dynein ATPase activity

The interaction between LIS1 and dynein HC ATPase domain has been suggested to play an important role for LIS1 in regulating dynein ATPase activity (Tai et al., 2002). To test directly whether LIS1 affected dynein ATPase activity, I performed the dynein ATPase assay in the presence or absence of recombinant LIS1 protein.

First, the purification of cytoplasmic dynein complex from bovine brain extract was according to the method developed in this laboratory (Paschal et al., 1987). Aliquots at each step were analyzed by immunoblotting of $p150^{Glued}$, IC and LIS1. The amount of proteins in each step was quantified by densitometer (see Fig. 5A and graph). A moderate amount of LIS1 protein co-pelleted with polymerized microtubules through two rounds of buffer washing, suggesting a stable interaction. Comparing the amount of proteins present in the GTP and ATP eluates, dynein and dynactin were preferentially eluted in the presence of ATP, while LIS1 did not show this preference. After sucrose gradient centrifugation of the ATP eluate, LIS1 fractions were again separated from the 20S dynein fractions, showing a fractionation profile similar to that of a COS crude extract (Fig. 5B & 4A). Fractions marked as the 20S were pooled and used in the ATPase assay.

Figure 5. Steps of cytoplasmic dynein preparation. Cytoplasmic dynein was purified to 90% purity by using ATP-mediated extraction from taxol-stabilized microtubule copelleting method (Paschal et al., 1991). (A) Progression of purification was monitored by both coomassie staining (top) and immunoblotting (middle three rows) using anti-IC, anti-p150^{Glued} and anti-LIS1 antibodies. Density of individual band for each protein was determined by densitometry and plotted accordingly (bottom). (B) Sucrose gradient centrifugation of the ATP-extractable microtubule-associated proteins. A 5-20% sucrose gradient in Tris-KCl buffer (Paschal et al., 1987) was used to resolve the ATP eluate followed by centrifugation. Aliquots of fractions were collected and analyzed by both coomassie staining (top) and immunoblotting (bottom three rows). The bottom fraction (1) showed higher amount of all three proteins, which might represent non-specific aggregation of proteins. Significant amount of p150^{Glued} and IC were present in the low S fractions, which indicates dissociation of these proteins from their intact complex at 20S (Paschal et al., 1993). Note LIS1 was co-extracted with dynein and dynactin in the presence of ATP, it did not co-sediment with these protein complexes at 20S. CE, cytosolic extract; S, supernatant; P, pellet; DHC, dynein heavy chain; Kin, kinesin; Tub, tubulin.

A

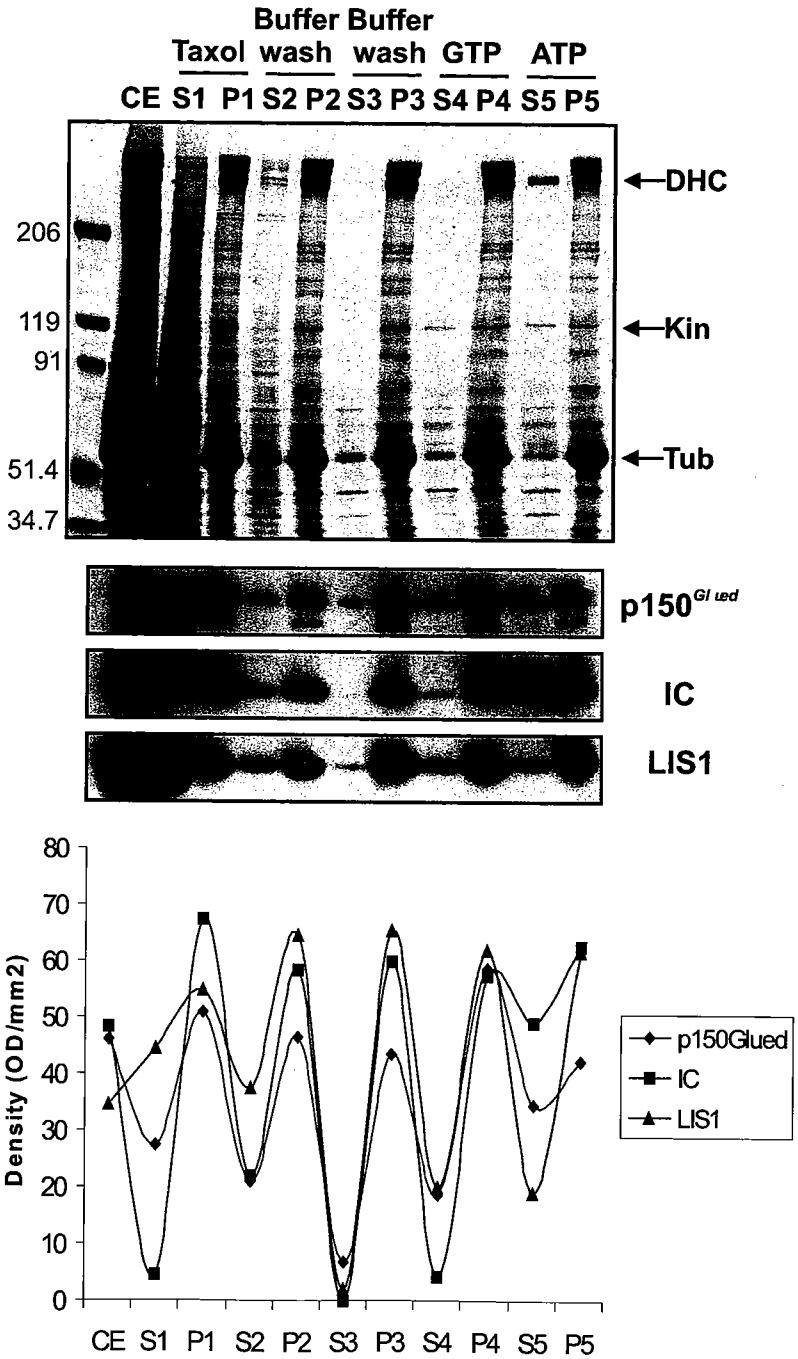
Buffer Buffer
Taxol wash wash GTP ATP
CE S1 P1 S2 P2 S3 P3 S4 P4 S5 P5
206
119
91
51.4
34.7
DHC
Kin
Tub
p150Glued
IC
LIS1
Density (OD/mm2)
80
70
60
50
40
30
20
10
0
CE S1 P1 S2 P2 S3 P3 S4 P4 S5 P5
p150Glued
IC
LIS1

B

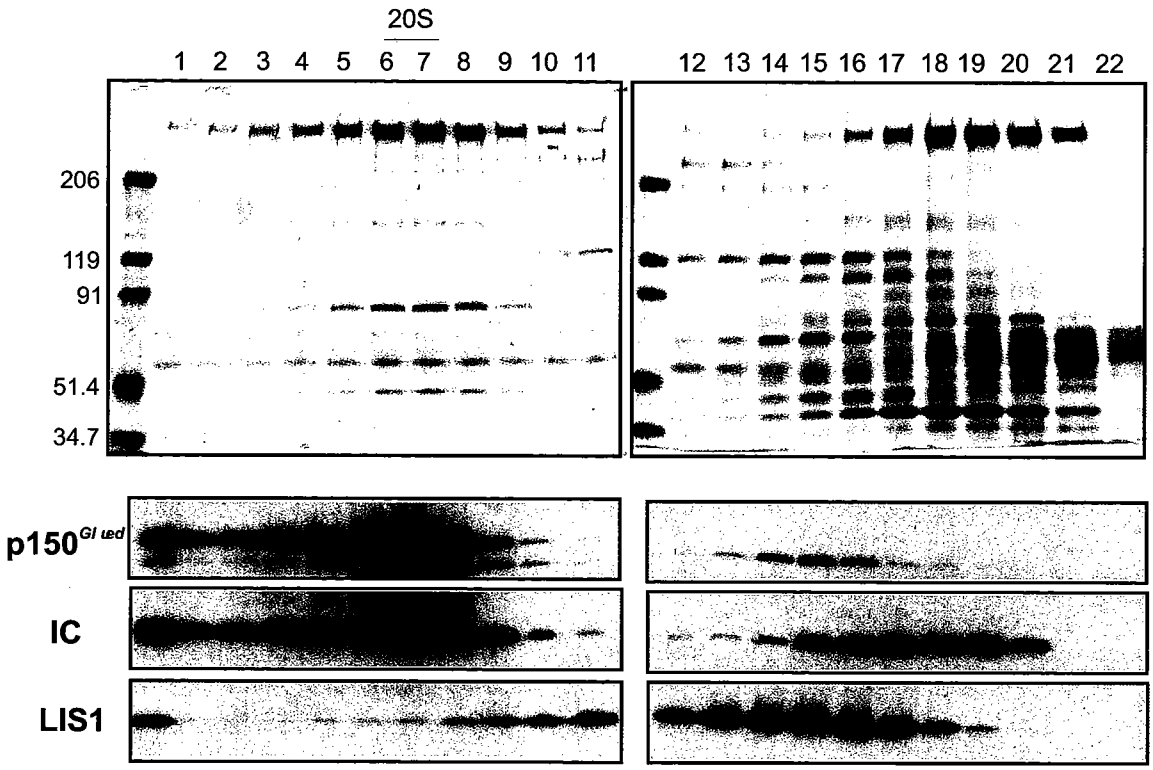
20S
1 2 3 4 5 6 7 8 9 10 11
12 13 14 15 16 17 18 19 20 21 22
206
119
91
51.4
34.7
p150Glued
IC
LIS1

Second, the recombinant LIS1 protein was produced by the baculoviral system (Fig. 6A), and added into the dynein preparation to allow measurement of the ATPase activity using a radioactive method (Paschal et al., 1991). A storable enhancement of dynein ATPase specific activity was detected with increasing amounts of LIS1 protein added (Fig. 6B). This storable curve was observed a few times (data not shown). In addition, ATPase assays with boiled or non-boiled LIS1 protein were also used as negative controls, which did not significantly change dynein enzymatic activity (Fig. 6C). Interestingly, LIS1 activated dynein ATPase by 1.6 fold, whereas BSA had no obvious effect on dynein ATPase (Fig. 6B & C). The basal dynein ATPase specific activity was in the range of 40-80 mol Pi/min/mg, which was consistent with the activities reported previously (Paschal et al., 1987; Shelter et al., 1988). A decline in ATPase activities was observed sometimes at much higher LIS1 concentration (Fig. 6C), but this inhibition was rarely observed and varied from batch to batch.

Figure 6. LIS1 activates dynein ATPase activity *in vitro*. (A) Purification of recombinant 6xHis-tagged LIS1 from baculoviral expression system. Aliquot of each step during the purification was resolved by SDS-PAGE, followed by coomassie staining (M, markers; TL, total lysate; PL, precleared lysate; FT, flow through; W1-W3, wash1-3; E1-3, eluate1-3). The 6His-tagged LIS1 protein was confirmed by immunoblotting using either anti-6His or anti-LIS1 monoclonal antibodies (U, uninfected control; I, infected). (B) The specificity activity of dynein ATPase was stimulated by the addition of the recombinant LIS1 protein in a dose dependent manner. (C) Another example of dynein ATPase assay including bovine serum albumin (BSA) and boiled LIS1 protein as negative controls. Error bars represent the range of duplicate points.

A

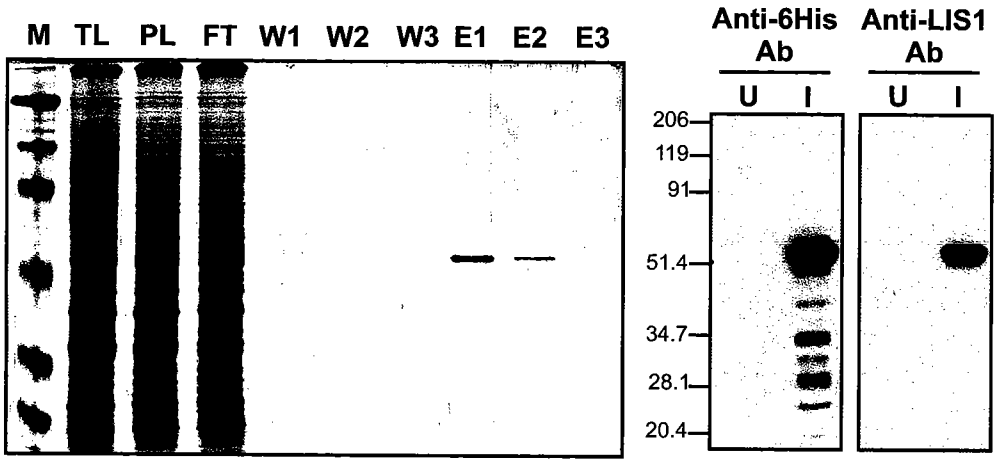
M TL PL FT W1 W2 W3 E1 E2 E3
Anti-6His Ab
Anti-LIS1 Ab
U I
U I
206
119
91
51.4
34.7
28.1
20.4

B

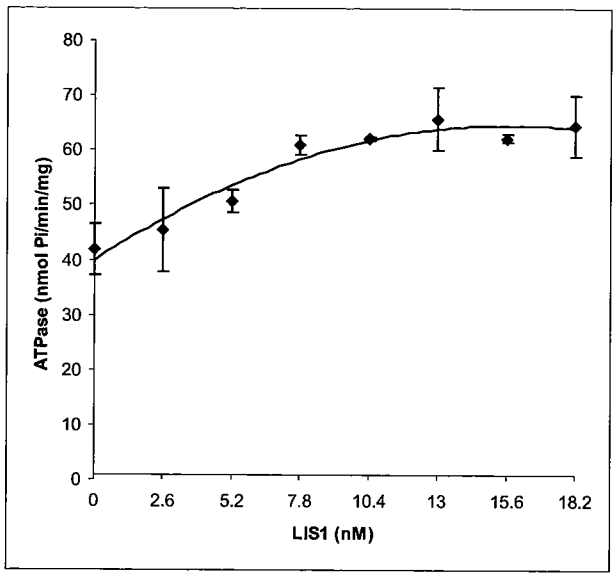
ATPase (nmol Pi/min/mg)
80
70
60
50
40
30
20
10
0
0
2.6
5.2
7.8
10.4
13
15.6
18.2
LIS1 (nM)

C

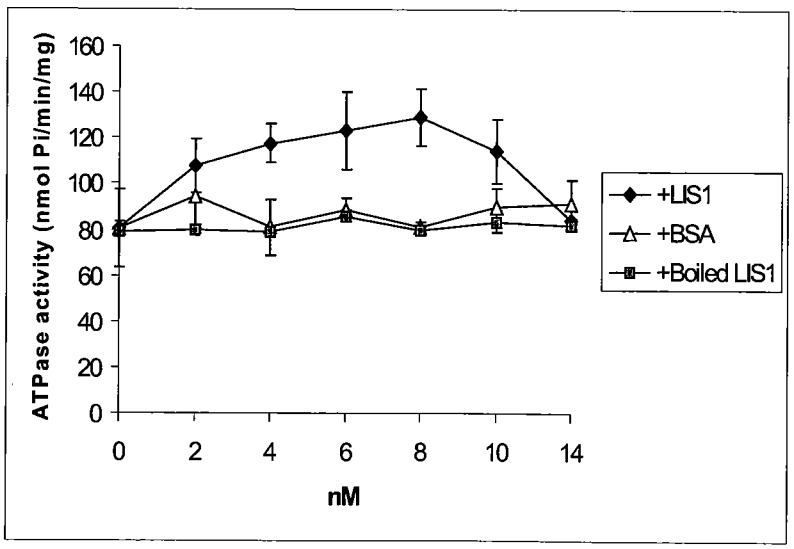
ATPase activity (nmol Pi/min/mg)
160
140
120
100
80
60
40
20
0
0
2
4
6
8
10
14
nM
+LIS1
+BSA
+Boiled LIS1

Discussion

Intricate protein-protein interactions at microtubule plus ends

The distinct pattern and length of EB1 and p150^{Glued} staining at microtubule plus ends indicated a difference in the microtubule binding property of these proteins (Fig. 1B). EB1 was found to mediate the microtubule plus end targeting of APC (Askham et al., 2000), whereas p150^{Glued} was indicated in recruiting dynein to the plus ends (Fig. 2)(Vaughan et al., 2002), suggesting a functional difference between EB1 and p150^{Glued} at microtubule plus ends. However, EB1 was found to interact with p150^{Glued} (Berrueta et al., 1999), but the significance of this interaction remains unclear.

The microtubule plus end binding property of p150^{Glued} has also been suggested to function at the loading step of vesicular transport (Vaughan et al., 2002). This view was disputed by the finding that p150^{Glued} was displaced from the microtubule plus ends in LIS1 overexpressing cells (Fig. 3A), and the morphologies and distributions of Golgi, endosomes and lysosomes remained unaltered (Faulkner et al., 2000; Tai et al., 2002).

When either the LIS1 N or WD fragment was overexpressed, dynein microtubule plus end localizations were abolished completely (Chapter III Fig. 3) and mitotic progressions of the transfected cells were severely perturbed (Chapter II Fig. 1)(Tai et al., 2002). These striking phenotypes suggested that LIS1 might not only regulate proper microtubule plus end binding of dynein, but also dynein-mediated mitotic functions.

The role of LIS1 in dynein motor activity

Previously a dynein-dynactin supercomplex can be purified at 30S in a sucrose density gradient (Kini and Collins, 2001), however, this result has never been reproduced by us and others. We could only obtain 20S fractions containing dynein and dynactin, indicating that the two protein complexes were separated during isolation procedures. A small amount of LIS1 was found to interact with dynein and dynactin at the 20S peak (Fig. 4 & 5B). Coimmunoprecipitation analyses indicated that LIS1 interacted with both complexes separately. This result strengthened the idea that LIS1 did not just interact with free subunits of dynein and dynactin, but with entire intact complexes (Chapter II)(Tai et al., 2002).

LIS1 was shown to interact with the P-loop mutant of dynein HC, suggesting that ATP hydrolysis was not required for binding (Tai et al., 2002). Furthermore, the LIS1-dynein interaction was unaffected in the absence or in the presence of ATP, GTP, AMP-PNP and ADP (data not shown). These results demonstrated that the binding between LIS1 and the dynein ATPase domain was not regulated by the status of nucleotides bound to the motor protein.

In the presence of increasing amounts of LIS1, the ATPase activity of dynein was stimulated and reached a maximum of 1.6 fold ± 0.4 enhancement (average of three independent experiments). These results clearly showed a true dynein ATPase activation

by LIS1, but the accurate Km and Vmax remain to be determined. IC has been suggested to serve as an inhibitory function of dynein HC ATPase activity (Kini and Collins, 2001). Thus, the ability of LIS1 to interact with both HC and IC raised the possibility that the stimulation could be the indirect result of LIS1-IC interactions. To exclude this possibility, a recombinant HC motor domain (380 kDa) protein purified from the baculoviral system was used for the ATPase assay instead of using the purified brain dynein complex. Preliminary results showed that the ATPase activity could be activated in a similar manner by the recombinant LIS1 as the purified dynein complex (CYT-unpublished result). However, the purity of this HC motor domain protein was not perfect, thus further purifications are required in order to confirm this finding.

A decline in LIS1-stimulated dynein ATPase activity was observed when an excess amount of LIS1 protein was added in the reactions (Fig. 5B). This decline has been observed in another set of reactions containing, again, excess amount of LIS1 protein. The consistency of this decline remains to be verified.

GENERAL CONCLUSIONS AND FUTURE DIRECTIONS

I believe that this thesis study has contributed to our understanding of how LIS1 functions in the cytoplasmic dynein pathway. First, I found that LIS1 regulated CLIP-170 kinetochore localization in a dynein/dynactin-dependent manner, and hence it contributed positively to the stability of kinetochore-microtubule interactions during the process of chromosome alignment. Second, domain analysis unequivocally showed the WD-repeat domain of LIS1 interacted with heavy-, intermediate-chains of dynein and dynamitin of dynactin. Third, I showed that LIS1 served as a dynein ATPase activator, a direct demonstration of the biological activity of LIS1 protein. Lastly, the finding of displacing dynein from microtubule plus ends by overexpressing LIS1, suggesting a role for LIS1 in regulating plus end-related functions of dynein during mitosis.

LIS1 at the kinetochore

I found that LIS1 was localized at the kinetochore through its associations with three subunits in the dynein and dynactin complexes (Tai et al., 2002). Subsequently, I discovered that LIS1 mediated CLIP-170 kinetochore targeting, suggesting a role for LIS1 in stabilizing the kinetochore-microtubule interactions. Others also showed that LIS1 interacted directly with CLIP-170 *in vitro*, complementing my *in vivo* results (Coquelle et al., 2002).

CLIP-170 was characterized as a microtubule-associated protein, which regulated vesicular transport (Pierre et al., 1992) and kinetochore-microtubule interactions (Dujardin et al., 1998). The functional importance of CLIP-170 at the kinetochore was further confirmed by studies of its yeast homologue, Bik1p, which was found to localize at the yeast kinetochores and to regulate chromosome segregation in polypoid yeast cells (Lin et al., 2001). We reported previously that interference of LIS1 function by an injection of anti-LIS1 antibody caused defects in chromosome alignment onto the metaphase plate (Faulkner et al., 2000). While the connections between spindle microtubules and kinetochores have not been examined in the anti-LIS1 antibody injected cells, it is tempting to speculate that defective spindle microtubule-kinetochore interactions would be observed in the injected cells. In addition, it was also unclear whether the mis-alignments of chromosomes at the metaphase plate were caused by the dysfunctions of CLIP-170 and/or dynein.

Domain analysis of LIS1 protein

The linear structure of LIS1 protein can be divided into two modules, the N-terminal 87 a.a. fragment containing a 28 a.a. coiled-coil motif and the C-terminal seven WD-repeat domain. Mutations in the LIS1 gene discovered in lissencephalic patients are scattered throughout its entire open reading frame, implying that the two structural domains of the encoded LIS1 protein are equally important for its structural/functional integrity.

In this study, the N-terminal domain was found to participate in self-association, and overexpressing this fragment prevented endogenous LIS1 protein from binding to kinetochores. The N-terminal domain was found to participate in self-association, possibly into a dimer (Ahn and Morris, 2001; Tai et al., 2002). Overexpression of this domain displaced the endogenous LIS1 from the kinetochore (Tai et al., 2002), suggesting an intact LIS1 homo-oligomer was crucial for its kinetochore localization. I found that when I deleted the 28 a.a. coiled-coil region from the N-terminal domain of LIS1, the self-association ability was retained, suggesting this region was dispensable for the process of self-association (Tai et al., 2002). The only know protein to interact with this domain was NudE, suggesting this N-terminal domain could interact with proteins other than itself (Kitagawa et al., 2000). Only one copy of the LIS1 protein was found in the PAFAH complex (Hattori et al., 1993), suggesting that LIS1 did not always function in the dimeric form.

The WD-repeat domain of LIS1, on the other hand, was the kinetochore-targeting domain, and was capable of interacting with the HC and IC of dynein, and dynamitin of dynactin. The WD-repeat domain has also been found to interact with several other proteins, including: CLIP-170 (Coquelle et al., 2002), doublecortin (Caspi et al., 2000), and catalytic subunits of PAFAH 1b (Kitagawa et al., 2000; Sweeney et al., 2000). A similar WD-repeat domain has been characterized in the β subunit of heterotrimeric G protein, and there have been more than fifteen different protein-protein interactions found within that domain (reviewed in Smith et al., 1999), suggesting that the multi-protein

interaction property seemed to be a general feature among proteins containing WD repeats.

The implications of LIS1 acting as a dynein ATPase activator

I found that LIS1 could stimulate dynein ATPase activity *in vitro*. In addition, this activation was saturable when LIS1 was added at equal molar ratios of LIS1 to dynein HC molecules present in the assays, suggesting the 1:1 ratio of LIS1 and HC was required for the full strength of activation. This LIS1 concentration-dependent activation of dynein ATPase activity was also tested when a recombinant dynein motor domain was used. A similar curve of activation was observed, suggesting the interaction between LIS1 and the ATPase domain was specifically responsible for this activation. However, a decrease in the degree of activation was also observed in a few experiments when LIS1 was added in excess amount. I noted that the decrease never dropped below the basal level of dynein ATPase activity, suggesting the excess amount of LIS1 protein repressed it's own activation activity rather than further inhibiting the basal activity of dynein ATPase. This suggests that the perturbation of mitotic progression that we observed when LIS1 was overexpressed (Faulkner et al., 2000; Tai et al., 2002) could represent an inhibition of its own activation function of dynein ATPase activity. It is worthwhile to test whether the velocity of dynein moving along the microtubule will be affected by the addition of LIS1 protein or not.

Microtubules and phospholipids have also been demonstrated to stimulate the ATPase activity of dynein as well (Ferro and Collins, 1995; Paschal et al., 1987). Microtubules form the tracks for dynein, and this ATPase activation ability of microtubules perpetuated the motility of dynein on the way to the minus end (Paschal et al., 1987). The phospholipids represent a form of vesicular cargo for dynein, and this phospholipid-stimulated dynein ATPase may represent another way to sustain the hydrolytic power of dynein during vesicular trafficking.

LIS1 at microtubule plus ends

Overexpression of LIS1 full-length or its fragments displaced dynein and dynactin from the microtubule plus ends (Chapter III; Faulkner et al., 2000). CLIP-170 has been reported to participate in the recruitment of LIS1 and dynactin to the microtubule plus ends (Coquelle et al., 2002; Valetti et al., 1999). This result supported our finding that the overexpressed LIS1 was unable to remove CLIP-170 from the microtubule plus ends (Chapter III; Faulkner et al., 2000). Thus, LIS1 was suggested to be the linker between CLIP-170 and dynactin (Coquelle et al., 2002). The microtubule-binding domain of $p150^{Glued}$ alone was able to localize at the microtubule plus ends, suggesting this domain was sufficient to target the whole dynactin complex to the plus ends (Vaughan et al., 2002). Thus, the absolute requirement of LIS1 in the microtubule plus end targeting of dynactin remains to be elucidated.

The perturbation of mitotic progression seen in LIS1 fragment overexpressing cells could be in part explained by the displacement of dynein and dynactin from the microtubule plus ends. First, mis-orientation of mitotic spindles was found in LIS1 FL overexpressers, suggesting that interruptions occurred between the plus ends of astral microtubules and the cell cortex (Faulkner et al., 2000). However, dynein and dynactin were mislocalized rather than completely displaced from the cell cortex (Faulkner et al., 2000). A detailed investigation of the relations between the microtubule plus ends and the cell cortex may clarify the exact mechanism of the spindle mis-orientation observed in LIS1 overexpressing cells. Second, overexpression of LIS1 FL and WD may prevent dynein and dynactin from interacting with the spindle microtubule plus ends as well as CLIP-170 from binding to the kinetochore (Tai et al., 2002). Both interruptions could hinder the interactions between the microtubule plus ends and kinetochores.

Dynein in neuronal migration

The link between LIS1 and neuronal migration has been suggested by the study of *LIS1* mutant mice. Defects in neuronal migration were observed in *LIS1* mutant mice (Hirotsune et al., 1997), which have provided the only evidence regarding the involvement of LIS1 in neuronal migration.

It is unknown whether dynein plays any role in the process of neuronal migration. The analogy drawn between neuronal migration and the nuclear migration of filamentous fungi seemed to be far-fetched. First, the massive waves of multiple-cell migrations

observed in neuronal migration cannot be compared with the multiple nuclei movements within a single cell observed in fungi. Second, radial glial cells are involved in guiding the process of neuronal migration, whereas there is no other cell type involved in the fungi nuclear migration. Even though dynein was found to participate in the nuclear migration process of filamentous fungi, there is no evidence whatsoever that dynein was involved in neuronal migration.

We reported in two consecutive research articles that LIS1 was involved in the mitotic dynein functions (Faulkner et al., 2000; Tai et al., 2002), suggesting a possibility that the cell cycle progression during neurogenesis might affect the process of neuronal migration (Vallee et al., 2000; Vallee et al., 2001). Again, our research did not address the role of dynein in neuronal migration, and this outstanding question needs to be answered in the future.

REFERENCES

Addinall, S.G., P.S. Mayr, S. Doyle, J.K. Sheehan, P.G. Woodman, and V.J. Allan. 2001. Phosphorylation by cdc2-CyclinB1 kinase releases cytoplasmic dynein from membranes. *J Biol Chem.* 276:15939-44.

Ahn, C., and N.R. Morris. 2001. Nudf, a fungal homolog of the human LIS1 protein, functions as a dimer in vivo. *J Biol Chem.* 276:9903-9.

Arai, H., H. Koizumi, J. Aoki, and K. Inoue. 2002. Platelet-Activating Factor Acetylhydrolase (PAF-AH). *J Biochem (Tokyo).* 131:635-40.

Askham, J.M., P. Moncur, A.F. Markham, and E.E. Morrison. 2000. Regulation and function of the interaction between the APC tumour suppressor protein and EB1. *Oncogene.* 19:1950-8.

Aumais, J.P., J.R. Tunstead, R.S. McNeil, B.T. Schaar, S.K. McConnell, S.H. Lin, G.D. Clark, and L.Y. Yu-Lee. 2001. NudC associates with Lis1 and the dynein motor at the leading pole of neurons. *J Neurosci.* 21:RC187.

Baes, M., P. Gressens, E. Baumgart, P. Carmeliet, M. Casteels, M. Fransen, P. Evrard, D. Fahimi, P.E. Declercq, D. Collen, P.P. van Veldhoven, and G.P. Mannaerts. 1997. A mouse model for Zellweger syndrome. *Nat Genet.* 17:49-57.

Banks, J.D., and R. Heald. 2001. Chromosome movement: dynein-out at the kinetochore. *Curr Biol.* 11:R128-31.

Benashski, S.E., A. Harrison, R.S. Patel-King, and S.M. King. 1997. Dimerization of the highly conserved light chain shared by dynein and myosin V. *J Biol Chem.* 272:20929-35.

Berrueta, L., J.S. Tirnauer, S.C. Schuyler, D. Pellman, and B.E. Bierer. 1999. The APC-associated protein EB1 associates with components of the dynactin complex and cytoplasmic dynein intermediate chain. *Curr Biol.* 9:425-8.

Bix, G.J., and G.D. Clark. 1998. Platelet-activating factor receptor stimulation disrupts neuronal migration In vitro. *J Neurosci.* 18:307-18.

Bowman, A.B., R.S. Patel-King, S.E. Benashski, J.M. McCaffery, L.S. Goldstein, and S.M. King. 1999. Drosophila roadblock and Chlamydomonas LC7: a conserved family of dynein-associated proteins involved in axonal transport, flagellar motility, and mitosis. *J Cell Biol.* 146:165-80.

Bruno, K.S., J.H. Tinsley, P.F. Minke, and M. Plamann. 1996. Genetic interactions among cytoplasmic dynein, dynactin, and nuclear distribution mutants of Neurospora crassa. *Proc Natl Acad Sci U S A.* 93:4775-80.

Burkhardt, J.K., C.J. Echeverri, T. Nilsson, and R.B. Vallee. 1997. Overexpression of the dynamitin (p50) subunit of the dynactin complex disrupts dynein-dependent maintenance of membrane organelle distribution. *J Cell Biol.* 139:469-84.

Caggese, C., R. Moschetti, G. Ragone, P. Barsanti, and R. Caizzi. 2001. dtctex-1, the Drosophila melanogaster homolog of a putative murine t- complex distorter encoding a dynein light chain, is required for production of functional sperm. *Mol Genet Genomics.* 265:436-44.

Cardoso, C., R.J. Leventer, N. Matsumoto, J.A. Kuc, M.B. Ramocki, S.K. Mewborn, L.L. Dudlicek, L.F. May, P.L. Mills, S. Das, D.T. Pilz, W.B. Dobyns, and D.H. Ledbetter. 2000. The location and type of mutation predict malformation severity in isolated lissencephaly caused by abnormalities within the LIS1 gene. *Hum Mol Genet.* 9:3019-28.

Caspi, M., R. Atlas, A. Kantor, T. Sapir, and O. Reiner. 2000. Interaction between LIS1 and doublecortin, two lissencephaly gene products. *Hum Mol Genet.* 9:2205-13.

Chenn, A., and S.K. McConnell. 1995. Cleavage orientation and the asymmetric inheritance of Notch1 immunoreactivity in mammalian neurogenesis. *Cell.* 82:631-41.

Coquelle, F.M., M. Caspi, F.P. Cordelieres, J.P. Dompierre, D.L. Dujardin, C. Koifman, P. Martin, C.C. Hoogenraad, A. Akhmanova, N. Galjart, J.R. De Mey, and O. Reiner. 2002. LIS1, CLIP-170's key to the dynein/dynactin pathway. *Mol Cell Biol.* 22:3089-102.

des Portes, V., F. Francis, J.M. Pinard, I. Desguerre, M.L. Moutard, I. Snoeck, L.C. Meiners, F. Capron, R. Cusmai, S. Ricci, J. Motte, B. Echenne, G. Ponsot, O. Dulac, J. Chelly, and C. Beldjord. 1998. doublecortin is the major gene causing X-linked subcortical laminar heterotopia (SCLH). *Hum Mol Genet.* 7:1063-70.

Diamantopoulos, G.S., F. Perez, H.V. Goodson, G. Batelier, R. Melki, T.E. Kreis, and J.E. Rickard. 1999. Dynamic localization of CLIP-170 to microtubule plus ends is coupled to microtubule assembly. *J Cell Biol.* 144:99-112.

Dick, T., K. Ray, H.K. Salz, and W. Chia. 1996. Cytoplasmic dynein (ddlc1) mutations cause morphogenetic defects and apoptotic cell death in Drosophila melanogaster. *Mol Cell Biol.* 16:1966-77.

Dujardin, D., U.I. Wacker, A. Moreau, T.A. Schroer, J.E. Rickard, and J.R. De Mey. 1998. Evidence for a role of CLIP-170 in the establishment of metaphase chromosome alignment. *J Cell Biol.* 141:849-62.

Dujardin, D.L., and R.B. Vallee. 2002. Dynein at the cortex. *Curr Opin Cell Biol.* 14:44-9.

Echeverri, C.J., B.M. Paschal, K.T. Vaughan, and R.B. Vallee. 1996. Molecular characterization of the 50-kD subunit of dynactin reveals function for the complex in chromosome alignment and spindle organization during mitosis. *J Cell Biol.* 132:617-33.

Eckley, D.M., S.R. Gill, K.A. Melkonian, J.B. Bingham, H.V. Goodson, J.E. Heuser, and T.A. Schroer. 1999. Analysis of dynactin subcomplexes reveals a novel actin-related protein associated with the arp1 minifilament pointed end. *J Cell Biol.* 147:307-20.

Espindola, F.S., D.M. Suter, L.B. Partata, T. Cao, J.S. Wolenski, R.E. Cheney, S.M. King, and M.S. Mooseker. 2000. The light chain composition of chicken brain myosin-Va: calmodulin, myosin-II essential light chains, and 8-kDa dynein light chain/PIN. *Cell Motil Cytoskeleton.* 47:269-81.

Faulkner, N.E., D.L. Dujardin, C.Y. Tai, K.T. Vaughan, C.B. O'Connell, Y. Wang, and R.B. Vallee. 2000. A role for the lissencephaly gene LIS1 in mitosis and cytoplasmic dynein function. *Nat Cell Biol.* 2:784-91.

Faust, P.L., and M.E. Hatten. 1997. Targeted deletion of the PEX2 peroxisome assembly gene in mice provides a model for Zellweger syndrome, a human neuronal migration disorder. *J Cell Biol.* 139:1293-305.

Feng, Y., E.C. Olson, P.T. Stukenberg, L.A. Flanagan, M.W. Kirschner, and C.A. Walsh. 2000. LIS1 regulates CNS lamination by interacting with mNudE, a central component of the centrosome. *Neuron.* 28:665-79.

Feng, Y., and C.A. Walsh. 2001. Protein-protein interactions, cytoskeletal regulation and neuronal migration. *Nat Rev Neurosci.* 2:408-16.

Ferro, K.L., and C.A. Collins. 1995. Microtubule-independent phospholipid stimulation of cytoplasmic dynein ATPase activity. *J Biol Chem.* 270:4492-6.

Fleck, M.W., S. Hirotsune, M.J. Gambello, E. Phillips-Tansey, G. Suares, R.F. Mervis, A. Wynshaw-Boris, and C.J. McBain. 2000. Hippocampal abnormalities and enhanced excitability in a murine model of human lissencephaly. *J Neurosci.* 20:2439-50.

Fox, J.W., E.D. Lamperti, Y.Z. Eksioglu, S.E. Hong, Y. Feng, D.A. Graham, I.E. Scheffer, W.B. Dobyns, B.A. Hirsch, R.A. Radtke, S.F. Berkovic, P.R. Huttenlocher, and C.A. Walsh. 1998. Mutations in filamin 1 prevent migration of cerebral cortical neurons in human periventricular heterotopia. *Neuron.* 21:1315-25.

Garces, J.A., I.B. Clark, D.I. Meyer, and R.B. Vallee. 1999. Interaction of the p62 subunit of dynactin with Arp1 and the cortical actin cytoskeleton. *Curr Biol.* 9:1497-500.

Gee, M.A., J.E. Heuser, and R.B. Vallee. 1997. An extended microtubule-binding structure within the dynein motor domain. *Nature.* 390:636-9.

Geiser, J.R., E.J. Schott, T.J. Kingsbury, N.B. Cole, L.J. Totis, G. Bhattacharyya, L. He, and M.A. Hoyt. 1997. Saccharomyces cerevisiae genes required in the absence of the CIN8- encoded spindle motor act in functionally diverse mitotic pathways. *Mol Biol Cell.* 8:1035-50.

Gibbons, B.H., and I.R. Gibbons. 1987. Vanadate-sensitized cleavage of dynein heavy chains by 365-nm irradiation of demembranated sperm flagella and its effect on the flagellar motility. *J Biol Chem.* 262:8354-9.

Gibbons IR, R.A. 1965. Dynein: a protein with adenosine triphosphate activity from cilia. *Science.* 149:424.

Gill, S.R., T.A. Schroer, I. Szilak, E.R. Steuer, M.P. Sheetz, and D.W. Cleveland. 1991. Dynactin, a conserved, ubiquitously expressed component of an activator of vesicle motility mediated by cytoplasmic dynein. *J Cell Biol.* 115:1639-50.

Gleeson, J.G., K.M. Allen, J.W. Fox, E.D. Lamperti, S. Berkovic, I. Scheffer, E.C. Cooper, W.B. Dobyns, S.R. Minnerath, M.E. Ross, and C.A. Walsh. 1998. Doublecortin, a brain-specific gene mutated in human X-linked lissencephaly and double cortex syndrome, encodes a putative signaling protein. *Cell.* 92:63-72.

Goldstein, L.S., and Z. Yang. 2000. Microtubule-based transport systems in neurons: the roles of kinesins and dyneins. *Annu Rev Neurosci.* 23:39-71.

Grimm, C., R. Sporle, T.E. Schmid, I.D. Adler, J. Adamski, K. Schughart, and J. Graw. 1999. Isolation and embryonic expression of the novel mouse gene Hic1, the homologue of HIC1, a candidate gene for the Miller-Dieker syndrome. *Hum Mol Genet.* 8:697-710.

Grissom, P.M., E.A. Vaisberg, and J.R. McIntosh. 2002. Identification of a Novel Light Intermediate Chain (D2LIC) for Mammalian Cytoplasmic Dynein 2. *Mol Biol Cell.* 13:817-29.

Gupta, A., L.H. Tsai, and A. Wynshaw-Boris. 2002. Life is a journey: a genetic look at neocortical development. *Nat Rev Genet.* 3:342-55.

Han, G., B. Liu, J. Zhang, W. Zuo, N.R. Morris, and X. Xiang. 2001. The Aspergillus cytoplasmic dynein heavy chain and NUDF localize to microtubule ends and affect microtubule dynamics. *Curr Biol.* 11:719-24.

Hattori, M., H. Adachi, M. Tsujimoto, H. Arai, and K. Inoue. 1994. Miller-Dieker lissencephaly gene encodes a subunit of brain platelet- activating factor acetylhydrolase. *Nature.* 370:216-8.

Hattori, M., H. Arai, and K. Inoue. 1993. Purification and characterization of bovine brain platelet-activating factor acetylhydrolase. *J Biol Chem.* 268:18748-53.

Hirotsune, S., M.W. Fleck, M.J. Gambello, G.J. Bix, A. Chen, G.D. Clark, D.H. Ledbetter, C.J. McBain, and A. Wynshaw-Boris. 1998. Graded reduction of Pafah1b1 (Lis1) activity results in neuronal migration defects and early embryonic lethality. *Nat Genet.* 19:333-9.

Hirotsune, S., S.D. Pack, S.S. Chong, C.M. Robbins, W.J. Pavan, D.H. Ledbetter, and A. Wynshaw-Boris. 1997. Genomic organization of the murine Miller-Dieker/lissencephaly region: conservation of linkage with the human region. *Genome Res.* 7:625-34.

Hoffmann, B., W. Zuo, A. Liu, and N.R. Morris. 2001. The LIS1-related protein NUDF of Aspergillus nidulans and its interaction partner NUDE bind directly to specific subunits of dynein and dynactin and to alpha- and gamma-tubulin. *J Biol Chem.* 276:38877-84.

Holleran, E.A., S. Karki, and E.L. Holzbaur. 1998. The role of the dynactin complex in intracellular motility. *Int Rev Cytol.* 182:69-109.

Holleran, E.A., M.K. Tokito, S. Karki, and E.L. Holzbaur. 1996. Centractin (ARP1) associates with spectrin revealing a potential mechanism to link dynactin to intracellular organelles. *J Cell Biol.* 135:1815-29.

Holzbaur, E.L., J.A. Hammarback, B.M. Paschal, N.G. Kravit, K.K. Pfister, and R.B. Vallee. 1991. Homology of a 150K cytoplasmic dynein-associated polypeptide with the Drosophila gene Glued. *Nature.* 351:579-83.

Hong, S.E., Y.Y. Shugart, D.T. Huang, S.A. Shahwan, P.E. Grant, J.O. Hourihane, N.D. Martin, and C.A. Walsh. 2000. Autosomal recessive lissencephaly with cerebellar hypoplasia is associated with human RELN mutations. *Nat Genet.* 26:93-6.

Hughes, S.M., K.T. Vaughan, J.S. Herskovits, and R.B. Vallee. 1995. Molecular analysis of a cytoplasmic dynein light intermediate chain reveals homology to a family of ATPases. *J Cell Sci.* 108:17-24.

Kamal, A., and L.S. Goldstein. 2000. Connecting vesicle transport to the cytoskeleton. *Curr Opin Cell Biol.* 12:503-8.

Karcher, R.L., S.W. Deacon, and V.I. Gelfand. 2002. Motor-cargo interactions: the key to transport specificity. *Trends Cell Biol.* 12:21-7.

Karki, S., and E.L. Holzbaur. 1995. Affinity chromatography demonstrates a direct binding between cytoplasmic dynein and the dynactin complex. *J Biol Chem.* 270:28806-11.

King, S.J., M. Bonilla, M.E. Rodgers, and T.A. Schroer. 2002. Subunit organization in cytoplasmic dynein subcomplexes. *Protein Sci.* 11:1239-50.

King, S.J., and T.A. Schroer. 2000. Dynactin increases the processivity of the cytoplasmic dynein motor. *Nat Cell Biol.* 2:20-4.

King, S.M., E. Barbarese, J.F. Dillman, III, R.S. Patel-King, J.H. Carson, and K.K. Pfister. 1996. Brain cytoplasmic and flagellar outer arm dyneins share a highly conserved Mr 8,000 light chain. *J Biol Chem.* 271:19358-66.

Kini, A.R., and C.A. Collins. 2001. Modulation of cytoplasmic dynein ATPase activity by the accessory subunits. *Cell Motil Cytoskeleton.* 48:52-60.

Kitagawa, M., M. Umezu, J. Aoki, H. Koizumi, H. Arai, and K. Inoue. 2000. Direct association of LIS1, the lissencephaly gene product, with a mammalian homologue of a fungal nuclear distribution protein, rNUDE. *FEBS Lett.* 479:57-62.

Kobayashi, K., Y. Nakahori, M. Miyake, K. Matsumura, E. Kondo-Iida, Y. Nomura, M. Segawa, M. Yoshioka, K. Saito, M. Osawa, K. Hamano, Y. Sakakihara, I.

Nonaka, Y. Nakagome, I. Kanazawa, Y. Nakamura, K. Tokunaga, and T. Toda. 1998. An ancient retrotransposal insertion causes Fukuyama-type congenital muscular dystrophy. *Nature*. 394:388-92.

Lambert de Rouvroit, C., and A.M. Goffinet. 2001. Neuronal migration. *Mech Dev.* 105:47-56.

Lane, J.D., M.A. Vergnolle, P.G. Woodman, and V.J. Allan. 2001. Apoptotic cleavage of cytoplasmic dynein intermediate chain and p150(Glued) stops dynein-dependent membrane motility. *J Cell Biol.* 153:1415-26.

Lee, I.H., S. Kumar, and M. Plamann. 2001. Null mutants of the neurospora actin-related protein 1 pointed-end complex show distinct phenotypes. *Mol Biol Cell.* 12:2195-206.

Leventer, R.J., C. Cardoso, D.H. Ledbetter, and W.B. Dobyns. 2001a. LIS1 missense mutations cause milder lissencephaly phenotypes including a child with normal IQ. *Neurology*. 57:416-22.

Leventer, R.J., C. Cardoso, D.H. Ledbetter, and W.B. Dobyns. 2001b. LIS1: from cortical malformation to essential protein of cellular dynamics. *Trends Neurosci.* 24:489-92.

Lin, H., P. de Carvalho, D. Kho, C.Y. Tai, P. Pierre, G.R. Fink, and D. Pellman. 2001. Polyploids require Bik1 for kinetochore-microtubule attachment. *J Cell Biol.* 155:1173-84.

Liu, Z., R. Steward, and L. Luo. 2000. Drosophila Lis1 is required for neuroblast proliferation, dendritic elaboration and axonal transport. *Nat Cell Biol.* 2:776-83.

Lo, K.W., S. Naisbitt, J.S. Fan, M. Sheng, and M. Zhang. 2001. The 8-kDa dynein light chain binds to its targets via a conserved (K/R)XTQT motif. *J Biol Chem.* 276:14059-66.

Ma, S., L. Trivinos-Lagos, R. Graf, and R.L. Chisholm. 1999. Dynein intermediate chain mediated dynein-dynactin interaction is required for interphase microtubule organization and centrosome replication and separation in Dictyostelium. *J Cell Biol.* 147:1261-74.

Mazumdar, M., A. Mikami, M.A. Gee, and R.B. Vallee. 1996. In vitro motility from recombinant dynein heavy chain. *Proc Natl Acad Sci U S A.* 93:6552-6.

McConnell, S.K. 1988. Fates of visual cortical neurons in the ferret after isochronic and heterochronic transplantation. *J Neurosci.* 8:945-74.

McConnell, S.K., and C.E. Kaznowski. 1991. Cell cycle dependence of laminar determination in developing neocortex. *Science.* 254:282-5.

McManus, L.M., and R.N. Pinckard. 2000. PAF, a putative mediator of oral inflammation. *Crit Rev Oral Biol Med.* 11:240-58.

McNally, F.J. 2001. Cytoskeleton: CLASPing the end to the edge. *Curr Biol.* 11:R477-80.

Mikami, A., S.H. Tynan, T. Hama, K. Luby-Phelps, T. Saito, J.E. Crandall, J.C. Besharse, and R.B. Vallee. 2002. Molecular structure of cytoplasmic dynein 2 and its distribution in neuronal and ciliated cells. Accepted by *J Cell Sci.*

Minke, P.F., I.H. Lee, J.H. Tinsley, K.S. Bruno, and M. Plamann. 1999. Neurospora crassa ro-10 and ro-11 genes encode novel proteins required for nuclear distribution. *Mol Microbiol.* 32:1065-76.

Mocz, G., and I.R. Gibbons. 2001. Model for the motor component of dynein heavy chain based on homology to the AAA family of oligomeric ATPases. *Structure (Camb).* 9:93-103.

Mok, Y.K., K.W. Lo, and M. Zhang. 2001. Structure of Tctex-1 and its interaction with cytoplasmic dynein intermediate chain. *J Biol Chem.* 276:14067-74.

Neuwald, A.F., L. Aravind, J.L. Spouge, and E.V. Koonin. 1999. AAA+: A class of chaperone-like ATPases associated with the assembly, operation, and disassembly of protein complexes. *Genome Res.* 9:27-43.

Niclas, J., V.J. Allan, and R.D. Vale. 1996. Cell cycle regulation of dynein association with membranes modulates microtubule-based organelle transport. *J Cell Biol.* 133:585-93.

Niethammer, M., D.S. Smith, R. Ayala, J. Peng, J. Ko, M.S. Lee, M. Morabito, and L.H. Tsai. 2000. NUDEL is a novel Cdk5 substrate that associates with LIS1 and cytoplasmic dynein. *Neuron.* 28:697-711.

Nurminsky, D.I., M.V. Nurminskaya, E.V. Benevolenskaya, Y.Y. Shevelyov, D.L. Hartl, and V.A. Gvozdev. 1998. Cytoplasmic dynein intermediate-chain isoforms with different targeting properties created by tissue-specific alternative splicing. *Mol Cell Biol.* 18:6816-25.

Ogura, T., and A.J. Wilkinson. 2001. AAA+ superfamily ATPases: common structure--diverse function. *Genes Cells*. 6:575-97.

Palazzo, A.F., H.L. Joseph, Y.J. Chen, D.L. Dujardin, A.S. Alberts, K.K. Pfister, R.B. Vallee, and G.G. Gundersen. 2001. Cdc42, dynein, and dynactin regulate MTOC reorientation independent of Rho-regulated microtubule stabilization. *Curr Biol.* 11:1536-41.

Paschal, B.M., E.L. Holzbaur, K.K. Pfister, S. Clark, D.I. Meyer, and R.B. Vallee. 1993. Characterization of a 50-kDa polypeptide in cytoplasmic dynein preparations reveals a complex with p150GLUED and a novel actin. *J Biol Chem.* 268:15318-23.

Paschal, B.M., A. Mikami, K.K. Pfister, and R.B. Vallee. 1992. Homology of the 74-kD cytoplasmic dynein subunit with a flagellar dynein polypeptide suggests an intracellular targeting function. *J Cell Biol.* 118:1133-43.

Paschal, B.M., H.S. Shpetner, and R.B. Vallee. 1987. MAP 1C is a microtubule-activated ATPase which translocates microtubules in vitro and has dynein-like properties. *J Cell Biol.* 105:1273-82.

Paschal, B.M., H.S. Shpetner, and R.B. Vallee. 1991. Purification of brain cytoplasmic dynein and characterization of its in vitro properties. *Methods Enzymol.* 196:181-91.

Pazour, G.J., B.L. Dickert, and G.B. Witman. 1999. The DHC1b (DHC2) isoform of cytoplasmic dynein is required for flagellar assembly. *J Cell Biol.* 144:473-81.

Pfister, K.K., M.W. Salata, J.F. Dillman, 3rd, E. Torre, and R.J. Lye. 1996a. Identification and developmental regulation of a neuron-specific subunit of cytoplasmic dynein. *Mol Biol Cell.* 7:331-43.

Pfister, K.K., M.W. Salata, J.F. Dillman, 3rd, K.T. Vaughan, R.B. Vallee, E. Torre, and R.J. Lye. 1996b. Differential expression and phosphorylation of the 74-kDa intermediate chains of cytoplasmic dynein in cultured neurons and glia. *J Biol Chem.* 271:1687-94.

Pierre, P., J. Scheel, J.E. Rickard, and T.E. Kreis. 1992. CLIP-170 links endocytic vesicles to microtubules. *Cell.* 70:887-900.

Purohit, A., S.H. Tynan, R. Vallee, and S.J. Doxsey. 1999. Direct interaction of pericentrin with cytoplasmic dynein light intermediate chain contributes to mitotic spindle organization. *J Cell Biol.* 147:481-92.

Rakic, P. 1978. Neuronal migration and contact guidance in the primate telencephalon. *Postgrad Med J.* 54:25-40.

Rakic, P. 1988. Specification of cerebral cortical areas. *Science.* 241:170-6.

Rakic, P. 1990. Principles of neural cell migration. *Experientia.* 46:882-91.

Rasmusson, K., M. Serr, J. Gepner, I. Gibbons, and T.S. Hays. 1994. A family of dynein genes in Drosophila melanogaster. *Mol Biol Cell.* 5:45-55.

Reiner, O., R. Carrozzo, Y. Shen, M. Wehnert, F. Faustinella, W.B. Dobyns, C.T. Caskey, and D.H. Ledbetter. 1993. Isolation of a Miller-Dieker lissencephaly gene containing G protein beta-subunit-like repeats. *Nature.* 364:717-21.

Ross, M.E., and C.A. Walsh. 2001. Human brain malformations and their lessons for neuronal migration. *Annu Rev Neurosci.* 24:1041-70.

Sapir, T., M. Eisenstein, H.A. Burgess, D. Horesh, A. Cahana, J. Aoki, M. Hattori, H. Arai, K. Inoue, and O. Reiner. 1999. Analysis of lissencephaly-causing LIS1 mutations. *Eur J Biochem.* 266:1011-20.

Sapir, T., M. Elbaum, and O. Reiner. 1997. Reduction of microtubule catastrophe events by LIS1, platelet- activating factor acetylhydrolase subunit. *Embo J.* 16:6977-84.

Sasaki, S., A. Shionoya, M. Ishida, M.J. Gambello, J. Yingling, A. Wynshaw-Boris, and S. Hirotsune. 2000. A LIS1/NUDEL/cytoplasmic dynein heavy chain complex in the developing and adult nervous system. *Neuron.* 28:681-96.

Sauer, F.C. 1935. Mitosis in the neuraltube. *J. Comp. Neurol.* 62:377-405.

Schroer, T.A., and M.P. Sheetz. 1991. Two activators of microtubule-based vesicle transport. *J Cell Biol.* 115:1309-18.

Schuyler, S.C., and D. Pellman. 2001. Microtubule "plus-end-tracking proteins": The end is just the beginning. *Cell.* 105:421-4.

Shpetner, H.S., B.M. Paschal, and R.B. Vallee. 1988. Characterization of the microtubule-activated ATPase of brain cytoplasmic dynein (MAP 1C). *J Cell Biol.* 107:1001-9.

Signor, D., K.P. Wedaman, J.T. Orozco, N.D. Dwyer, C.I. Bargmann, L.S. Rose, and J.M. Scholey. 1999. Role of a class DHC1b dynein in retrograde transport of IFT motors and IFT raft particles along cilia, but not dendrites, in chemosensory neurons of living Caenorhabditis elegans. *J Cell Biol.* 147:519-30.

Smith, D.S., M. Niethammer, R. Ayala, Y. Zhou, M.J. Gambello, A. Wynshaw-Boris, and L.H. Tsai. 2000. Regulation of cytoplasmic dynein behaviour and microtubule organization by mammalian Lis1. *Nat Cell Biol.* 2:767-75.

Smith, T.F., C. Gaitatzes, K. Saxena, and E.J. Neer. 1999. The WD repeat: a common architecture for diverse functions. *Trends Biochem Sci.* 24:181-5.

Starr, D.A., B.C. Williams, T.S. Hays, and M.L. Goldberg. 1998. ZW10 helps recruit dynactin and dynein to the kinetochore. *J Cell Biol.* 142:763-74.

Stebbings, H. 2001. Cytoskeleton-dependent transport and localization of mRNA. *Int Rev Cytol.* 211:1-31.

Susalka, S.J., K. Nikulina, M.W. Salata, P.S. Vaughan, S.M. King, K.T. Vaughan, and K.K. Pfister. 2002. The roadblock light chain binds a novel region of the cytoplasmic dynein intermediate chain. *J Biol Chem.* 20:20.

Swan, A., T. Nguyen, and B. Suter. 1999. Drosophila Lissencephaly-1 functions with Bic-D and dynein in oocyte determination and nuclear positioning. *Nat Cell Biol.* 1:444-9.

Sweeney, K.J., G.D. Clark, A. Prokscha, W.B. Dobyns, and G. Eichele. 2000. Lissencephaly associated mutations suggest a requirement for the PAFAH1B heterotrimeric complex in brain development. *Mech Dev.* 92:263-71.

Tai, A.W., J.Z. Chuang, C. Bode, U. Wolfrum, and C.H. Sung. 1999. Rhodopsin's carboxy-terminal cytoplasmic tail acts as a membrane receptor for cytoplasmic dynein by binding to the dynein light chain Tctex-1. *Cell.* 97:877-87.

Tai, C.Y., D.L. Dujardin, N.E. Faulkner, and R.B. Vallee. 2002. Role of dynein, dynactin, and CLIP-170 interactions in LIS1 kinetochore function. *J Cell Biol.* 156:959-68.

Tanaka, Y., Z. Zhang, and N. Hirokawa. 1995. Identification and molecular evolution of new dynein-like protein sequences in rat brain. *J Cell Sci.* 108:1883-93.

Tynan, S.H., M.A. Gee, and R.B. Vallee. 2000a. Distinct but overlapping sites within the cytoplasmic dynein heavy chain for dimerization and for intermediate chain and light intermediate chain binding. *J Biol Chem.* 275:32769-74.

Tynan, S.H., A. Purohit, S.J. Doxsey, and R.B. Vallee. 2000b. Light intermediate chain 1 defines a functional subfraction of cytoplasmic dynein which binds to pericentrin. *J Biol Chem.* 275:32763-8.

Vaisberg, E.A., P.M. Grissom, and J.R. McIntosh. 1996. Mammalian cells express three distinct dynein heavy chains that are localized to different cytoplasmic organelles. *J Cell Biol.* 133:831-42.

Valetti, C., D.M. Wetzel, M. Schrader, M.J. Hasbani, S.R. Gill, T.E. Kreis, and T.A. Schroer. 1999. Role of dynactin in endocytic traffic: effects of dynamitin overexpression and colocalization with CLIP-170. *Mol Biol Cell.* 10:4107-20.

Vallee, R.B., N.E. Faulkner, and C.Y. Tai. 2000. The role of cytoplasmic dynein in the human brain developmental disease lissencephaly. *Biochim Biophys Acta.* 1496:89-98.

Vallee, R.B., C. Tai, and N.E. Faulkner. 2001. LIS1: cellular function of a disease-causing gene. *Trends Cell Biol.* 11:155-60.

Vallee, R.B., J.S. Wall, B.M. Paschal, and H.S. Shpetner. 1988. Microtubule-associated protein 1C from brain is a two-headed cytosolic dynein. *Nature*. 332:561-3.

Vaughan, K.T., S.H. Tynan, N.E. Faulkner, C.J. Echeverri, and R.B. Vallee. 1999. Colocalization of cytoplasmic dynein with dynactin and CLIP-170 at microtubule distal ends. *J Cell Sci*. 112:1437-47.

Vaughan, K.T., and R.B. Vallee. 1995. Cytoplasmic dynein binds dynactin through a direct interaction between the intermediate chains and p150Glued. *J Cell Biol*. 131:1507-16.

Vaughan, P.S., J.D. Leszyk, and K.T. Vaughan. 2001. Cytoplasmic dynein intermediate chain phosphorylation regulates binding to dynactin. *J Biol Chem*. 276:26171-9.

Vaughan, P.S., P. Miura, M. Henderson, B. Byrne, and K.T. Vaughan. 2002. A role for regulated binding of p150Glued to microtubule plus ends in organelle transport. *J Cell Biol*. 158:305-319.

Walsh, C.A. 1999. Genetic malformations of the human cerebral cortex. *Neuron*. 23:19-29.

Waterman-Storer, C.M., S. Karki, and E.L. Holzbaur. 1995. The p150Glued component of the dynactin complex binds to both microtubules and the actin-related protein centractin (Arp-1). *Proc Natl Acad Sci U S A*. 92:1634-8.

Willins, D.A., B. Liu, X. Xiang, and N.R. Morris. 1997. Mutations in the heavy chain of cytoplasmic dynein suppress the nudF nuclear migration mutation of Aspergillus nidulans. *Mol Gen Genet*. 255:194-200.

Willins, D.A., X. Xiang, and N.R. Morris. 1995. An alpha tubulin mutation suppresses nuclear migration mutations in Aspergillus nidulans. *Genetics*. 141:1287-98.

Xiang, X., S.M. Beckwith, and N.R. Morris. 1994. Cytoplasmic dynein is involved in nuclear migration in Aspergillus nidulans. *Proc Natl Acad Sci U S A*. 91:2100-4.

Xiang, X., A.H. Osmani, S.A. Osmani, M. Xin, and N.R. Morris. 1995. NudF, a nuclear migration gene in Aspergillus nidulans, is similar to the human LIS-1 gene required for neuronal migration. *Mol Biol Cell*. 6:297-310.

Ye, G.J., K.T. Vaughan, R.B. Vallee, and B. Roizman. 2000. The herpes simplex virus 1 U(L)34 protein interacts with a cytoplasmic dynein intermediate chain and targets nuclear membrane. *J Virol*. 74:1355-63.